Resource Management with Smart Antenna in CDMA Systems

by

Yu Lei

Thesis submitted to the Faculty of the
Virginia Polytechnic Institute & State University
in partial fulfillment of the requirements for the degree of

MASTER OF SCIENCE
in
Electrical Engineering

Approved:

_____
Dr. Annamalai Annamalai, Chairman

_____ _____
Dr. Lamine Mili Dr. Luiz DaSilva

September 15, 2001
Alexandria, Virginia

Keywords: Smart Antenna, Resource Management, Wideband CDMA, Wireless Communications, Simulation

Resource Management with Smart Antenna in CDMA Systems

Yu Lei

(ABSTRACT)

Third generation (3G) mobile communication systems will provide services supporting high-speed data network and multimedia applications in addition to voice applications. The Smart antenna technique is one of the leading technologies that helps to meet the requirement by such services to radio network capacity. Resource management schemes such as power control, handoff and channel reservation/assignment are also essential for providing the seamless services with high quality. Smart antenna techniques will help to enhance the capability of resource management through more efficient and flexible use of resources. In this thesis, adaptive array and switched beam antenna techniques are compared in terms of algorithm, performance, complexity and hardware requirements. Based on these comparisons, sub-optimal code gate algorithm are most likely the suitable algorithms for next generation code division multiple access (CDMA) systems due to its good performances, robustness, and low complexity. A multi-cell CDMA simulator is developed for investigating the gain from smart antenna techniques in both bit error rate (BER) performance improvement and enhancement to resource management schemes. Our study shows that smart antenna techniques can significantly improve the performance of the system and help to build more powerful and flexible resource management schemes. With eight array elements, the system capacity can be increased by a factor of four. Power control command rates can be reduced through the tradeoff with the interference reduction by smart antennas. Smart antennas will also reduce handover failure rates and further increase the system capacity by reducing the resources reserved for soft handover.

Acknowledgments

I would like to express my gratitude to Dr. Annamalai Annamalai for his precious guidance, support and encouragement during the last one year, essential to my thesis work. I also thank Dr. Luiz DaSilva and Dr. Lamine Mili for their careful review of my thesis and valuable suggestions. I also want to express my thankfulness to LG Electronics for sponsoring the project on which this thesis is based.

Special thanks to Fakhrul Alam and Paulo Cardieri whose works on simulating W-CDMA systems and resource management gave me introductory knowledge in constructing my simulation model. I would also like to thank James Hicks and Kazi Zahid who gave me insight on smart antenna techniques. Shakheela H. Marikar, and Vikash Srivastava deserve my thankfulness for their help in building the simulation model.

I would give my thanks to all the faculty members and friends who helped me in Blacksburg as well as Alexandria during my course and research works for the last two years.

Finally, I want to thank my parents and family for their unreserved love and support from where comes the motivation and inspiration for the completion of my thesis work.

List of Content

1. Introduction 1
1.1 Evolution of Cellular Systems 1
1.2 WCDMA Features 3
1.3 Overview of Smart Antenna Techniques 5
1.4 Overview of Radio Resource Management 6
1.5 Objective and Outline of the Thesis 8

2. Smart Antenna Techniques 10
2.1 Antenna Array Basics 10
2.1.1 Uniformly Spaced Isotopic Liner Array Synthesis 11
2.1.2 Beamforming 12
2.1.3 Sidelobe Reduction 14
2.2 Switched Beam Systems 15
2.3 Adaptive Beamforming 19
2.3.1 Algorithm Basics 19
2.3.2 Blind Algorithms 22
2.3.3 Blind Algorithms in CDMA Systems 24
2.4 Complexities and Hardware Requirements of CDMA SA Algorithms 27
2.5 Application Issues of SA in CDMA systems 29
2.5.1 Performance and Beam Pattern 29
2.5.2 AOA Spread and 2-D RAKE 32
2.5.3 SA Applications in CDMA Systems 35

3. Radio Resource Management 36
3.1 Introduction to Resource Management 36

3.2 Resource management in TDMA/FDMA systems 37
3.3 Power Control in CDMA Systems 40
3.4 Handover in CDMA Systems 44
3.5 Call Admission Control in CDMA Systems 46
3.6 Capacity Reservation/Channel Assignment in CDMA systems 47

4. Simulation Model on SA and RRM in CDMA Systems 51
4.1 General Description of The Simulator 51
4.2 Mobility and Geographic Model 53
4.3 Event Simulator 60
4.4 Channel Simulator 62
4.5 Signal Processor 65
4.6 Smart Antenna Processing 70
4.7 Resource Management 71

5. Simulation Result and Discussions 73
5.1 General Description of the Simulation Setup 73
5.2 Simulation Study in Single Cell Scenario 74
5.2.1 Single User BER Performance and Power Control 74
5.2.2 Multi-user BER Performance and Smart Antenna 80
5.2.3 Cell Capacity, Block/Drop Rate and Smart Antenna 84
5.3 Simulation Study in Multi-cell Scenario 87

6. Conclusion and Future Work 93
6.1 Conclusions 93
6.2 Future Works 94

Reference 96
Abbreviations 102
VITA 104

List of Tables

Table 1.1 WCDMA, GSM and IS-95 Air Interfaces..... 3
Table 1.2 Experimental SA Systems and Commercially Available Products..... 6
Table 1.3 Comparisons of RRM of FDMA/TDMA and CDMA systems 7
Table 2.1 Criteria for Optimal Weights 20
Table 2.2 Performance of Switched Beam and Adaptive Array 33
Table 4.1 Cluster Sets for Distance Adjustment 60
Table 4.2 Vehicular Outdoor Channel PDF 63
Table 5.1 Number of Users with respect to Arrival/Departure Ratio 84

List of Figures

Fig 1.1 UTRAN Architecture 4
Fig 2.1 Uniformly Spaced Isotopic Linear Array 12
Fig 2.2 Beam Pattern of a 8 Element Linear Array 14
Fig 2.3 Comparison of Beam Pattern with Different SLR 15
Fig 2.4 Switched Beam System Block Diagram 17
Fig 2.5 Multi-beam Generating Algorithms 18
Fig 2.6 Multi-beam Patterns of Switched Beam Systems 18
Fig 2.7 Reference Generation in Decision Direct Algorithm 23
Fig 2.8 CGA Beamformer Block Diagram 26
Fig 2.9 CGA and Sub-Optimal CGA Computing process 28
Fig 2.10 Complexity of the Smart Antenna Algorithms 28
Fig 3.1 Transmitting Power vs. System Load 43
Fig 3.2 IS-95A Handover Process 44
Fig 3.3 WCDMA Handover Process 45
Fig 3.4 Channel Reservation Scheme 50
Fig 4.1 General Block Diagram of The Simulator 52
Fig 4.2 PDF of Mobile Directions and Speeds 54
Fig 4.3 Overlapping Area of Cell Styles 55
Fig 4.4 Coverage Area and Cell Layout 56
Fig 4.5 Concept of Toroidal Structure 57
Fig 4.6 Toroidal Adjustment of Mobile Locations and MS to BS Distances 58
Fig 4.7 Mobile Location Adjustment 59
Fig 4.8 Events Generating and Scheduling 61
Fig 4.9 Time Varying Channel 65

Fig 4.10 WCDMA Physical Channel Spreading and Modulation..... 67
Fig 4.11 Receiver Structure 69
Fig 4.12 Smart Antenna Processing..... 70
Fig 4.13 CAC and Channel Reservation Scheme..... 72
Fig 5.1 Received Signal at BS 75
Fig 5.2 Fading Curves with Different Doppler Spreads..... 76
Fig 5.3 BER with PC under Different Doppler Spread 77
Fig 5.4 Power Control Error with Respect to Doppler Spreads 78
Fig 5.5 BER with Respect to Doppler Spreads..... 79
Fig 5.6 BER with Respect to Shadowing and Fast/Slow PC..... 80
Fig 5.7 BER with respect to PC and Sectoring..... 81
Fig 5.8 BER with respect to SA and Number of Users 82
Fig 5.9 BER with respect to SA and No. of Users 83
Fig 5.10 BER with respect to PC Rate and SA..... 84
Fig 5.11 Cell Capacity with respect to Antenna, Call Admission and Drop Threshold... 85
Fig 5.12 Number of Users with Finite Cell Capacity 86
Fig 5.13 Block / Drop Rate and the Antenna..... 87
Fig 5.14 Call Drop Rate with respect to Antenna Types, SR, and Reservation 88
Fig 5.15 Handover Rate with respect to Antenna Type and SR..... 89
Fig 5.16 Handover Failure Rate with respect to Antenna and SR..... 90
Fig 5.17 Call Blocking Rates with respect to Antenna Types and SR 91
Fig 5.18 Call Blocking Rate with respect to Antenna and Reservation 91
Fig 5.19 Handover Failure Rate with respect to Antenna and Reservation..... 92

Chapter 1

Introduction

1.1 Evolution of Cellular Systems

In the current telecommunication market, mobile phones are predicted to outnumber the fixed line phones and the mobile phone coverage exceeds 70% in countries with the most advance wireless markets [1]. So far, cellular technology has been evolving over two and currently to its third generation. Third generation mobile telecommunication networks are developed in competing with the traditional wired networks not only in number of subscribers but also in types of service they provide.

First generation cellular networks are analog systems using Frequency Division Multiple Access (FDMA). Deployed in 1983 [2], the Advanced Mobile Phone System (AMPS) is representative of the first generation systems employing FM technology and cellular concept with frequency reuse and planning.

Second generation systems (2G) dominate the current cellular market. Second generation cellular systems transmit and process digital signals with sophisticated signaling, access control and resource management scheme. Global System for Mobile Communications (GSM) deployed from 1990 [2] is the largest network in Europe and employs Time Division Multiple Access (TDMA). In the United States, major 2G standards include IS-95 (cdmaOne) adopted in 1993 [3] based on Code Division Multiple Access (CDMA) and IS-54/IS-136 based on TDMA. Second generation systems provide

a wide range of services such as voice, paging, facsimile, and low speed data network services.

Third generation systems (3G) have been developed from 2G systems to provide seamless and integrated voice and data services such as multi-media transmission and high-speed Internet access with a uniform infrastructure. Basic characteristics of 3G systems include [4]:

- A common global frequency band for both terrestrial and satellite components
- A small pocket terminal with worldwide roaming
- Maximizing the commonality and optimization of radio interfaces for multiple environments
- High speed circuit- and packet-switched data transmission and multi-media service
- Support for both symmetric and asymmetric data capabilities in all environments
- Compatibility with pre-existing networks and new services
- Spectrum efficiency and overall cost improvement

Major proposals for 3G systems based on CDMA techniques include cdma2000, WCDMA (UTRA, ARIB), CDMA I / CDMA II, and TD-SCDMA. Although most of the standard proposals avoid adopting specific requirements that result in new receiver structures, new technologies are available and may be implemented in 3G systems. Technologies for 3G and 4G systems include smart antenna techniques, multi-user detection, new receivers structure (such as LMMSE receivers), space-time receiver, turbo coding, and software radio, etc. [5].

1.2 WCDMA Features

WCDMA (UTRA) evolves from GSM system and combines Wideband Direct Sequence CDMA (DS-CDMA) air interface with GSM radio network structure. Major characteristics of W-CDMA systems are tabulated below with comparison to GSM and IS-95 systems [1].

Table 1.1 WCDMA, GSM and IS-95 Air Interfaces

CHARACTORISTICS	WCDMA	GSM	IS-95
Carrier Spacing	5 MHz	200 kHz	1.25 MHz
Chip Rate	3.84 Mcps	N/A	1.2288 Mcps
Frequency Reuse Factor	1	1-18	1
BS Synchronization	Not needed	N/A	Typically via GPS
Inter-frequency Handover	Yes	N/A	Possible
Power Control Frequency	1500 Hz	2 Hz or Lower	800Hz
Resource Management	Efficient radio resource management algorithms	Frequency planning	Not needed for speech only networks
Frequency Diversity	Rake receiver	Frequency hoping	Rake receiver
Packet Data	Load-based scheduling	Time-slot based scheduling with GPRS	As short circuit switched calls
Downlink Trans Diversity	Supported	Not supported but applicable	Not supported

Other characteristics of WCDMA are:

- Support for both Frequency Division Duplex (FDD) and Time Division Duplex (TDD)
- Frame length is 10 ms
- Multi-user detection and smart antennas supported but optional in implementation
- Data rate of 384 kbps for outdoor to indoor and pedestrian, 2 Mbps for indoor office
- Support for variable rate data service

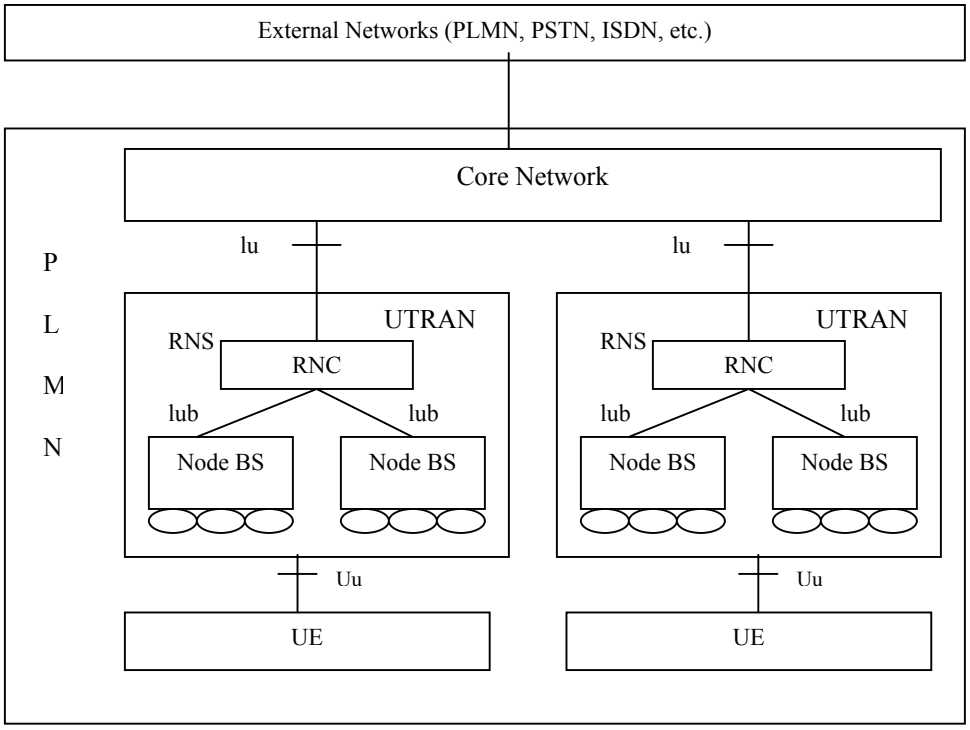

Fig 1.1 UTRAN Architecture

Figure 1.1 shows the overall structure of the third generation mobile network based on W-CDMA air interface [1], [44]. The Public Land Mobile Networks (PLMN) consists of a core network, multiple radio network subsystems (RNS), also called the Universal Terrestrial Radio Access Networks (UTRAN), and User Equipment (UE). UTRAN consists of one Radio Network Controller (RNC) and multiple Node BS (Base Station)

under control. Among several interfaces in the system, *Uu* is the WCDMA air interface and *lub* is the interface between a BS and its RNC.

Radio links will be established between Node BS and UE. Smart antenna is set up at Node BS. Power control will involve both Node BS and UE. Handover, call admission control (CAC) and channel assignment will in addition involve the RNC.

1.3 Overview of Smart Antenna Techniques

Smart Antenna (SA) techniques employ Digital Beam Forming (DBF) originated in the sonar and radar communities. Instead of generating an omni-directional beam pattern, a smart antenna can point one beam to a particular direction from which the desired user signal comes and nulls the interfering signals from other users. Additional gains also come from the spatial and angular diversity provided by an antenna array. The carrier to noise ratio also increases when signals from array elements combine, which yields multiplied received signal power at the output of the combiner.

Two smart antenna techniques have been developed and implemented in cellular systems. Switched beam systems use multiple beams of fixed number and directions while adaptive arrays steer one beam to one individual user. Table 1.2 shows the experimental and commercially available smart antenna systems [7].

In addition to switched beam and adaptive array, overloaded arrays combine the techniques of adaptive array and multi-user detection to serve users who outnumber the array elements by several times. Overloaded array algorithms have been considered mainly in airborne systems due to it's increased complexity as compared to the other two.

Table 1.2 Experimental SA Systems and Commercially Available Products

Designer	Air Interface	Antenna (M)	SA Receiver Algorithm	Remarks	Ref
SA Experimental Systems					
Ericsson & Manesmann Mobilefunk	GSM/DCS 1800	8	**Up-link**: DOB **Down-link**: DOB switched beam and adaptive	Several BS with SA in network	[8]
Ericsson Research (SW/US)	IS-136 (D-AMPS)	Spacing up-link 15λ & pol. div.	**Up-link**: MRC and IRC, **Down-link**: fixed beam approach		[9]
AT&T Labs-Research (US)	IS-136	4	**Up-link**: adaptive TRB, DMI Algorithm **Down-link**: switched beam with or without PC	Up and down links are independent	[10]
NTT DoCoMo (Japan)	UMTS	6	**Up-link**: Decision directed MMSE (tentative data and pilot) 4-finger 2D Rake **Down-link**: Calibration of weights for reverse link	Include 3 cell sites data transmission up to 2 Mbps	[11]
TSUNAMI Consortium (EU)	DECT -> DCS 1800		ULA with MUSIC for AoA estimation, tracking with Kalman filtering	SDMA was studied based on DECT	[12]
CNET & CSF-THOMPSON (F)	GSM/DCS 1800	10 circular	**Up-link**: DOB based BF Capon, MUSIC for AoA estimation **Down-link**: DOB		[13]
Uppsala University (SW)	DCS 1800	10 circular	Up-link only: TRB with DMI	Data traffic from DCS-1800 used	[14]
Commercially Available Products					
Metawave (US) Spotlight™ 2000	AMPS, CDMA	12	**Up-and down link**: 12 switched beam		[15]
Raytheon (US)	Flexible upgraded by SW	8	**Up-link**: DOB	SA can be directly connected at RF input at BS	[16]
ArrayComm "IntelliCell"™ (US)	WLL, PHS, GSM	4	**Up-link**: ESPRIT algorithm Adaptive interference cancellation	First mass market commercial product	[17]

1.4 Overview of Radio Resource Management

Radio Resource Management (RRM) is essential for efficient utilization of available air interface and transmitting power, maximizing the system capacity, and guaranteeing Quality of Service (QoS). Resource management includes functions such as power

control (PC), handover, channel assignment, load control and packet scheduling. Such resource management mechanisms may also interact with each other and desire joint consideration.

Sophisticated resource management schemes are adopted in 2G systems such as GSM and IS-95. Although their goals are the same, RRM schemes differ greatly between FDMA / TDMA systems [18] with fixed number of channels and CDMA systems with soft capacity. Comparisons of RRM between FDMA/TDMA systems and CDMA systems are summarized below.

Table 1.3 Comparisons of RRM of FDMA/TDMA and CDMA systems

Access Method	**FDMA/TDMA**	**CDMA**
Power Control	Centralized / distributed minimum variance, signal-level-based, or signal to interference ratio balancing	Target signal power or SIR identical for all served users
Handover	Hard handover	Soft handover
Channel Assignment	Fixed channel allocation (FCA), dynamic channel allocation (DCA) (can be combined with PC)	Channel reservation / call admission control

Resource management in 3G systems should be developed to meet requirements for combined high speed data and voice services satisfying QoS. Smart antenna technique can be considered as an approach helping to enhance 2G RRM into 3G RRM.

1.5 Objective and Outline of the Thesis

The objective of our research is to compare different smart antenna techniques (switched beam and adaptive array) in aspects including performance, complexity, and hardware requirements, and to investigate the performance improvement, capacity increment and resource management (power control, hand off, and channel assignment / reservation) enhancements brought about by SAs.

Many smart antenna algorithms can be found in literature [6], [19], [22], [23], [24], [25]. [21] also compared switched beam algorithms with a tracking beam algorithm (maximum power Lagrange). This thesis studies comprehensively on comparisons among different smart antenna algorithms subjected to various applications and environments. Detail comparisons are made to switched beam and adaptive array algorithms applied in CDMA systems.

Radio resource management (RRM) has been studies by many researchers, e.g. [33]-[38], [42]. However, there are little discusses on smart antennas effects on radio resource management in CDMA systems. This thesis studies how smart antenna affect radio resource management schemes such as power control, handover and radio resource management.

This research also provides a multi-cell cellular system simulator based on WCDMA and IS-95 standards that includes smart antenna and resource management schemes. [18] discussed a simulation model of multi-cell cellular systems in TDMA systems. There are also works on simulating WCDMA transmitting and receiving structures [45] in single cell scenario. Different to these works, we developed a CDMA system simulator in a multi-cell scenario. A new method is presented to generate an accurate geographic model with toroidal structures essential for studying RRM. Smart antenna algorithms and radio resource management schemes are also simulated. These

simulation are process in WCDMA signals and with mobile movements instead of by theoretical models.

This thesis is organized as follows. Chapter two introduces beamforming basics and various smart antenna algorithms. Also discussed are applications of SA in cellular systems and the comparison between switched beam systems and adaptive array systems. Chapter three discusses resource management schemes, especially in WCDMA and IS-95 systems. Chapter four describes the simulator for homogeneous or heterogeneous multi-cell WCDMA cellular systems. Simulation results and observations from the results are summarized in Chapter five.

Chapter 2

Smart Antenna Techniques

Smart antenna began to draw intensive attention from the cellular community in the early 1990s despite the long history of antenna array applications in radar and sonar systems. Smart antenna techniques improve point-to-point communications by providing spatial processing capability. SA techniques not only increase the capacity of the systems but also provide additional degrees of freedom for the radio network control and planning.

SA techniques can be integrated into existing and future cellular networks without major obstacles because of its relative independence to other components of cellular systems. A large number of algorithms have been developed to meet the need of different applications and environments. SA can easily be combined with other techniques such as space-time processing, multi-user detection, and channel coding [7]. SA techniques can also easily be integrated with radio resource management schemes and provide additional enhancement and flexibility to the schemes.

2.1 Antenna Array Basics

An antenna array is a set of antenna elements that are spatially distributed at fixed locations. A beamformer electronically forms the main beam and/or places nulls in any direction by changing the phase and amplitude of the exciting currents in each of the antenna elements. Linear, circular and planar arrays are common geometric arrangements of antenna elements. Linear arrays have their elements aligned along a straight line, and

are further called uniformly spaced linear array if the spacing between the array elements is equal. Circular arrays have their elements placed on a circle. Both linear arrays and circular arrays belong to the set termed planar array, with all their elements lying on a plane. Arrays whose elements do not lie on a single plane but conform to a given non-planar surface are categorized into conformal arrays.

The radiation pattern of an array is determined by the radiation pattern of the individual elements, their orientations and relative positions in space, as well as the amplitudes and phases of the feeding currents. If each element of the array is an isotropic point source, the radiation pattern of the array will depend solely on the geometry and feeding current of the array [5].

2.1.1 Uniformly Spaced Isotopic Liner Array Synthesis

As illustrated in figure 2.1, a uniformly spaced isotopic linear array has equal distance *d* between elements and θ as the angle of arrival (AoA) (from broadside to incident direction). Thus wave front delay between each two adjacent elements is $d\sin\theta$ assuming that the array is illuminated by a plane wave. The received signal can be expressed as:

$$\mathbf{x}(t) = \boldsymbol{\alpha}(\theta)x_1(t) \tag{2.1}$$

where

$$\mathbf{x}(t) = \begin{bmatrix} x_1(t) \\ x_2(t) \\ \vdots \\ x_M(t) \end{bmatrix} \qquad \boldsymbol{\alpha}(\theta) = \begin{bmatrix} 1 \\ e^{-j\frac{2\pi}{\lambda}d\sin\theta} \\ \vdots \\ e^{-j\frac{2\pi}{\lambda}(M-1)d\sin\theta} \end{bmatrix}$$

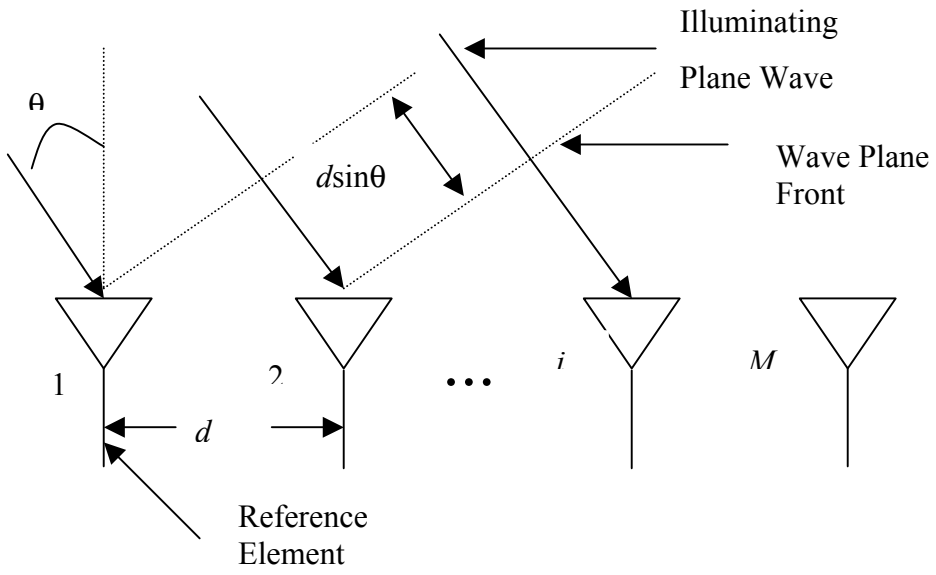

Fig 2.1 Uniformly Spaced Isotopic Linear Array

2.1.2 Beamforming

Beamforming is a process that generates a radiation pattern from the output of array elements such that the energy either focuses or disseminates along a specific direction in space. Electronically scanning of the antenna array can be done using a power dividing beamforming matrix such as the Butler matrix [19], phase array approaches or optimal combining.

It is desirable for its simplicity and flexibility to electronically scan the beam of an antenna by changing the phase of the output from the antenna elements. If only the phases are shifted with the amplitude unchanged when a beam is steered, the array is called a phased array [6]. The combined signal after beamforming thus becomes:

$$y(t) = \mathbf{w}^H \mathbf{x}(t) \tag{2.2}$$

where

$$\mathbf{W} = \begin{bmatrix} w_1 \\ w_2 \\ \vdots \\ w_M \end{bmatrix}$$

is the weight vector and H denotes the Hermitian transpose. The array response can be expressed as

$$g(\theta) = \mathbf{w}^H \boldsymbol{\alpha}(\theta) \tag{2.3}$$

Assuming that the weights are all ones, we have

$$\begin{aligned} g(\theta) &= \sum_{i=1}^{M} e^{-j\frac{2\pi}{\lambda}(i-1)d\sin\theta} \\ &= \frac{\sin(\pi\frac{Md}{\lambda}\sin\theta)}{\sin(\pi\frac{d}{\lambda}\sin\theta)} e^{-j\pi\frac{(M-1)d}{\lambda}\sin\theta} \end{aligned} \tag{2.4}$$

The discriminating capability of a beamformer depends on the ratio of the spatial aperture of the array to the wavelength. The null-to-null beam width is

$$\theta_{BW} = 2\arcsin(\frac{\lambda}{Md}) \tag{2.5}$$

Large spacing $d > \lambda/2$ will cause spatial alias and create additional main lobes, while excessively small spacing would bring mutual coupling effect and enlarge beam width. Thus, it is desired to keep $d = \lambda/2$ and accordingly beam width will only be determined by the number of array elements.

It is also noticeable that near the endfire area, the beam width will grow because $d\sin(\theta)$, when AoA deviates from the center of the beam, increases more slowly at the endfire zone than at the broadside. Also noticeable is that for a linear array, array

response is symmetric across the two sides of the array since illuminations from both sides are identical. As for steering, if the weights vector $\mathbf{w}$ is chosen as equal to the natural array response $\boldsymbol{\alpha}$, the amplitude of the array response after beamforming will reach its maximum at the AoA θ.

2.1.3 Sidelobe Reduction

The array response pattern (space factor) of an 8-element array is shown in Figure 2.2. The sidelobe ratio (SLR) is about 13 dB. SLR will level at 13.26 dB when the number of array elements increases. It is desirable to do sidelobe reduction to further reduce the possible interference coming from the sidelobe direction if SLR is of major concern.

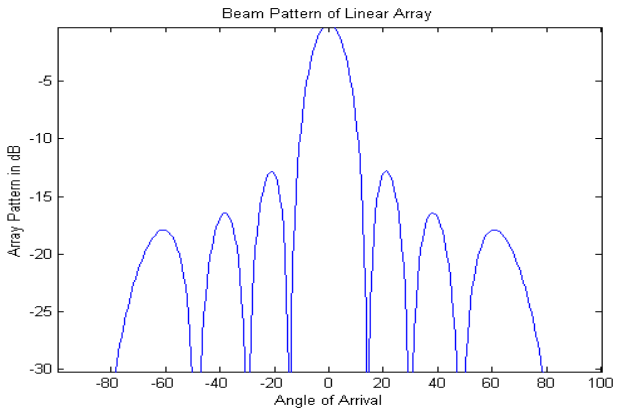

Fig 2.2 Beam Pattern of a 8 Element Linear Array

A half-wave spaced array yields maximum directivity for a given sidelobe ratio when all sidelobes are of equal height. Chebyshev polynomials are ideally suited for this purpose [20]. The Dolph-Chebyshev array algorithm is represented by the following equations.

$$x_0 = \cosh\frac{\arccos hSLR}{N-1} = \frac{1}{2}\left[SLR + \sqrt{SLR^2 - 1}\right]^{1/N} \tag{2.6}$$

$$w_n = \frac{1}{N}\sum_m T_{N-1}(x_0 \cos\frac{\pi m}{N}) \exp\left\{-j\left[(2n - N - 1)\frac{\pi m}{N}\right]\right\} \tag{2.7}$$

The beam pattern illustrated in Figure 2.3 shows that for a fixed number of array elements, there is a tradeoff between sidelobe reduction (SLR) and discriminating capability (beam width) which may reduce the benefit from sidelobe reduction.

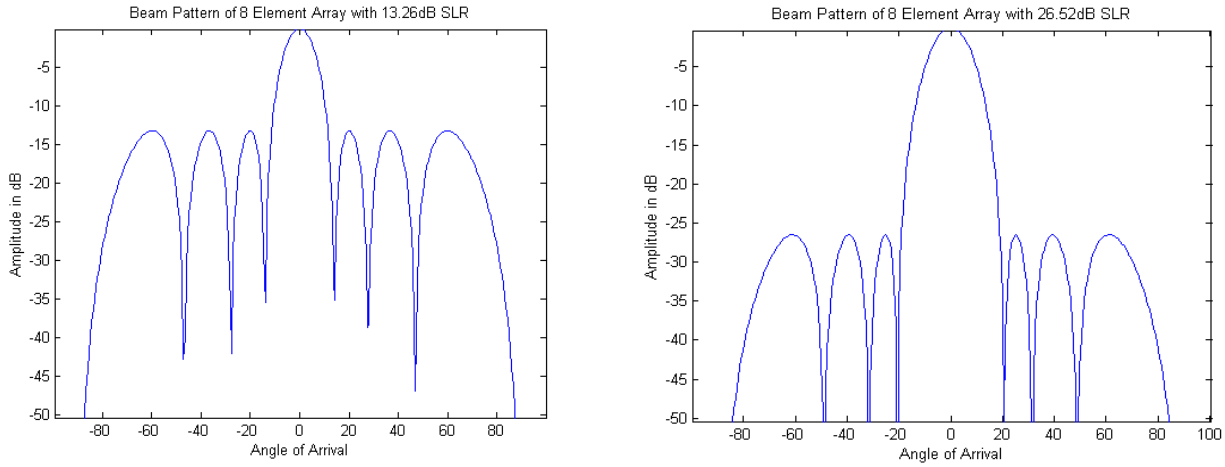

Fig 2.3 Comparison of Beam Pattern with Different SLR

2.2 Switched Beam Systems

The array system that has a number of fixed narrow beams and selects one for each subscriber at each sampling period is refereed to as a "switched-beam array" (SBA) [21]. A switched-beam system is shown in Figure 2.4.

There are two steps in designing a switched beam system. A multi-beam beam pattern needs to be generated and a beam-selecting algorithm needs to be designed.

An antenna array can generate multiple fixed beams through beamforming network (BFN) or phase array approaches. A well-known BFN uses the Butler Matrix method [19]. Others include simple Power Divider BFN, Blass and Nolen Matrices or 2-D BFN such as Mcfarland 2-D matrix. Another BFN family is lenses BFN including Rotman Lens BFN, Bootlace Lenses, Dome Lenses, etc. All of these methods divide the output signals from the antenna elements and feed them into an array processing network to generate combined signals. BFN have been implemented in hardware and served in systems such as Globalstar [20]. However, these methods are not computationally efficient as compared to phased array methods.

Two approaches have been configured to implement a multi-beam array system. The first method is to transplant the Butler matrix method into a phased array approaches. The algorithm is illustrated in Figure 2.5 where M is the number of arrays, and $l = 1 : L$ (L is the number of beams). θ determines the direction of the first beam and the angular space to the next beam. Choosing θ carefully according to the number of beams can generate multiple beams covering an arbitrary desired area. The second approach selects a set of uniformly spaced angles covering a predefined area and sets the weight vectors equal to the array responses. The algorithms of these two approaches are illustrated by the following flow chart in Figure 2.5 where θ_0 is the starting angle clockwise; θ_1 is the angelica area covered; and $\mathbf{m} = [1,2,...M]$.

The beam patterns generated by these two methods are shown in Figure 2.6. While the first method results in same level of beam intersections, second method generates uniformly spaced steering directions. The difference does not have significant effect on beamformer's performance.

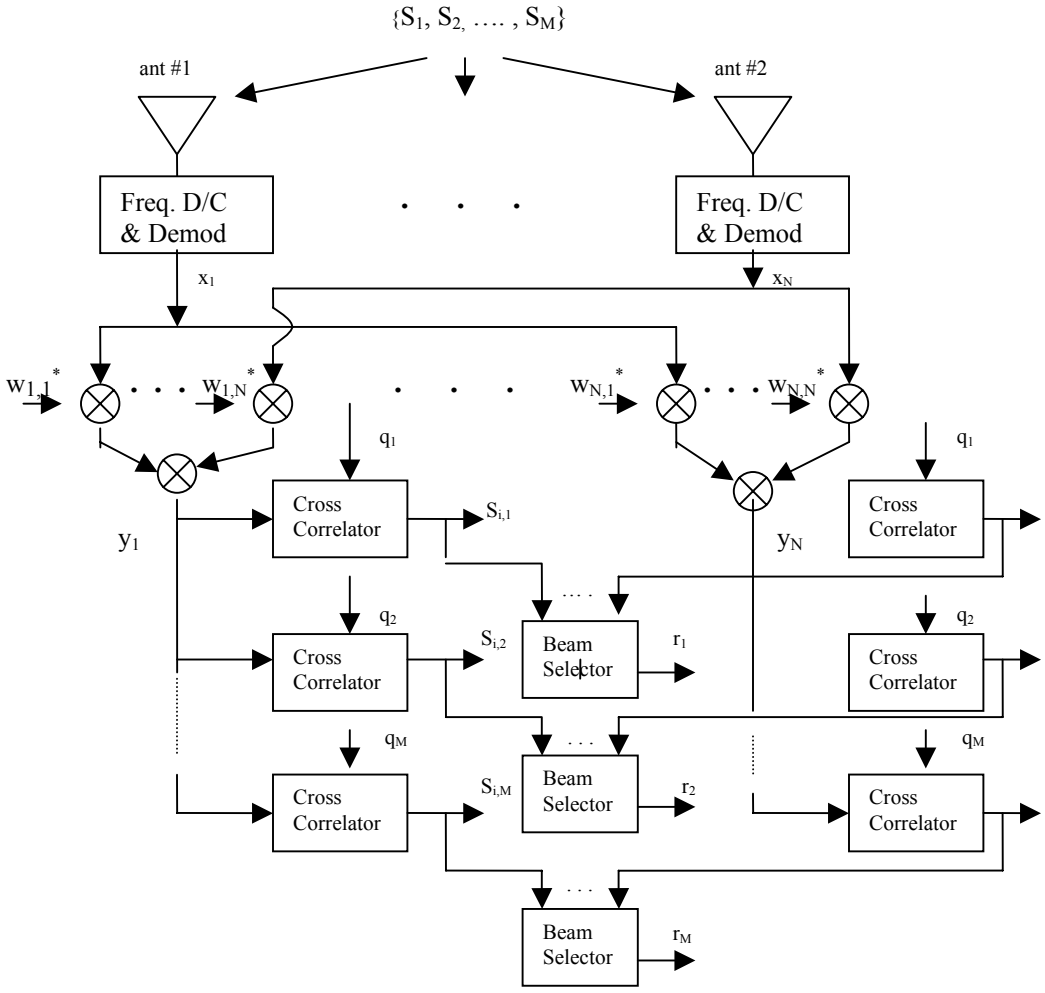

Fig 2.4 Switched Beam System Block Diagram

There are two ways to select a particular beam from the set to serve a certain user. One is to use a threshold and start selection from the first beam (set of weights). Whenever the output from the cross correlators ($S_{i,m}$ in Figure 2.4) is larger than the threshold, the corresponding weights $w_{i1},...,w_{iM}$ are chosen. A second method is to choose the weights that generate the strongest output from the cross correlators. Selection by threshold will somewhat reduces the beamforming time.

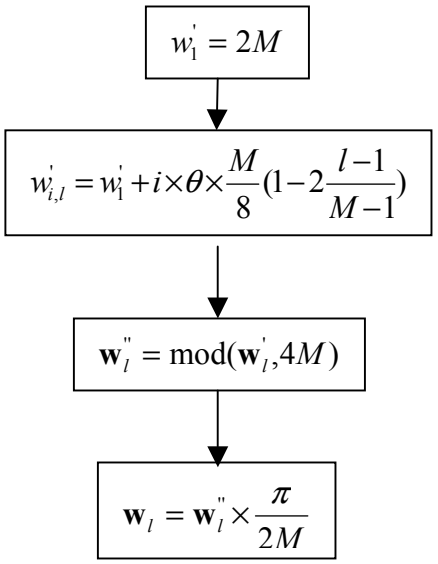

(1)

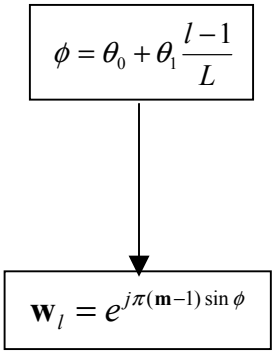

(2)

Fig 2.5 Multi-beam Generating Algorithms

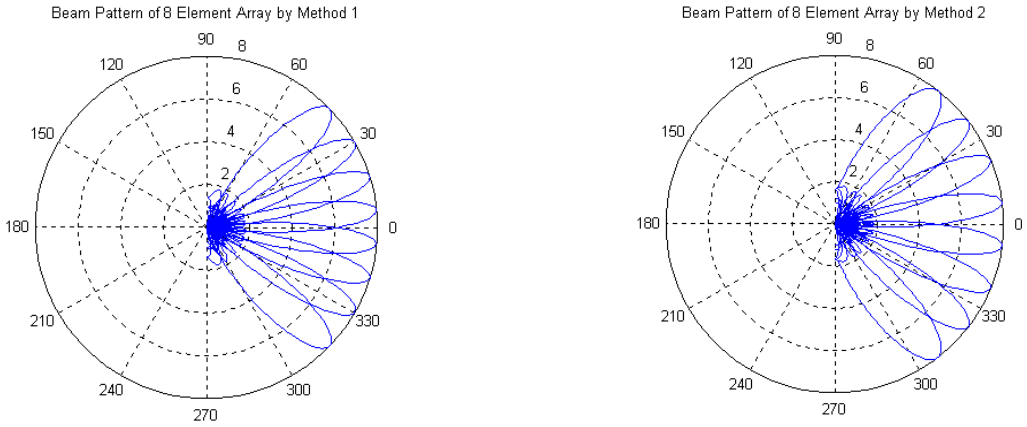

Fig 2.6 Multi-beam Patterns of Switched Beam Systems

2.3 Adaptive Beamforming

Adaptive beamformers are able to automatically optimize the beam pattern by adjusting the controlling weights of the array elements to satisfy a prescribed objective function [6]. Unlike fixed beam systems, not only the steering directions but also the entire beam patterns are automatically formed during the adaptation process. Adaptive beamformers can tract the desired user signal and/or put nulls toward interferes' signals provided that there are more array elements than interferers. Adaptive beamforming algorithms can be categorized into non-blind and blind algorithms. Non-blind algorithms use training signals while blind algorithms explore prior knowledge of certain properties of the desired signal.

2.3.1 Algorithm Basics

Many algorithms have been developed for adaptive beamforming. However, all these algorithms share the same foundation and follow basic approaches each of which include a criteria and an adaptive process. Criteria for optimal weights are summarized in Table 2.1 [6].

In Table 2.1, $\mathbf{R} = E(\mathbf{x}\mathbf{x}^H)$, $\mathbf{R}_u = E(\mathbf{u}\mathbf{u}^H)$, $\mathbf{R}_s = E(\mathbf{s}\mathbf{s}^H)$, $\mathbf{r} = E\{d^*(t)\mathbf{x}(t)\}$ and $\mathbf{x}, \mathbf{u}, \mathbf{s}, \mathbf{v}, \mathbf{w}, d, d^*$, are array output, interference signal, desired user signal, array response, controlling weights, desired signal and reference signal, respectively. Solutions for all three types of criteria can be generalized as the Wiener solution where β is a scalar coefficient.

Adaptive algorithms are used to resolve the matrix inverse and eigenvalue problems existing in seeking the Wiener solution. It is important that the algorithm designed converge fast and incur less computational complexity. Three commonly used algorithms

[6] are shown below, while others such as by neural networks are also presented in literature.

Table 2.1 Criteria for Optimal Weights

Criteria	Minimum Mean Square (MMSE)	Minimum Signal to Interference Ratio (MSIR)	Minimum Variance (MV)
Methods	Minimize the distance between the reference signal and the array output $\varepsilon^2(t) = [d^*(t) - \mathbf{w}^H \mathbf{x}(t)]^2$	Maximize the signal to interference ratio $SIR = \frac{\mathbf{w}^H \mathbf{R}_s \mathbf{w}}{\mathbf{w}^H \mathbf{R}_u \mathbf{w}}$	Minimize the output noise variance $Var(y) = \mathbf{w}^H \mathbf{R}_s \mathbf{w} + \mathbf{w}^H \mathbf{R}_u \mathbf{w}$
Equation	$\nabla \mathbf{w}(E\{\varepsilon^2(t)\})$ $= -2\mathbf{r} + 2\mathbf{R}\mathbf{w}$ $= 0$	$\mathbf{R}_u^{-1}\mathbf{R}_s \mathbf{w} = \lambda_{\max} \mathbf{w}$	$\nabla \mathbf{w}(\frac{1}{2}\mathbf{w}^H \mathbf{R}_u \mathbf{w} + \beta[1 - \mathbf{w}^H \mathbf{v}])$ $= \mathbf{R}_u \mathbf{w} - \beta \mathbf{v}$ $= 0$
Solution	$\mathbf{w}_{opt} = \beta \mathbf{R}_u^{-1} \mathbf{v}$ $\beta = \frac{E\{d^2(t)\}}{1 + E\{d^2(t)\}\mathbf{v}^H \mathbf{R}_u^{-1} \mathbf{v}}$	$\mathbf{w}_{opt} = \beta \mathbf{R}_u^{-1} \mathbf{v}$ $\beta = \frac{E\{d^2(t)\}}{SIR} \mathbf{v}^H \mathbf{w}_{opt}$	$\mathbf{w}_{opt} = \beta \mathbf{R}_u^{-1} \mathbf{v}$ $\beta = \frac{g}{\mathbf{v}^H \mathbf{R}_u^{-1} \mathbf{v}}$

Least Mean Squares Algorithms employ simple recursive equations (2.8) based on the equation of MMSE in Table 2.1.

$$\begin{aligned} \mathbf{w}(n+1) &= \mathbf{w}(n) + \frac{1}{2}\mu[-\nabla(E\{\varepsilon^2(n)\})] \\ &= \mathbf{w}(n) + \mu[\mathbf{r} - \mathbf{R}\mathbf{w}(n)] \end{aligned} \tag{2.8}$$

Instant estimates of $\mathbf{R}$ and $\mathbf{r}$ ($\hat{\mathbf{R}}(n) = \mathbf{x}(n)\mathbf{x}^H(n)$ and $\hat{\mathbf{r}}(n) = d^*(n)\mathbf{x}(n)$) are used such that

$$\begin{aligned} \hat{\mathbf{w}}(n+1) &= \hat{\mathbf{w}}(n) + \mu \mathbf{x}(n)[d^*(n) - \mathbf{x}^H(n)\hat{\mathbf{w}}(n)] \\ &= \hat{\mathbf{w}}(n) + \mu \mathbf{x}(n)\varepsilon^*(n) \end{aligned} \tag{2.9}$$

The LMS algorithm is simple but its convergence depends on the ratio of the largest eigenvalue to the others, especially the second largest one. Also, the accurate estimation of $\mathbf{R}$ and $\mathbf{r}$ depends on the stationary properties of the signals.

Direct Sample Covariance Matrix Inversion (DSCMI) employs the direct inversion of the covariance matrix $\mathbf{R}$ in MMSE equation in Table 2.1. $\mathbf{R}$ and $\mathbf{r}$ are estimated in the same way but from a block of samples. The least square solution will then be applied to

$$\hat{\mathbf{w}} = \hat{\mathbf{R}}^{-1}\hat{\mathbf{r}} \qquad\qquad e = \hat{\mathbf{R}}\mathbf{w}_{opt} - \hat{\mathbf{r}} \tag{2.10}$$

The DSCMI method converges faster than LMS but with higher complexity and finite precision problems causing instability when inverting a matrix.

Recursive Least Square (RLS) uses the weighted sum instead of a square window to estimate $\mathbf{R}$ and $\mathbf{r}$ by the equation below where $0 < \gamma < 1$ is the weighting factor

$$\hat{\mathbf{R}}(n) = \gamma\hat{\mathbf{R}}(n-1) + \mathbf{x}(n)\mathbf{x}^H(n) \tag{2.11}$$

$$\hat{\mathbf{r}}(n) = \gamma\hat{\mathbf{r}}(n-1) + d^*(n)\mathbf{x}(n) \tag{2.12}$$

The weight can be updated as

$$\mathbf{R}^{-1}(n) = \gamma^{-1}[\mathbf{R}^{-1}(n-1) - \mathbf{q}(n)\mathbf{x}(n)\mathbf{R}^{-1}(n-1)] \tag{2.13}$$

$$\mathbf{q}(n) = \frac{\gamma^{-1}\mathbf{R}^{-1}(n-1)\mathbf{x}(n)}{1+\gamma^{-1}\mathbf{x}^H(n)\mathbf{R}^{-1}(n-1)\mathbf{x}(n)} \tag{2.14}$$

$$\hat{\mathbf{w}}(n) = \hat{\mathbf{w}}(n-1) + \mathbf{q}(n)[d^*(n) - \hat{\mathbf{w}}^H(n-1)\mathbf{x}(n)] \tag{2.15}$$

The RLS algorithm replaces the inversion of the covariance matrix $\mathbf{x}(n)$ by scalar division and is an order of magnitude faster than the LMS algorithm [6].

2.3.2 Blind Algorithms

Blind algorithms do not need an explicit training sequence but rather generate their own references. Some commonly seen blind algorithms are summarized in this section with specific algorithms suitable for CDMA systems addressed in the next section.

DOA estimation algorithms such as MUSIC [22] and ESPRIT [23] use prior knowledge of array response or array manifold to estimate the DOA. Performance of DOA estimation algorithms depends on the accuracy and reliability of this knowledge. Furthermore, these algorithms can only estimate DOA up to the number of the array elements, a major disadvantage for application in cellular environments where multipath exists and the number of users is far greater than the number of array elements.

Constant Modulus algorithms take advantage of the constant modulus property that exists in signals of angle modulations, such as frequency modulation (FM), phase-shift keying (PSK), frequency-shift-keying (FSK), etc. Constant Modulus Algorithms define the cost function as the variation of the signal modulus as below:

$$\varepsilon = E[(r_p(n)1-|\, y(n)\,|^p)^2] \quad ; \quad r_p(n) = \frac{E[|\, s(n)\,|^{2p}]}{E[|\, s(n)\,|^p]} \tag{2.16}$$

Let $p = 1$ and scale $|\, s(n)\,|$ to unity, and use instantaneous estimation such that

$$\nabla(E\{\varepsilon(n)\}) = \mathbf{x}(n)(y(n) - \frac{y(n)}{|\, y(n)\,|})^* \tag{2.17}$$

controlling weights will be updated as

$$\begin{aligned} \mathbf{w}(n+1) &= \mathbf{w}(n) + \mu[-\nabla(E\{\varepsilon(n)\})] \\ &= \mathbf{w}(n) + \mu\mathbf{x}(n)\varepsilon^*(n) \end{aligned} \tag{2.18}$$

where $$\varepsilon(n) = y(n) - \frac{y(n)}{|\, y(n)\,|} \tag{2.19}$$

It is easy to see that the updating equation is similar to that of LMS methods except that the reference for CMA is implicit as the constant modulus of the signal.

The CMA algorithm does not require an explicit reference signal. However its performance depends on the constant amplitude of the desired signal. In reality this can not be true as the signals are subject to multipath effect and imperfect power control.

In Decision-Direct Algorithms (DDA), the beamformer output is demodulated and the decision-maker makes a decision based on the demodulated signal. A reference signal is generated by modulating the decision. The process is shown in Figure 2.7 below [6].

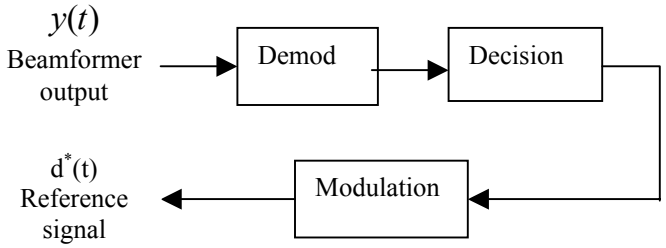

Fig 2.7 Reference Generation in Decision Direct Algorithm

DDA updates the weights by adaptive algorithms such as LMS. DDA and CMA cannot guarantee the convergence of the adaptive process because of the non-convex property of the cost function.

2.3.3 Blind Algorithms in CDMA Systems

Signals in CDMA systems have some properties that favor certain types of adaptive beamforming algorithms. These algorithms include Maximum Power Lagrange (MPL) algorithm [24] and Code Gate Algorithm (CGA) [25].

The Maximum Power Lagrange algorithm explores the fact that with reasonable power control quality, the despread desired user signal is stronger than that of each individual interferer by approximately the amount of processing gain. Therefore, the steering vector to the target signal source is approximately equal to the eigenvector corresponding to the largest eigenvalue of the auto-covariance matrix of the received signals [26]. The problem of beamforming thus turn into following eigenvalue problems:

$$\mathbf{R}_{xx}\mathbf{w} = \lambda_{\max}\mathbf{w} \tag{2.20}$$

The cost function is chosen as a Lagrange formula in order to find the eigenvector corresponding to the largest eigenvalue.

$$J(\mathbf{w}, r) = \mathbf{w}^H \mathbf{R}_{xx}\mathbf{w} + r(1 - \mathbf{w}^H\mathbf{w}) \tag{2.21}$$

where $\mathbf{w}^H\mathbf{w} = 1$ and r is the Lagrange multiplier. $\mathbf{R}_{xx}$ is the auto-covariance matrix of received despread signal $\mathbf{x}$ and can be obtained by

$$\mathbf{R}_{xx}(k) = f\mathbf{R}_{xx}(k-1) + \mathbf{x}(k)\mathbf{x}^H(k) \tag{2.22}$$

where f is the forgetting factor.

The control weight thus is obtained by

$$\mathbf{w}(k+1) = [[1 - \mu r(k)]\mathbf{I} + \mu\mathbf{R}_{xx}(k)]\mathbf{w}(k) \tag{2.23}$$

where μ is the adaptive gain factor that determines the convergence speed.

Like other approaches such as CGA, a simplified version of MPL method sets f to zero, i.e. uses instant estimation to reduce the complexity..

The CGA algorithm is based on maximum total signal to interference and noise ratio (TSINR) shown in Table 2.1 and has the solution as the eigenvector of the following equation

$$\mathbf{R}_u^{-1}\mathbf{R}_s\mathbf{w} = \lambda_{\max}\mathbf{w} \tag{2.24}$$

It is natural to use the despread array output as the reference to the signal of the desired user, and from it and by proper process generate the estimation of interference. The reference acquiring process is illustrated in Figure 2.8 where c_i is the spreading code for the *i*th user. The reference to the desired signal comes directly from a low pass filter fed with the despread array outputs.

$$\mathbf{y}_i(n) = \frac{1}{\sqrt{T_b}}\int_{(n-1)T_b+\tau_i}^{nT_b+\tau_i} x_i(t)dt \tag{2.25}$$

The interference reference can be obtained by subtracting the desired reference signal from the total signal as

$$\mathbf{u}(n) = \alpha\mathbf{x}(n) - \beta\mathbf{y}(n) \tag{2.26}$$

The general eigenvalue problem as Equation 2.24 can be solved by adaptive algorithms such as Generalized Lagrange Multiplier Method (GLM), Adaptive Matrix Inversion Method (AMI) or others like those discussed in Section 2.3.1.

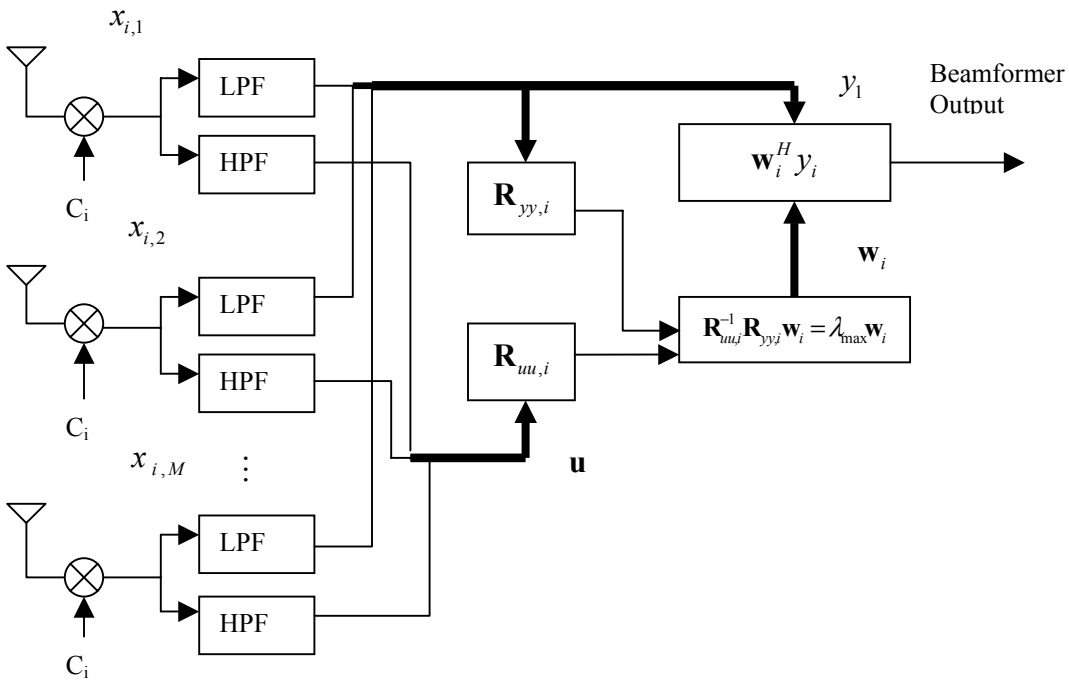

Fig 2.8 CGA Beamformer Block Diagram

The CGA algorithm is designed to take advantage of the existing despread signal in the CDMA receiver, which simplifies the reference acquisition process. However, the estimation of α and β in Equation 2.26 may not be straightforward and often degrades algorithm performance. Indirect matrix inversion operations also face problems such as singularity of the matrix and finite precision of processors. These problems degrade the performance of the optimal beamformer such that in reality a sub-optimal beamformer may outperform an optimal beamformer [25].

If the interference and noise signal $\mathbf{u}(n)$ is spatially and temporally white, we can maximize the beamformer output due to a desired user signal by following sub-optimal CGA equation

$$\mathbf{R}_{yy}\mathbf{w} = \lambda_{\max}\mathbf{w} \tag{2.27}$$

which is exactly the same as Equation 2.20. This illustrates that sub-optimal CGA problem and solution are exactly the same as those of MPL.

2.4 Complexities and Hardware Requirements of CDMA SA Algorithms

Ideal smart antenna algorithms should achieve interference reduction with low computational complexity and hardwire requirements subject to the application environment. CGA and sub-optimal CGA (or MPL) are designed for CDMA systems. Their complexity and hardware requirements are compared to the switched beam systems.

Figure 2.9 illustrates the computational process and complexity of CGA, sub-optimal CGA and switch beam algorithms. Variable N in Figure 2.9 is the number of array elements used and also represents N complex multiplication when referring to computational complexity. We can conclude that CGA will have approximately O(8N) complexity per iteration and Sub-Optimal CGA will have O(5N) complexity per iteration. It is worth noticing that the complexity of the adaptive algorithms is independent to the number of users in the system. It is also easy to see that the switch-beam system will have O(N*M) complexity where M denote the number of users. The complexities of the algorithms are shown in figure 2.10 assuming that the adaptive process converges after 4 iterations.

Hardware requirements do not differ much for all three algorithms. The number of RF fronts and cross correlators required is equal to the number of array elements and independent of smart antenna algorithms. Requirement on DSP is based on the computational complexity shown above. In addition, CGA requires N high pass and low pass filters while sub-optimal CGA requires N low pass filters only. Switched beam

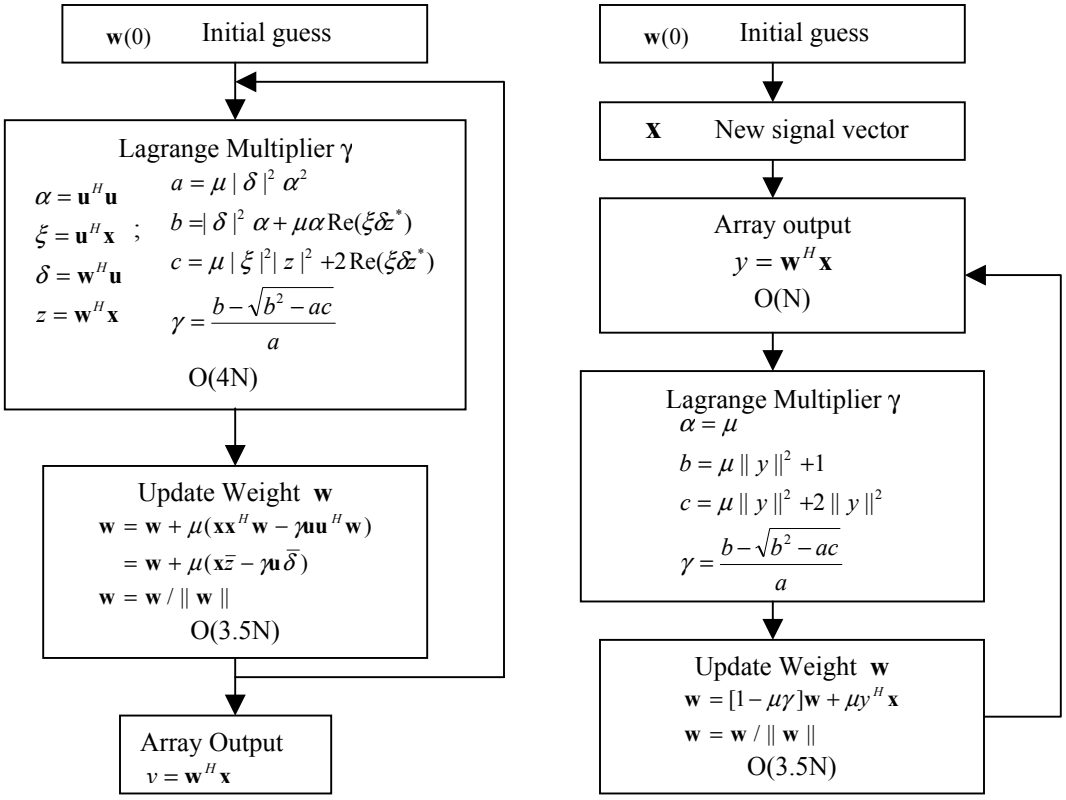

Fig 2.9 CGA and Sub-Optimal CGA Computing process

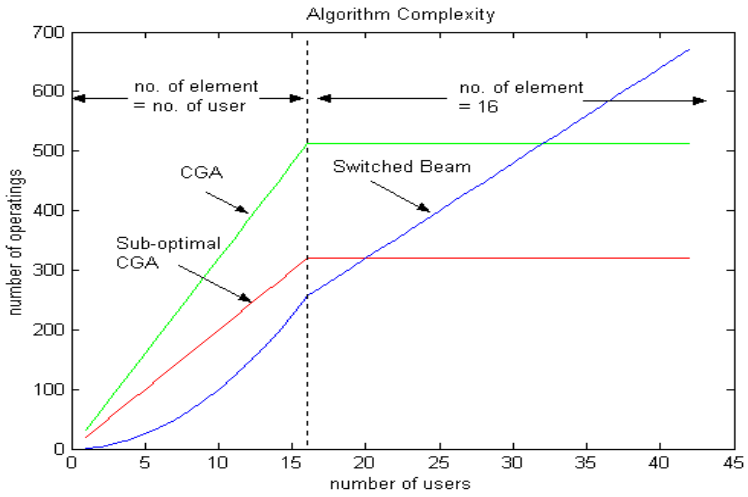

Fig 2.10 Complexity of the Smart Antenna Algorithms

systems, on the other hand, need an additional signal selector. These additional requirements can either be satisfied by employing specific hardware or increasing computational load on DSP.

It can be concluded from the above discussions that from the implementation point of view, the sub-optimal CGA algorithm is better than switched beam systems. Comparison of performance and other aspects of switch-beam and adaptive arrays will be given in the next section and chapter 5.

2.5 Application Issues of SA in CDMA systems

2.5.1 Performance and Beam Pattern

Performance of the smart antenna systems is closely related to the beam pattern. Theoretically, it is possible to maximize the desired signal power and at the same time completely null out all the interfering signals if the signal satisfies certain conditions illustrated by the following equations.

$$\delta_s^2 = E\{|\ \mathbf{w}^H\mathbf{s}\ |^2\} = \mathbf{w}^H\mathbf{R}_s\mathbf{w} \tag{2.28}$$

$$\delta_u^2 = E\{|\ \mathbf{w}^H\mathbf{u}\ |^2\} = \mathbf{w}^H\mathbf{R}_u\mathbf{w} \tag{2.29}$$

If $\|\ \mathbf{R}_u\ \| = 0$, it is possible to choose a certain $\mathbf{w}$ such that $\delta_u^2 = 0$. Meanwhile, if there is still freedom in choosing $\mathbf{w}$, it is possible to maximize δ_s^2 at the same time. The following examples illustrate how the beamformer maximizes the desire signal gain and nulls out the interferers.

Example 1 [6]:

Assuming that the desired signal $s(t)$ arrives from broadside and the interferer from $\pi/6$. The beamformer outputs due to the desired signal and interferer respectively are

$$\begin{aligned} y_d(t) &= s(t)(\mathbf{w}_1 + \mathbf{w}_2) \\ y_i(t) &= i(t)(\mathbf{w}_1 + e^{j\pi/2}\mathbf{w}_2) \end{aligned} \qquad \text{(note: } 2\pi\frac{d}{\lambda}\sin(\pi/6) = \pi/2\text{)} \tag{2.30}$$

To maximize the desired signal output and null out the interferer, $\mathbf{w}_1, \mathbf{w}_2$ should satisfy

$$\begin{aligned} \mathrm{Re}[\mathbf{w}_1] + \mathrm{Re}[\mathbf{w}_2] &= 1 \\ \mathrm{Im}[\mathbf{w}_1] + \mathrm{Im}[\mathbf{w}_2] &= 0 \end{aligned} \quad \text{and} \quad \begin{aligned} \mathrm{Re}[\mathbf{w}_1] + \mathrm{Re}[j\mathbf{w}_2] &= 0 \\ \mathrm{Im}[\mathbf{w}_1] + \mathrm{Im}[j\mathbf{w}_2] &= 0 \end{aligned} \tag{2.31}$$

and the solution is $\mathbf{w}_1 = 0.5 - j0.5$, $\mathbf{w}_2 = 0.5 + j0.5$.

Example 2:

Assuming $\mathbf{u}_1, \mathbf{u}_2$ are two interferers and $[1, \mathbf{v}_1], [1, \mathbf{v}_2]$ are two array responses according to AoA of $\mathbf{u}_1, \mathbf{u}_2$, the covariance matrix is

$$\begin{aligned} \mathbf{R}_{uu} &= E\{[(u_1 + u_2), (u_1v_1 + u_2v_2)]^H \cdot [(u_1 + u_2), (u_1v_1 + u_2v_2)]\} \\ \|\mathbf{R}_{uu}\| &= E\{(u_1 + u_2)^2\}E\{(u_1v_1 + u_2v_2)^2\} - E\{\overline{(u_1 + u_2)}(u_1v_1 + u_2v_2)\}E\{(u_1 + u_2)\overline{(u_1v_1 + u_2v_2)}\} \end{aligned} \tag{2.32}$$

It is somewhat difficult to draw a general condition under which the above equation holds, but two case studies can illustrate the idea.

If there is just one interferer as u_1, $\|\mathbf{R}_{uu}\| = 0$ which means that one interferer can always been canceled by the antenna array. Another case is that two interferers with

identical AoA i.e. $v_1 = v_2$ would also give $\| \mathbf{R}_{uu} \| = 0$, which shows that two interfering signals from the same direction can always be canceled by antenna arrays.

However, possibility of complete null all interferers (optimum beamforming) depends on the interference signals, array response and how many degrees of freedom the controlling weights have.

Another issue concerned with join maximization of the desired signal and nulling the interferers comes from the process of getting $\mathbf{w}$. Although theoretically blind beamforming algorithms will automatically generate the beam patterns that completely null out the interferers if possible, it is generally not easy to get the optimal result when $\mathbf{R}_{uu}$ is singular.

Furthermore, if the interference and noise signal is spatially and temporally white, there is no gain by placing nulls toward the interferers in addition to pointing the main beam to the desired signal. It is obvious that because of the whiteness, the gain from nulling out one interferer will be lost since another interferer may be amplified. In addition, there is no way to completely simultaneously null out all the interferers by adjusting the beam patterns if the number of array elements is less than the number of interferers with distinct incident angles. The optimal algorithms will collapse [27] in such situations. It is possible to null out major interferers whose number is less than that of the array elements. However in a cellular system where interferers usually outnumber array elements many times, it is not quite clear whether the scheme will bring real benefits after paying the price of more complex processing.

Generally speaking, interference signals are spatially white when traffic comes from all the directions such as in the center of an urban area. On the other hand, it is unlikely to be spatially white in suburban areas when traffic flows mainly along highways and when the area around the base stations is not symmetrically populated. Similar conclusion

about the performance comparison of optimal and sub-optimal approaches can be found from reference [28].

If infinite processing gain is assumed, it is easy to find that the weights generated by sub-optimal CGA algorithm (Equation 2.27) correspond to the natural array response of the desired user signal scaled by a factor of $\sqrt{N}$, where N is the number of array elements. Using natural array response of the desired user instead of sub-optimal CGA would therefore slightly improve the performance. It is also worth noticing that sub-optimal CGA is a phase array approach while optimal beamforming generally is not (since the amplitude and the phase of the signal from array elements are both changed while, however, the norm remain the same).

2.5.2 AOA Spread and 2-D RAKE

Radio channel characteristics differ in densely populated urban areas with micro or pico-cells from that in large suburban areas with a macro cell environment. For a macro cell environment, there is likely to be a line of sight (LOS) component of the signal and the angular spread of the signal is small. In micro- or pico-cell environments, it is less likely to have a LOS component and the angular spread tends to be large. Models of AoA spread can be found in the literature, e.g. [29].

Another concern is whether the system is narrowband or wideband. For a narrowband system, all multipath components arrive with very small delay compared to the chip period (also called correlated) and cannot be resolved by temporal RAKE receivers. In the mean time, it is more likely that the multipath components will have a small angular spread because otherwise large delay shall arise. In wideband systems, all the multipath components arrive with sufficient separation (uncorrelated) and can be resolved by temporal RAKE receivers.

Smart antenna algorithms yield different performances in different environments. For wideband systems, 2-D RAKE receiver can be employed with either adaptive array or switched beam antenna. Table 2.2 below [30] shows the performance measured in maximum number of users supported at outage probability of 10% ($\Pr(BER > 10^2) < 10\%$) with perfect power control and processing gain equal to 31. SB stands for switched beam and OSF for optimal spatial filtering which is another term for adaptive array. Geometrically Based Single Bounce (GBSB) multipath model is used to compute the table.

Table 2.2 Performance of Switched Beam and Adaptive Array

(with uncorrelated multipath components)

Number of Multipath Components	Number of user supported at Pr(BER> 10^{-12})<10%				
	Omni	M=6, SB	M=6, OSF	M=12, SB	M=12, OSF
1	14	31	>31	>31	>31
6	6	20	28	20	>31
10	4	15	23	20	29
20	1	11	14	20	24
30	0	6	10	13	20

(with correlated multipath components)

Number of Multipath Components	Number of user supported at Pr(BER> 10^{-12})<10%				
	Omni	M=6, SB	M=6, OSF	M=12, SB	M=12, OSF
1	14	31	>31	>31	>31
6	0	16	>31	>31	>31
10	0	6	>31	25	>31
20	1	10	>31	21	>31
30	0	12	>31	14	>31

It can be seen that for correlated multipath components, switch beam system is not able to offer performance comparable to adaptive array systems even with more

elements, especially when the number of multipath components is large. It is clear that switched beam systems do not have the same ability as adaptive array in resolving multipath with small AoA spread.

In the wideband case, even for a large number of multipath components, switch beam system can still offer performance comparable to adaptive arrays. By a reasonable increase in elements, it can even outperform the adaptive array, but of course the computation complexity also increases.

Furthermore, the temporal RAKE combining possible in wideband systems will give major utilization to multipath diversity (temporal diversity). The spatial RAKE combining will further explore the angular diversity of the multipath and improve the combining effect. However, it may not bring significant difference to the performance compared with 1-D RAKE receiver. For the same reason, the performance difference between switched beam and adaptive array due to spatial RAKE combining is not substantial.

WCDMA system is wideband because of its high chip rate. Assuming spatial and temporal whiteness of the interfering signal, there would be some but small difference in performance analysis between 2-D RAKE and conventional RAKE receiver with either switched beam or adaptive array. In a macro-cell environment, it is still a wideband system even if the angular spread is small. Employing temporal RAKE receiver thus reduces the need for spatial filtering in combating multipath effect. It is reasonable to assume no angular spread of multipath components in both micro and macro cell environments in a simulation study on switched beam and adaptive array performance, which cuts down the complexity but still generating results with enough fidelity.

2.5.3 SA Applications in CDMA Systems

For downlink transmitting a beamformer can point a beam to the desired mobile and reduce the transmitting power. The interference to other mobiles reduces accordingly both because the transmission is along a specific direction and because the power is reduced. Downlink beamforming is thus capable of improving the received signal quality at mobiles as well as expanding and reshaping base station coverage area.

For uplink transmitting, there are four ways to utilize antenna arrays to improve performance. The major improvement comes from co-channel interference reduction through beamforming gain. Second is fading suppression via exploring angular diversity by pointing the beams to different multipath components and combining the output. The third method that also combats multipath fading is exploring spatial diversity from the separated antenna array. Finally SNR improvement is achieved when adding signals from several antenna elements multiplies the signal power over noise. Only co-channel interference reduction through beamforming will be studied in later part of the thesis. A temporal RAKE receiver will be used to mitigate the fading effect.

Chapter 3

Radio Resource Management

Radio Resource Management (RRM) is very important for efficient usage of radio resources and for guaranteeing Quality of Service (QoS). RRM manages and controls the usage of radio resources such as transmitting power, available spectrum and hardware (equipped channels). Although the number of equipped channels (modulation and demodulation modules) can limit the capacity of the system, the focus in this thesis will be on interference-based radio resource management. A brief discuss on resource management in TDMA/FDMA systems is given as an introductory complement followed by detail discussion on RRM in CDMA systems.

3.1 Introduction to Resource Management

Resource management in TDMA/FDMA and CDMA systems has the same goal yet takes different mechanisms because of different reuse factors in this two type of systems. In TDMA/FDMA systems available spectrum is divided into channels and assigned to different users in one cell and is reused in cells with a certain distance. Unlike TDMA/FDMA systems, CDMA systems assign entire available spectrum to every user in the cell and reuse it in all the neighboring cells. This means that all the users in the covered area share a same available broadband channel. Resource management for CDMA systems thus can facilitate some new functions such as soft handover and macro diversity to enhance the performance.

RRM consists of power control, handover, call admission control, channel

assignment and reservation as well as load control and packet scheduling. Load control and packet scheduling are typically addressed in radio network planning and are not discussed in this thesis.

Power control refers to controlling the transmitting power so that the signals will reach the receivers with enough energy while generate as little co-channel interference as possible to other signals. Handover happens when a mobile moves from one cell to another. Handover algorithms will ensure that the old serving base station is replaced by a new base station while trying to minimize the effect on the ongoing communication process. Call admission, channel assignment and channel reservation determine how the calls are accepted and resources are assigned with the objectives of minimizing the overall interference level, reducing the outage probability for ongoing calls and exploring the capacity of the system to its fullest extent possible.

3.2 Resource management in TDMA/FDMA systems

Power control error usually is not as crucial in a TDMA/FDMA system as in CDMA systems. Power control in TDMA/FDMA systems usually takes into account the long-term path loss variation without instantaneous fading effects. Power control in a TDMA/FDMA system may be implemented using centralized or distributed controllers based on either received power level or signal to noise and interference ratio. However, a centralized controller is not feasible because of the huge overhead for information transferring and processing as well as the corresponding delay. An SIR based distributed power control algorithm can be found in [18]. The SIR for a given link can be written as

$$\Gamma_i = \frac{P_i}{\sum_{j \neq i}^{M} \frac{G_{i,j}}{G_{i,i}} P_j} = \frac{P_i}{\sum_{j=1}^{M} Z_{i,j} P_j - P_i} \tag{3.1}$$

where P_i is the i th mobile power; $G_{i,j}$ is the path gain of the i th mobile to the j th base station and $Z_{i,j} = G_{i,j} / G_{i,i}$. It has been shown in [18] that the largest Γ_i is achieved by choosing power control vector $\mathbf{P}$ $(p_1, p_2, \ldots, p_N)$ equal to the eigenvector corresponding to the largest eigenvalue $\lambda_{\max}$ of $Z_{i,j}$. And by doing so, the largest Γ_i is also the smallest Γ_i so that the SIR is balanced. Several distributed algorithms driving the Γ_i to its balanced value are illustrated below [18] where Γ_t is the target SIR

$$P_i^K = \kappa P_i^{K-1}(1 + \frac{1}{\Gamma_i^{K-1}})$$

$$P_i^K = \xi \frac{P_i^{K-1}}{\Gamma_i^{K-1}} \tag{3.2}$$

$$P_i^K = P_i^{K-1} \frac{\Gamma_t}{\Gamma_i^{K-1}}$$

TDMA/ FDMA employs a hard handover algorithm when mobiles move from one cell to another. Each base station monitors the signal strength of the mobiles it serves and that of other mobiles in its neighboring cells, and transfers the information to a mobile switching center (MSC). When the MSC detects a pilot signal drop below the handover threshold for a certain period of time, it initiates the hand off process. Second generation mobile systems such as GSM use mobile assisted handover (MAHO) where mobiles monitor the pilot signal strength from their neighboring cells. A mobile station initiates a handover process when the signal strength from its serving base station drops below the signal strength from another base station by a certain amount for a period of time.

Handover parameters include handover hysteresis defined as $\Delta = P_{handoff} - P_{drop}$ and waiting time T_w . These parameters must be set carefully to provide enough time for the handover operation while avoiding unnecessary handovers due to temporary fading effects and non-crossing mobile moving at the boarder. Dwell time, the time when a call remains within a cell, is one statistics helpful to set the hysteresis. Other statistics drawn

from the signals can also provide information such as speed of the vehicles to assist in the handover process.

Channel assignment for TDMA/FDMA systems can be classified into fixed channel assignment (FCA) and dynamic channel assignment (DCA). In FCA scheme, channels of fixed number are assigned to a cell and are reused by a certain pattern. FCA is not adaptive to traffic changes. In the DCA scheme, all channels belong to a set from which any can be assigned to a mobile. The DCA scheme is traffic adaptive since the number of channels assigned to a cell is not fixed. DCA algorithms are usually based on co-channel interference. The maximum SIR (MSIR) algorithm selects an unused channel with maximum SIR to serve the new call. Channel segregation lists the channels by their selectability and chooses the serving channel by following pre-established rules.

When a new call arrives, one chooses the channel with the highest selectability and senses the channel. If the signal power is below threshold level, one selects the channel to serve the call, meanwhile increasing its selectability by

$$P(i) = \frac{P(i)N(i)+1}{N(i)+1}, N(i) = N(i)+1 \tag{3.3}$$

where $N(i)$ is how many times channel i was accessed. Otherwise, one decreases its selectability by

$$P(i) = \frac{P(i)N(i)}{N(i)+1}, N(i) = N(i)+1 \tag{3.4}$$

The channel segregation method can reduce call interruption or deadlock and can also be combined with the DCA algorithm generating a better management scheme. Details of the above algorithms can be found in [18].

The new serving base station can treat the handover request as a new call request or as a priory request when it reserves a certain number of channels (guarded channel) for

handover purposes only. If there is no channel available, a new call is rejected. If there is no reserved channel available, the handover request is rejected and the call is dropped (handover failure). Sometimes, a reserved channel can be borrowed to serve a new call based on careful consideration of handover statistic so that such borrowing will not increase handover failure rate.

3.3 Power Control in CDMA Systems

The performance of CDMA systems depends greatly upon power control. Since all the mobile stations share the same broadband channel in a CDMA system, a single high power transmitter will severely degrade performance on all other ongoing communications. A CDMA system is more vulnerable to fading due to the same reason. Power control in CDMA therefore must keep signals received at the BS from all the users served in the cell as close as possible to the same level. Fast power control thus is indispensable for combating fading effects. Meanwhile power control should also keep the transmitting power as low as possible to save energy and reduce interference under the condition of satisfying performance requirements.

CDMA power control schemes should first equalize the power levels at the BS of the received signals from local (within the cell) mobile stations, and then balance the SIR among cells over the coverage area. CDMA power control schemes that only achieve the first goal are power level based while schemes also balancing SIR are SIR based. Power level based PC algorithms can be described similarly as the SIR based algorithms except that a target signal power level $PS_{t\arg et}$ is set instead of a target signal to noise ratio $SIR_{t\arg et}$. A detailed description of a power control algorithm is given below based on the WCDMA proposal, which is a SIR based algorithm.

In the WCDMA frequency division duplexing (FDD) scheme [31], two loops of power control mechanism are suggested for ordinary up-link transmission. Outer-loop power control sets the SIR target ($SIR_{t\arg et}$) according to the bit error rate (BER) or frame

error rate (FER) and QoS requirements. The inner-loop power control function adjusts the UE transmitting power so that the signal-to-interference ratio (SIR) is maintained at a given SIR target (SIR_{target}). Inner-loop fast power control is discussed in the following part of the thesis.

The serving cells' BS (cells in the active set) should estimate signal-to-interference ratio SIR_{target} of the received up-link DPCH (dedicated physical channel). The serving cells' BS then generates TPC commands and transmits the commands once per slot according to the following rule:

If $SIR_{est} > SIR_{target}$, *the TPC command to transmit is "0",*

If $SIR_{est} < SIR_{target}$, *the TPC command to transmit is "1".*

Upon receipt of one or more TPC commands in a slot, the user equipment (UE) derives a single TPC command TPC_{cmd} . The UE combines multiple TPC commands if more than one is received in a slot. Two algorithms are suggested to be supported by the UE for deriving a TPC_{cmd} . Which of these two algorithms is used is determined by a UE-specific higher-layer parameter, "PowerControlAlgorithm" (PCA), and is under the control of the UTRAN. The first algorithm is described below.

When a UE is not in soft handover, only one TPC command will be received in each slot. In this case, the value of TPC_{cmd} shall be derived as follows:

- If the received TPC command is equal to 0, then TPC_{cmd} for that slot is –1.
- If the received TPC command is equal to 1, then TPC_{cmd} for that slot is 1.

When a UE is in soft handover, multiple TPC commands may be received in each slot from different cells in the active set. The UE conducts a soft symbol decision W_i on each of the power control commands TPC_i, where i = 1, 2, … , N, with N greater than 1

the number of TPC commands from radio links of different radio link sets. The UE then derives a combined TPC command, TPC_{cmd}, as a function of all the N soft symbol decisions W_i, that is, $TPC_{cmd} = \gamma(W_1, W_2, \ldots W_N)$, where TPC_{cmd} can take the values 1 or -1. The function γ shall fulfill the following criteria

If the N TPC_i commands are random and uncorrelated with equal probability of being transmitted as "0" or "1", the probability that the output of γ is equal to 1 shall be greater than or equal to 1/(2N), and the probability that the output of γ is equal to -1 shall be greater than or equal to 0.5. Furthermore, the output γ of shall be equal to 1 if the TPC commands from all the radio link sets are reliably "1", and the output of γ shall be equal to –1 if a TPC command from any of the radio link sets is reliably "0".

It is very important to set a proper target SIR_{target} that meets the QoS requirement and at the same time is feasible. In a balanced SINR power control scheme, the target SIR_{target} should not exceed the upper limit $SIR_{\max}$ determined by the number of users in the system. Otherwise the scheme will fail. The achievable balanced target $SIR_{\max}$ is not a function of radio resources but of the number of users and the interference reduction capability (spreading gain in the system). However, SINR based power control should set the transmitting power of every mobile to its minimum satisfying the performance requirement rather than the maximum value regardless of the system load c/pg (see Equation 3.5). It also balances the SINR and reduces interference accordingly. As a result, the system capacity is further increased. SIR_{target} is set at RNC by jointly considering the current system load and the QoS requirements. The following example shows how power control works to reduce the transmitting power in a single cell [33].

$$SIR_{target} = \frac{P}{\frac{c}{pg}P + N} \quad ; \quad P = \frac{N \times SIR_{target}}{1 - SIR_{target}\frac{c}{pg}} \tag{3.5}$$

where P is the received power from one mobile, N is the power of white noise, c is the number of interferers (number of user deducted by 1), pg is the processing gain. It is obvious that no matter what P is, $SIR_{t\arg et}$ cannot exceed c/pg. Under this condition, Figure 3.3 below shows the power level necessary to achieve certain SIR with the increase of the system load c/pg.

It is clear from Figure 3.1 that pursuing a high $SIR_{t\arg et}$ close to its upper limit requires a high level of transmitting power. Exceed power is defined as the ratio of the

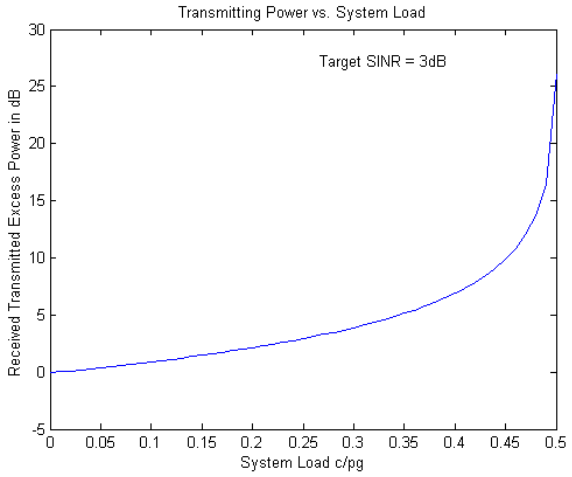

Fig 3.1 Transmitting Power vs. System Load

required power level with more than one interferers in the system to that with just one interferer. The absolute value depending on the noise power level is $P = P_{excess} + P(c = 1)$.

It is difficult to set a target SIR and pursue a multi-cell SIR balancing because the traffics in those cells vary. On the other hand, balancing the SIR can not improve the performance considerably if the system loads in different cells are close to each other.

3.4 Handover in CDMA Systems

CDMA systems employ soft handover algorithms that enable uninterrupted communications during the handover process. Since all the mobiles share a same broadband channel, every mobile in the soft handover region can communicate to more than one neighboring BS at the same time. When a mobile moves from one cell to another, it does not have to drop the link to the old BS before establishing one to the new BS. Soft handover provide a seamless handover process as well as macro-combining to mobiles in handover region.

Both IS-95A and WCDMA handover algorithm use CPICH (common pilot channel) pilot E_c / I_0 (definition of E_c / I_0 can be found in [1] p115) as the handover measurement. Handover algorithm in cdmaOne (IS-95A) can be illustrated as:

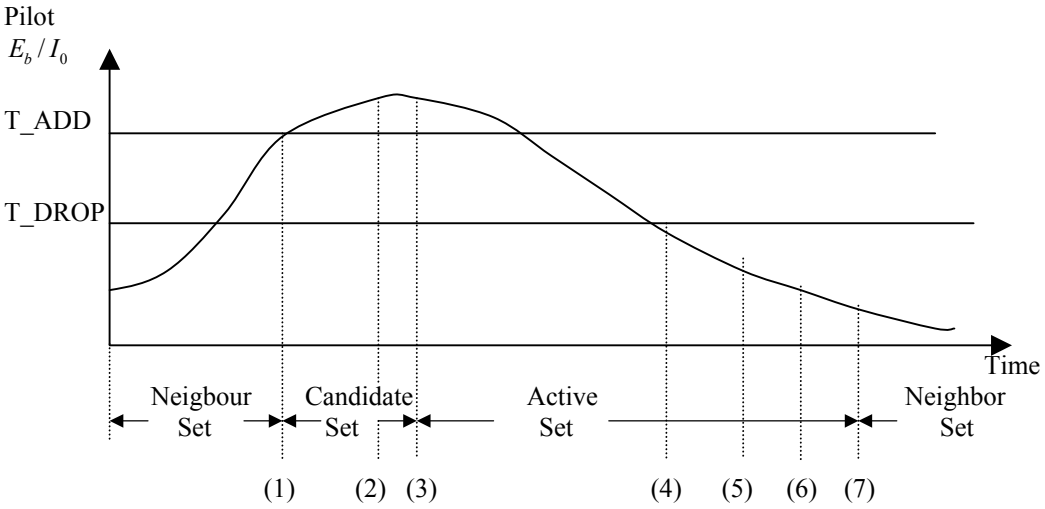

. Pilot strength exceeds T_ADD. Mobile station sends a Pilot Strength Measurement Message and transfers the pilot to the candidate set
. Base station sends a Handover Direction Message.
. Mobile station transfers the pilot to the active set and sends a Handover Completion Message.
. Pilot strength drops below T_DROP. Mobile station starts the handover drop timer.
. Handover drop timer expires. Mobile station sends a pilot Strength Measurement Message.
. Base station sends a handover Direction Message.
. Mobile station moves the pilot from the active set to the neighbor set and sends a Handover Completion Message.

Fig 3.2 IS-95A Handover Process

The range (T_DROP, T_ADD) or its corresponding area at the cell boundary is called the soft handover region (SR). It is obvious that handover rate increases with the increase of SR.

Handover algorithm in WCDMA [32] can be illustrated as

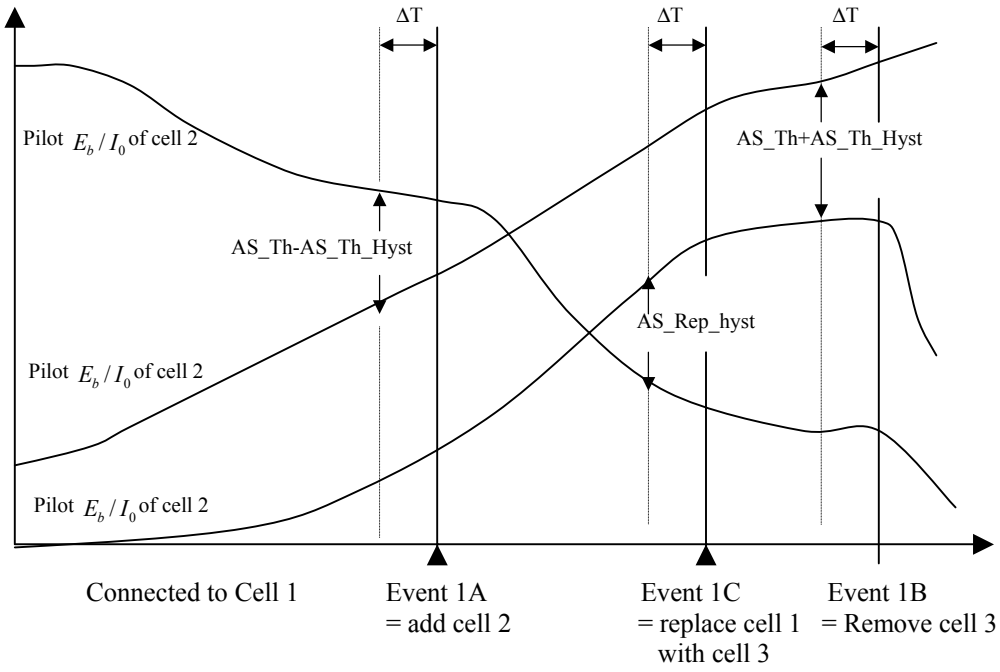

- If Meas_Sign is below (Best_Ss - As_Th - As_Th_Hyst) for a period of ΔT, remove the worst cell in the Active Set.
- If Meas_Sign is greater than (Best_Ss - As_Th + As_Th_Hyst) for a period of ΔT and the Active Set is not full, add Best cell outside the Active Set in the Active Set.
- If Active Set is full and Best_Cand_Ss is greater than (Worst_Old_Ss + As_Rep_Hyst) for a period of ΔT, add Best cell outside Active Set and Remove the worst cell in the Active Set.

Where

AS_Th: Threshold for macro diversity (reporting range);
AS_Th_Hyst: Hysteresis for the above threshold;
AS_Rep_Hyst: Replacement Hysteresis;
ΔT: Time to Trigger;
AS_Max_Size: Maximum size of Active Set.
Best_Ss :the best measured cell present in the Active Set;
Worst_Old_Ss: the worst measured cell present in the Active Set;
Best_Cand_Ss: the best measured cell present in the monitored set.
Meas_Sign :the measured and filtered quantity.

Fig 3.3 WCDMA Handover Process

WCDMA handover algorithm uses relative thresholds while IS-95A and IS-95B use absolute thresholds. All of these algorithms depend on the accurate measurement of the pilot E_c / I_0. E_c / I_0 can be obtained by filtering, which smooth the fading effect at the mobile station. Longer filtering periods will generate more precise measurement, but increases handover delay.

3.5 Call Admission Control in CDMA Systems

Network needs to know whether there is enough resource available to accommodate more users when a new call request arrives. Call admission control (CAC) must check not only the availability of those resources but also the effect to the system from the increased interference if the new call is admitted. A new call request must be denied if the admission will degrade the quality of any ongoing communications to an unacceptable level.

The total power received by a base station (current interference) can be used as the current interference level. The CAC estimates the total interference level assuming that the new call is admitted. The CAC rejects the call if the interference is higher than a certain threshold. Radio Network Controller (RNC) obtains the estimated interference levels from all of its cells and decides whether an incoming call be accepted or not. The following CAC algorithm is based on [34], [35]. Assuming that the pilot from BS k is the strongest and $h \in \Omega(k)$ is a nearby BS, the algorithm can be described as follows.

The MS measures $P_m(k)$ and $P_m(h)$, the received pilot strength from BS k and BS h respectively. $P(k)$ and $P(h)$ are the transmitted pilot strengths at BS k and h respectively. MS thus can compute the path losses as $l_m(k) = P_m(k) / P(k)$ and $l_m(h) = P_m(h) / P(h)$. The ratio of the path loses is $L_m(h,k) = l_m(h) / l_m(k)$. BS k periodically measures its reverse link SIR_k and updates the target signal power $P_t(k)$, while BS h measures SIR_h and updates $P_t(h)$. The information of SIR_k, SIR_h, $P_t(k)$,

$P_t(h)$ and $L_m(h,k)$ is transferred to RNC. RNC determines whether to admit the new call by the following rule.

The residue capacity R is estimated as

$$R = \begin{cases} \min\{R(j) \mid j = k \text{ or } j \in \Omega(k)\}, & \text{if } R(j) > 0\}; \\ 0, & \text{otherwise} \end{cases} \tag{3.6}$$

where

$$R(j) = \begin{cases} \left| \frac{1}{SIR_{TH}} - \frac{1}{SIR_k} \right|, & \text{if } j = k; \\ \left| \frac{1}{SIR_{TH}} - \frac{1}{SIR_h} - \frac{1}{L_m(h,k)\frac{P_t(h)}{P_t(k)}} \right|, & \text{if } j \in \Omega(k); \end{cases} \tag{3.7}$$

If $R > 0$, the call can be admitted. Otherwise, it is rejected.

The SIR threshold SIR_t is bounded by

$$SIR_{th} \le \left(n_h + R_h - 1 + \sum_{j \in \psi, j \ne h} \sum_{i=1}^{n_j} \left(\frac{r_{ij}}{r_{ih}} \right)^{\alpha} \times 10^{\zeta_{ih} - \xi_{ij}/10} + L_m(h,k)\frac{P_t(h)}{P_t(k)} \right)^{-1} \tag{3.8}$$

where r_{mh} is the distance from mobile m to BS h, and ξ_{mh} represents the shadowing effect. α is the path loss coefficient. n_h is the current number of mobiles in cell h and R_h is the residue capacity.

3.6 Capacity Reservation/Channel Assignment in CDMA systems

Capacity (channel) reservation works together with CAC. Handover requests in cellular systems are considered as having higher priority than new call requests since dropping an ongoing call is more annoying than rejecting a new call. A certain amount of resources must be reserved for handover.

An interference based channel assignment scheme for DS-CDMA cellular systems is proposed in [35]. The scheme reserves capacity by setting up a handover interference margin HIM. The algorithm is described below.

The bit energy to noise (including the interference) power spectral density ratio E_b / N_0 is given by

$$E_b / N_0 = \frac{S/(R \times \alpha)}{N_t + (N-1) \times S/W} \tag{3.9}$$

where N is the number of users in the cell; S is the received signal power; R is the bit rate; W is the chip rate; N_t is the thermal noise power spectrum density; and α is the voice activity factor. Rearranging the equation and replacing S with S_N, we have the received signal power required for supporting N users in the cell as

$$\begin{aligned} S_N &= \frac{N_t \times W}{\frac{W/(R\alpha)}{E_b/N_0} - (N-1)} \\ &= \frac{N_t \times W}{G - (N-1)} \qquad \text{where} \quad G = \frac{W/(R\alpha)}{E_b/N_0} \end{aligned} \tag{3.10}$$

Including the interference from other cells I_o, the total received power P_N should be

$$\begin{aligned} P_N &= N_t \times W + N \times S_N \\ &= \frac{G+1}{G+1-N}(N_t \times W + I_o) \end{aligned} \tag{3.11}$$

Thus,

$$\begin{aligned} P_{N+1} &= \frac{G+1}{G+1-(N+1)}(N_t \times W + I_o) \\ &= \frac{G+1-N}{G-N} P_N \end{aligned} \tag{3.12}$$

This result is similar to that from SIR balanced power control (section 3.2) by that SINR is kept constant and the target SINR (E_b / N_0) cannot exceed the system capacity. In addition, the power required increases faster when the system load approaches the system capacity.

TIM is defined as the total interference margin. TIM must be set to satisfy the target SINR (or E_b / N_0) with reasonable received signal power level. TIM can be set as $TIM = \beta G \times (N_t \times W)$ where β denotes the maximum system load. Current interference margin CIM is defined as equal to P_{N+1} in equation (3.12). Handover interference margin HIM is defined as

$$HIM = \frac{G + 1 - N}{G - N - R} P_N \tag{3.13}$$

where R represents the reserved capacity for handover. The capacity reservation scheme (combined with CAC) is illustrated in Figure 3.4.

The capacity reserved by the above approach is fixed. More complex are adaptive channel reservation schemes that adjust the reserved capacity according to handover statistics.

An adaptive capacity reservation scheme proposed in [37] explores explicitly the handover statistics. A new threshold T_RSRV below T_ADD is set to measure the likelihood that a mobile moves into the handover region. If the pilot from a neighboring BS becomes stronger than T_RSRV but lower than T_ADD, the mobile asks the corresponding BS to reserve a channel for a possible handover. If the pilot becomes stronger than T_ADD, soft handover happens and the reserved channel is used. If the pilot strength drops below T_RSRV for a predefined period, the reserved capacity is released.

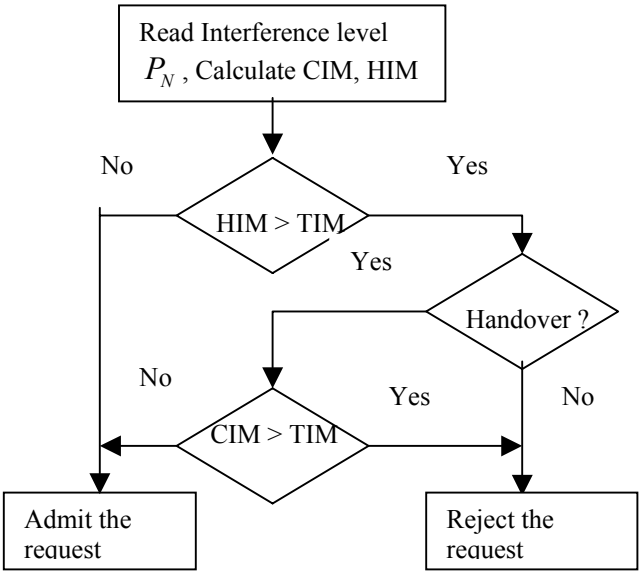

Fig 3.4 Channel Reservation Scheme

Another channel assignment scheme proposed in [38] reduces the soft handover region by increasing the T_DROP. Therefor, it not only releases the system capacity used in actual handover activities but also the capacity reserved for possible handovers.

Chapter 4

Simulation Model on SA and RRM in CDMA Systems

This chapter describes the simulation model developed for studying smart antenna and radio resource management in CDMA systems. The simulator is developed according to the IS-95 and W-CDMA proposals, but with simplifications. The up-link scenario of a multi-cell cellular system is simulated with omni-directional or smart antennas at the base stations. This simulator consists of six integrated components including a mobility and geographic model, an event simulator, a channel simulator, a signal processor, a smart antenna processor and a resource management model.

4.1 General Description of The Simulator

Figure 4.1 illustrates the general block diagram of the simulator. A brief description is given below about the functions of the blocks.

The mobility and geographical model generates the mobile speeds and the directions according to certain probability distributions; calculates the mobile locations accordingly; and calculates the path gains and AoA according to the mobile station (MS) locations. The event simulator generates and schedules events including the call arrivals and call departures, system status updates and mobile direction updates. The channel simulator generates Rayleigh fading data; simulates multipath effect and generates received signals from the channels. At the transmitters, the signal processor generates and spreads the data; performs pulse shaping, and executes power control command. At the receivers, the

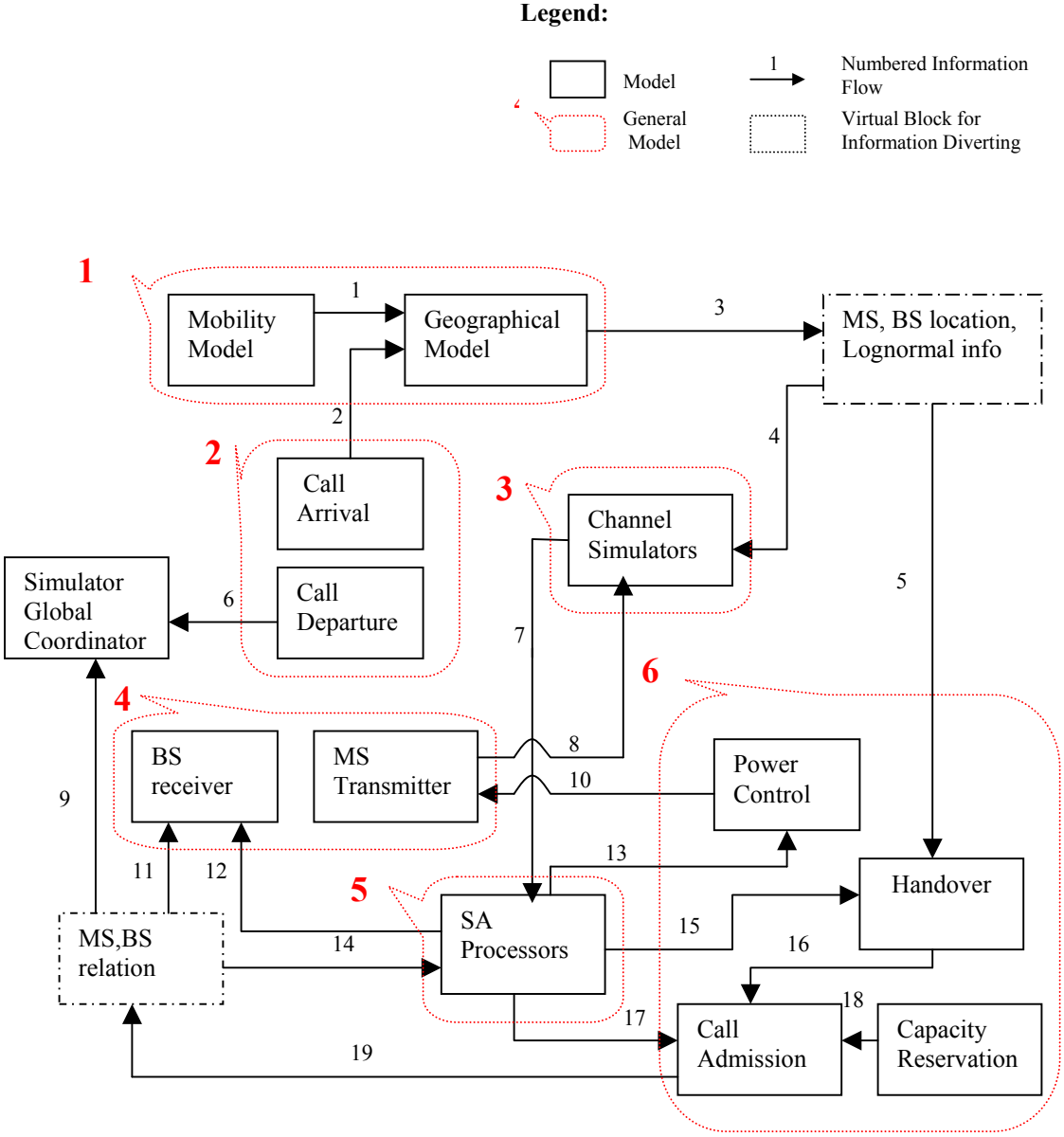

Information Flows:

1. MS locations
2. path gains, AoA
3. MS locations
4 Path gains
5. Path gains (pilot strengths)
6. MS IDs.
7. Received signals
8. Transmitted signals
9. MS's Serving BS
10. TPC
11. MS's serving BS
12. Array weights
13. Beamformer output of pilots
14. MS's serving BS
15. Beamformer output of all received signals
16. Handover requests
17. Same as 15
18. Reserved capacity
19. Admission decision

Fig 4.1 General Block Diagram of The Simulator

signal processor despreads the received signals and performs RAKE combining. The smart antenna processor generates combining weights and processes received signals accordingly. The resource management model generates power control commands, performs handover processes, call admission control and capacity reservation.

In addition, the simulator keeps tracking the records that match the mobile station IDs to handover active sets (AS), fading curves, serving base station IDs, power control commands, etc. The system parameters are defined in the preprocessor.

4.2 Mobility and Geographic Model

The mobility and geographic model is used to determine the mobile status whenever a new call arrives or the mobile status is updated. The mobility model updates the mobile station locations according to its speeds and directions. The geographic model determines the base station locations as well as adjusts the mobile locations by a toroidal structure. It also determines the distances and AoA from the mobile stations to the base stations.

The mobile stations are assumed to have constant speed during the call. However, the speed of each mobile is generated randomly following the half cosine probability density function (PDF). The half cosine PDF is illustrated in Figure 4.1. The range of the mobile speeds is from 0 to $v_{\max}$.

Mobile directions are also random variables following the cosine distribution. The mean values are the current directions. The distribution is illustrated below where K is the normalizing factor such that the total probability is one.

$$p_\theta(\theta) = \begin{cases} K\cos(\theta - \theta_{curent}), & \theta_{\text{current}} - \pi < \theta \le \theta_{current} + \pi \\ 0, & \text{Otherwise} \end{cases} \tag{4.1}$$

The two PDFs could be shown as

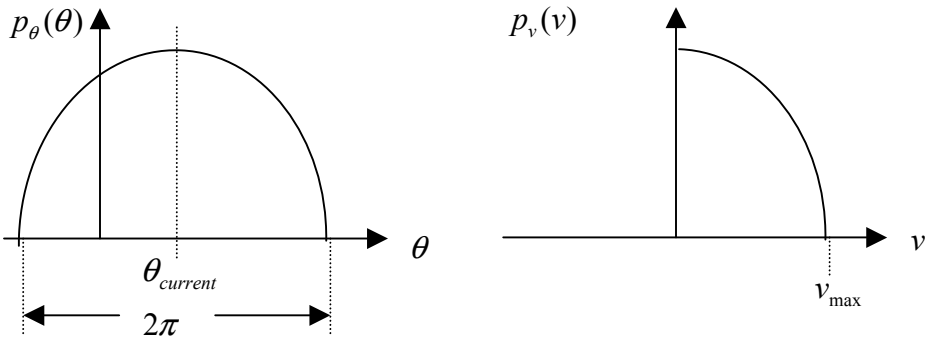

(a) Mobile Direction **(b)** Mobile Speed

Fig 4.2 PDF of Mobile Directions and Speeds

The geographic model includes a layout of a hexagonal cell coverage area and the corresponding BS locations, and the adjustment of the MS and BS locations according to the toroidal structure.

Cell design have significant impact on resource management such as power control and handover. Compared to other cell structures like square cells [42], hexagonal cells most closely resemble the natural isotropic radio radiation pattern.

In Figure 4.3, A refers to the intersecting point of the cells. It is easy to see that the overlapping areas of square cells are much larger than that of hexagonal cells. The large overlapping may causes the increase of soft handover rate and transmitting power, which means more resources as well as interference.

Also seen is that there are always some overlaps between the cells due to the isotropic radiation nature of the antennas. For example, mobile M1 and M2 have the same distances to BS2. Let us assume that the handover threshold is the pilot

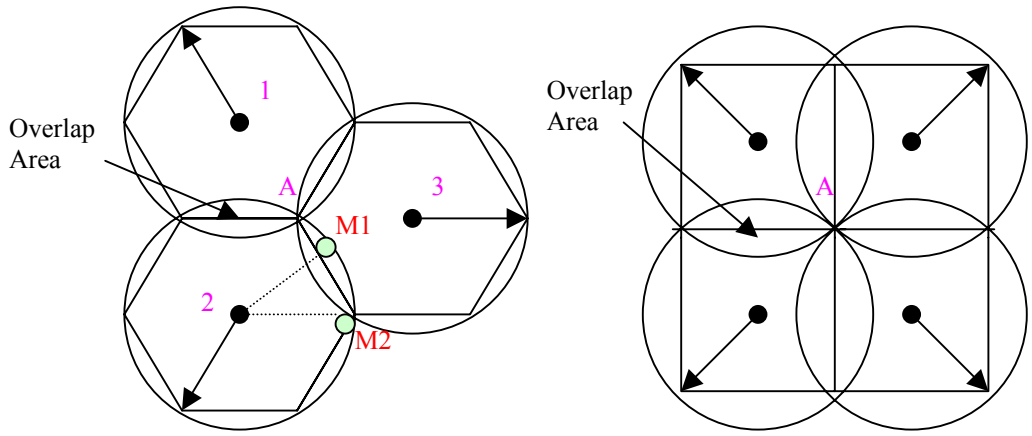

(a) Hexagonal Cell **(b)** Square cell

Fig 4.3 Overlapping Area of Cell Styles

strength at the farthest boarder. M1 and M2 will receive the pilots of same strength from BS2. However, mobile M1 is over the boarder into cell 3 while M2 is not. This means that the pilot strength M1 receives from BS3 is above the handover threshold, but the pilot strength M2 receives is not. Therefore, M1 is in soft handover while M2 is in regular communications. On the other hand, although reducing the cells size further will eliminate the soft handover area, it creates a spot at the intersection area where an MS cannot be served by any base stations.

Figure 4.4 shows the coverage area and the layout of the cells. O_c and O_a denote the cell centers and the area centers respectively. The area is covered by L cells horizontally and J cells vertically. The widths are x_width and y_width accordingly. The cells are increasingly numbered from the left lowest one to the right highest one. The Cartesian coordinates of cell centers are calculated by the following process.

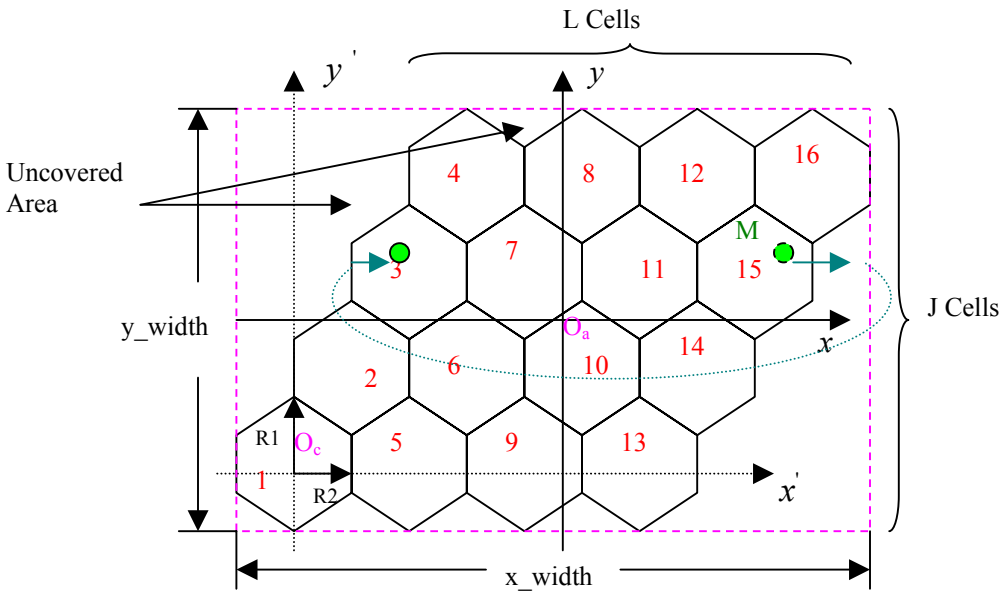

Fig 4.4 Coverage Area and Cell Layout

Assuming that the area center is O_c , the left lowest cell center, the centers of the cells shall be (x, y) such that

$$x(i,j) = (j-1)\times R2 + (l-1)\times 2R2$$
$$y(i,j) = (j-1)\times \frac{3}{2} R1 \qquad (4.2)$$

The location of the cell centers can be obtained by moving the origin of the coordinate system to O_a. i.e. deducting (x, y) with $0.5x\_width$ and $0.5y\_width$ respectively.

Toroidal structure is created by seaming up the boarder of the coverage area as illustrated in Fig 4.5. A mobile , ex. M1, will stay in the area no matter how it moves on a toroidal structure. In addition, the distance of two locations will change when a planar area is converted to its toroidal structure as illustrated in Fig 4.5

The creation of a planar cellular coverage area is illustrated in Figure 4.4. We then convert it into a toroidal circular pipe on o which a mobile cannot move out. Since every

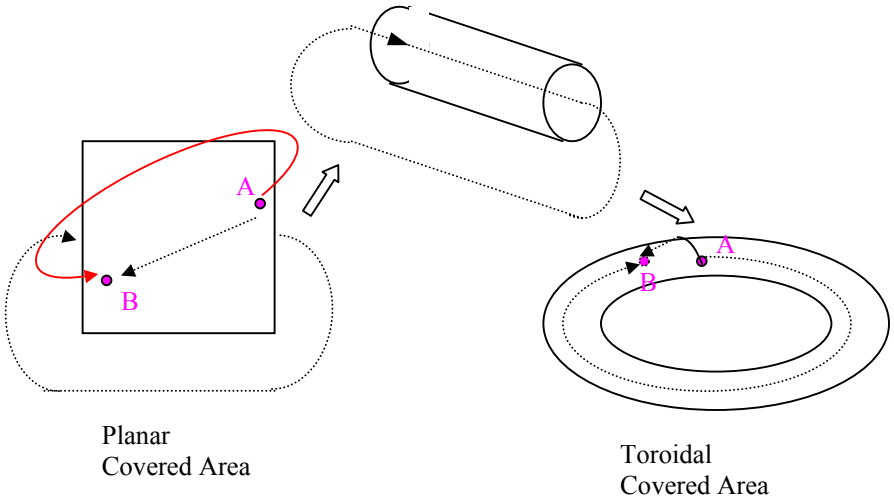

Fig 4.5 Concept of Toroidal Structure

cell on the circular pipe has the same neighboring situation (6 neighboring hexagonal cells), a small number of cells are enough to ensure the fidelity of the simulation. We also do not need to distinguish boarder cells from inner cells.

However, the simple converting scheme shown in Figure 4.5 will fail because that the actual coverage area is not square as shown in Figure 4.3, and some of the areas can not be covered. The converting method should seam the somewhat zigzagging boarder of the actual coverage areas. A new method illustrated by Figure 4.6 is discussed below.

In Figure 4.6 (a), cluster A is the coverage area and cluster B to G are the auxiliary virtual neighboring clusters used for toroidal adjustment. The centers of the neighboring cluster can be calculated by the following equations.

$$\begin{aligned} x(E) &= 2L \times R2 & x(D) &= J \times R2 & x(C) &= J \times R2 - 2L \times R2 \\ y(E) &= 0 & y(D) &= J \times 1.5R1 & y(C) &= J \times 1.5R1 \end{aligned} \tag{4.3}$$

$$\begin{aligned} x(B) &= -2L \times R2 & x(G) &= -J \times R2 & x(C) &= -(J \times R2 - 2L \times R2) \\ y(B) &= 0 & y(G) &= -J \times 1.5R1 & y(C) &= -(J \times 1.5R1) \end{aligned}$$

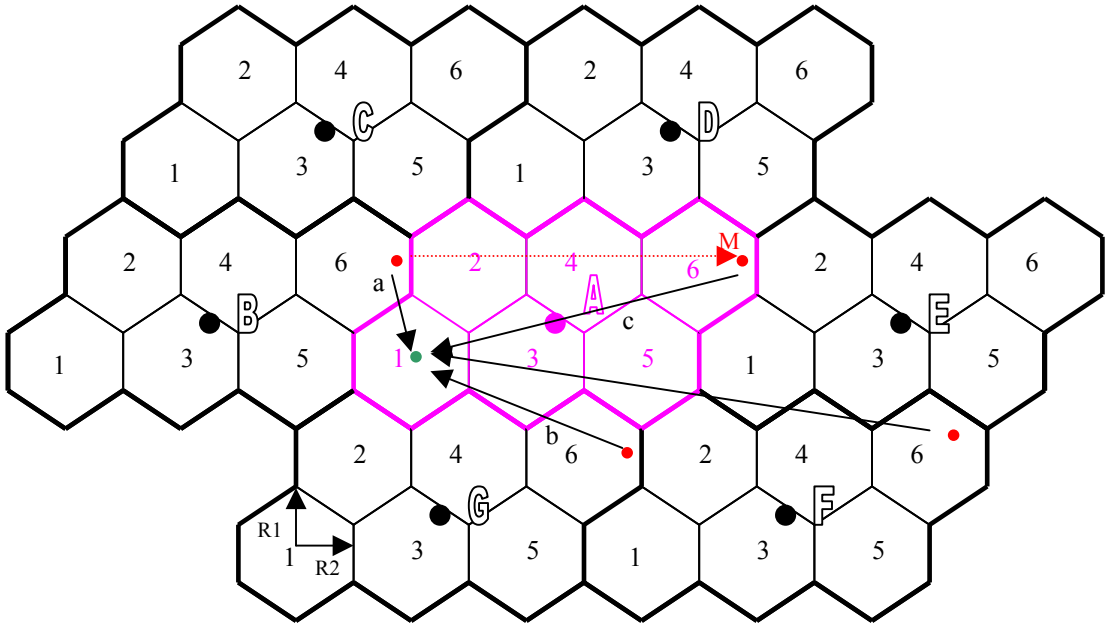

(a)

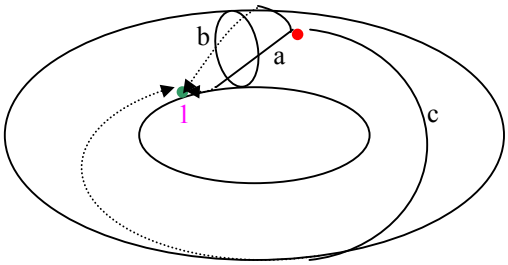

(b)

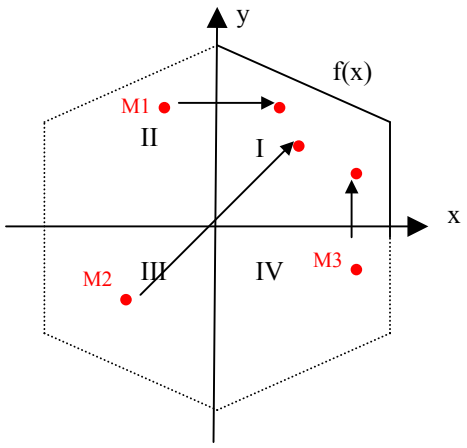

(c)

Fig 4.6 Toroidal Adjustment of Mobile Locations and MS to BS Distances

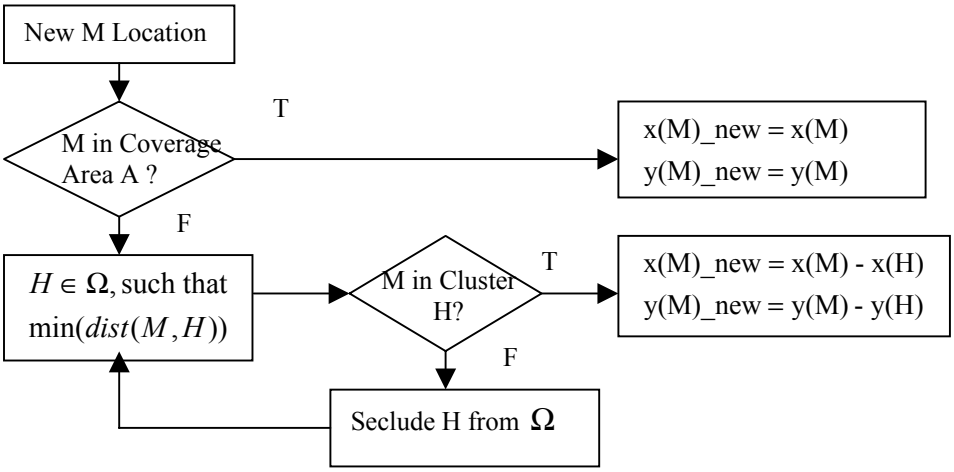

Fig 4.7 Mobile Location Adjustment

By toroidal adjustment, mobile M is relocated into cell 6 of the coverage area A when she moves out off the left boarder of cell 2. The distance from mobile M to base station 1 is the shortest of the distance a, b, and c. The detail algorithm is discussed below.

Mobile locations are checked and adjusted periodically. When a mobile moves out of the coverage area, the toroidal adjustment first determines which neighboring cluster it moves in and relocates it to the corresponding location in the coverage area. The relocating algorithm is illustrated below where Ω represents the neighboring cluster sets consisting of B-G.

The judgment of whether mobile M is in a certain cluster is made by the following steps illustrated by Figure 4.6 (c).

1. find the nearest cell center in the cluster to the mobile M
2. mapping the location of M into the first quadrant of that cell
3. M is in the cluster if $y(M) < f(x(M))$, otherwise not

After the adjustment of the mobile location, its distance to a base station illustrated in Figure 4.6 (a) is determined by the following algorithm.

In addition to the mobile location in coverage area A, other locations are obtained by mapping the mobile location to the cells with the same ID in the opposite clusters. In Figure 4.6 (a), M in cell 6 of coverage cluster A is mapped to cell 6 of cluster B and cell 6 of cluster G. The set Λ consists of the opposite clusters together with the coverage cluster.

The opposite clusters are chosen according to the following table.

Table 4.1 Cluster Sets for Distance Adjustment

Mobile Location (Quadrant)	I	II	III	IV
Opposite Clusters Set	(B, F, G)	(E, F, G)	(D, E, F)	(B, C, D)

The shortest distance among those from the mobile or its mapped locations to the BS is the distance from the mobile to the BS in toroidal structure. Such as in Figure 4.6 (a), arrow a among a, b ,c represents the distance.

In Figure 4.6 (a), M in cell 6 of A and its mapped locations in cell 6 of (B,F,G) are at the same location by toroidal structure. The multiple distances come from the different route and directions by which the distances are calculated. This observation is illustrated in Figure 4.6 (b).

4.3 Event Simulator

Four types of events including system status update, mobile direction change, call arrival, and call departure are generated and scheduled according to the methods

proposed in [39]. An event simulator consists of an events generator, an events scheduler and an events handler as shown in Figure 4.2.

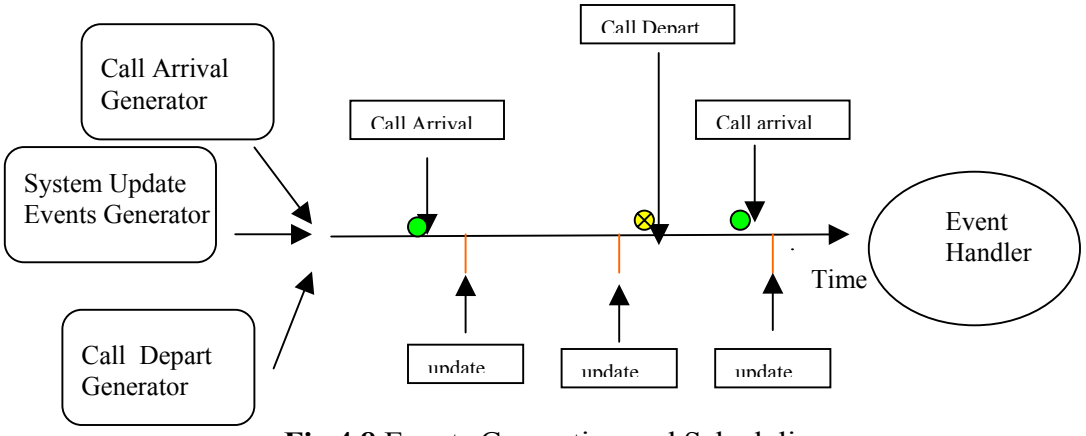

Fig 4.8 Events Generating and Scheduling

Event generator generates the events. The call arrivals are assumed following Poisson processes and the call departures have their service time exponentially distributed. The inter-arrival time τ of the new calls follow the exponential distribution as

$$p_T(\tau) = \lambda e^{-\lambda\tau} \tag{4.4}$$

where λ is the mean arrival rate. The service time s (call duration) also follow the exponentially distributed as

$$p_S(s) = \mu e^{-\mu s} \tag{4.5}$$

where μ is the mean call departure rate. The average service time is $H = 1/\mu$.

The processing of the call arrivals and departures by the system can be view as a M/M/m/m queue which has poison arrival (Markov), exponential departure times (Markov), m servers and the system capacity supporting m customers. Assuming block call clear, memoriless arrivals and infinite users, the theoretical blocking probability is given by Erlang B formula [40] as

$$P_B = \frac{A^C C!}{\sum_{k=0}^{C} A^k k!} \tag{4.6}$$

where $A = \lambda H$ is the offered traffic measured in Erlang and C is the number of available channels.

System status update is performed at a fixed rate. After every time interval T_s, the mobile statuses are updated and handovers are checked.

The events scheduler saves into a waiting list the type of a new event and its time stamp set as its arriving time. It picks up from the waiting list an event A with the smallest time stamps for processing. After calling the event handler, it deducts the time stamp T_A from the time stamps of all the events in the waiting list. Any event with a non-positive time stamp will be dropped from the waiting list.

Events handler will call the functions such as call arrival, call departure or system update according to the type of the events. Call arrival function will find the candidate serving BS and run CAC. Call departure function will delete the information of the departing mobile from certain status tracking lists. System update function will update the mobile locations and check possible handovers.

4.4 Channel Simulator

The channel simulator generates multipath profiles and the corresponding Rayleigh fading curves. The multipath profiles are assumed uniform over the coverage area. Each multipath component between a MS and a BS has a unique fading curve.

WCDMA systems adopt a chip rate as 3.84Mcps and are wideband systems where all the multipath components are resolvable. The method from [41] is used to generate multipath profiles. Vehicular outdoor channel profile is used to characterize the channel

model. The mobile speed is assumed to be 120 miles per hour and the corresponding Doppler spreads is 213 Hz. The power delay profile (PDF) is shown in Table 4.2.

Table 4.2 Vehicular Outdoor Channel PDF

Delay (ns)	0	310	710	1090	1730	2510
Avg. Power	0	-1	-9	-10	-15	-20

The continuous time based PDF is then converted to the discrete PDF using ray splitting method below.

Each multipath component (ray) is split into two rays at the adjacent sampling point by the following rule. The sum of the power of the split components is equal to that of the original component. The power of each split component is inversely proportional to its distance to the original component. If there are more than two split components at the same sampling point, they are added together as one discrete multipath component. All the discrete multipath components are normalized such that the channel does not change the signal energy.

One independent Rayleigh waveforms is generated for each multipath components using Clark's model [40]. A Doppler filter is created according to the Doppler spreads. Two complex Gaussian random variables are generated independently in frequency domain and passed through the Doppler filter which correlates the samples. The filtered samples are converted into time domain by inverse fast Fourier transformation (IFFT). The real parts of the outputs are used respectively as the real and imaginary parts of the Rayleigh fading coefficients. The complex curve has amplitudes following Rayleigh distribution and phases uniformly distributed between 0 and 2π.

Fading data should be continuous across the frames or slots. A large volume of fading data is generated so that the fading curves are continuous over a long period of time. Then, the curve is reused from the start. Interpolating and zero-order holding are used to generate interval sampling points of the fading data. A large number of fading curves are generated and stored. One fading curve is assigned to one multipath components of each existing link from a MS to a BS. Each time a new call arrives, free fading curves by the number of multipath components times the number of BS are selected from the pool and assigned to that MS.

Each channel from a MS to a BS is a linear time varying filter as in Figure 4.9 where $Z^{-\tau_i}$ denotes the delay of τ_i samples, c_i represents the strength of the multipath component and r_i is the Rayleigh waveform. White Gaussian noise is added at the receiver. The noise power is calibrated by the following process.

The carrier to noise power ratio is

$$\frac{C}{N} = \frac{E_b \times R_b}{N_0 \times W} \tag{4.7}$$

where C, N, R_b, W are signal power, noise power, bit rate, and chip rate respectively. Therefore, the noise power can be obtained as

$$\begin{aligned} N &= C \times \frac{W}{R_0} \Big/ \frac{E_0}{N_0} = C \times S_f \Big/ \frac{E_0}{N_0} \\ &= S_f \Big/ \frac{E_0}{N_0} \qquad \text{when C} = 1 \end{aligned} \tag{4.8}$$

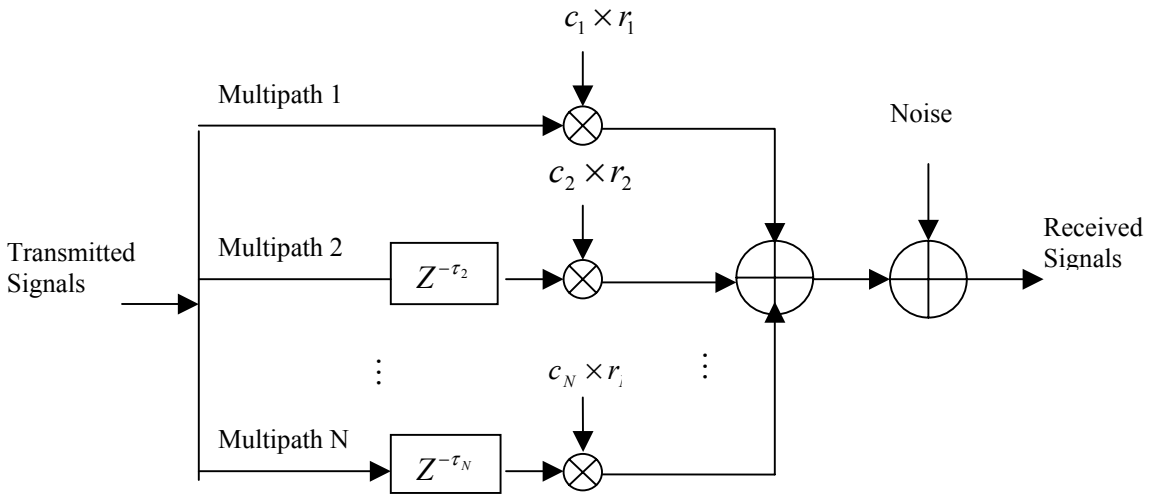

Fig 4.9 Time Varying Channel

4.5 Signal Processor

The signal processor includes a transmitter and a receiver. WCDMA physical layer structure is described in [43]. The up-link transmitting and receiving schemes are discussed below.

WCDMA up-link dedicated physical channels (DPCH) include several dedicated physical data channels (DPDCH) and one or none dedicated physical control channel (DPCCH). Spreading is applied to the physical channels in two steps. Channelization spreads the data in each channel with Orthogonal Variable Spreading Factor (OVSF) code with a gain factor. The spread DPDCH data are transmitted in I or Q channels and DPCCH data is transmitted only in Q channel. Scrambling code for UE identification are then multiplied to the complex data. The scrambled data is modulated as QPSK signals with real part into I channel and imaginary part into Q channel. The spreading and modulation processes are illustrated in Figure. 4.7. In simulation model, one DPDCH channel with no DPCCH is simulated for each user with the gain factor $\beta_d = 1$. Rectangular pulse shaping is used instead of standardized raise cosine filter with rolloff factor as 0.22.

The channelization codes are generated according to the following rule.

$$C_{ch,1,0} = 1 \tag{4.9}$$

$$\begin{bmatrix} C_{ch,2,0} \\ C_{ch,2,1} \end{bmatrix} = \begin{bmatrix} C_{ch,1,0} & C_{ch,1,0} \\ C_{ch,1,0} & -C_{ch,1,0} \end{bmatrix} = \begin{bmatrix} 1 & 1 \\ 1 & -1 \end{bmatrix} \tag{4.10}$$

$$\begin{bmatrix} C_{ch,2^{n+1},0} \\ C_{ch,2^{n+1},1} \\ C_{ch,2^{n+1},2} \\ C_{ch,2^{n+1},3} \\ \vdots \\ C_{ch,2^{n+1},2^{n+1}-2} \\ C_{ch,2^{n+1},2^{n+1}-1} \end{bmatrix} = \begin{bmatrix} C_{ch,2^n,0} & C_{ch,2^n,0} \\ C_{ch,2^n,0} & -C_{ch,2^n,0} \\ C_{ch,2^n,1} & C_{ch,2^n,1} \\ C_{ch,2^n,1} & -C_{ch,2^n,1} \\ \vdots & \\ C_{ch,2^n,2^{n-1}} & C_{ch,2^n,2^{n-1}} \\ C_{ch,2^n,2^{n-1}} & -C_{ch,2^n,2^{n-1}} \end{bmatrix} \tag{4.11}$$

$C_{ch,i,j}$ refers to the j th channel code with spreading factor (SF) as i. OVSF code preservers the orthogonality between the signals in any two physical channels of a user. Codes are selected in the following steps.

1. The DPDCH channel is always spread by $C_c = C_{ch,256,0}$
2. When only one DPDCH exist, it is spread by $C_{d,1} = C_{ch,SF,k}$ where SF is the spreading factor and $k = SF/4$.
3. For multiple DPDCH, all DPDCH have the spreading factor $SF = 4$, $C_{d,n} = C_{ch,4,k}$ where $k = 1$ if $n \in (1,2)$, $k = 2$ if $n \in (5,6)$, and $k = 3$ if $n \in (3,4)$

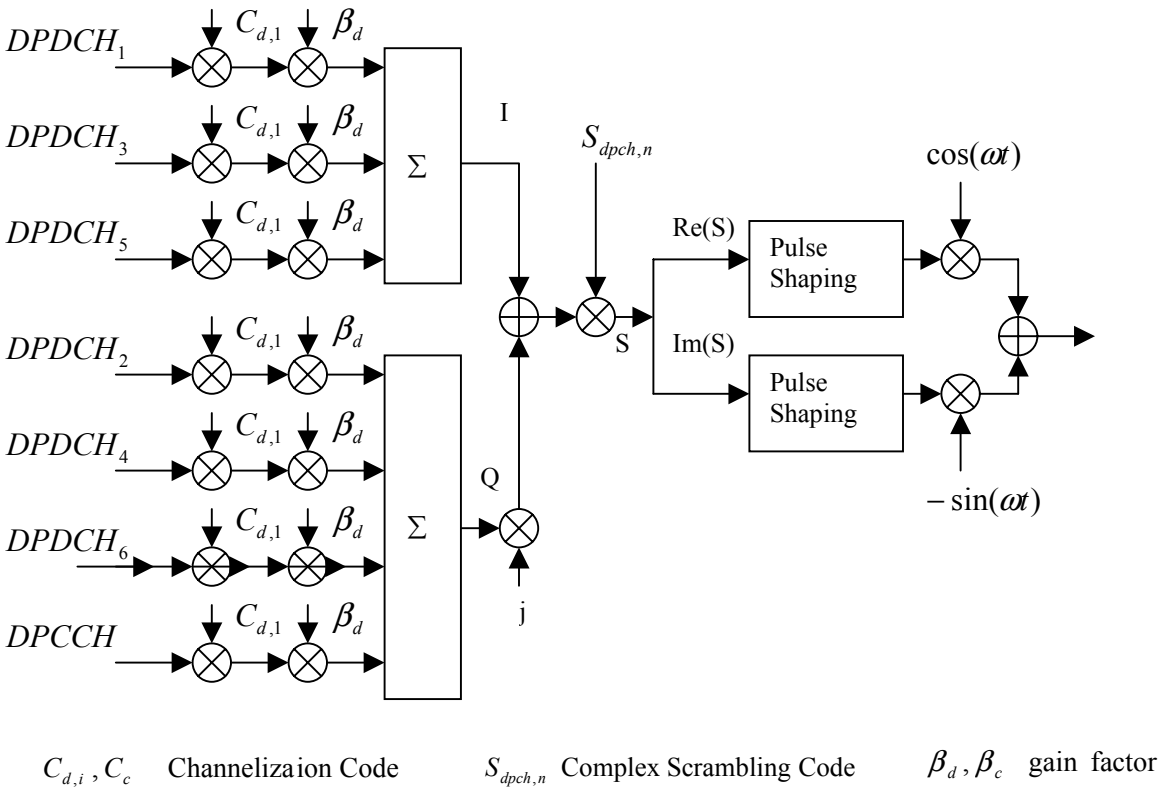

Fig 4.10 WCDMA Physical Channel Spreading and Modulation

The long scrambling sequences $c_{long,1,n}$ and $c_{long,2,n}$ are constructed from the modulo 2 sum of two binary *m*-sequences generated from two generator polynomials of degree 25. Let *x* and *y* be the two *m*-sequences respectively. The *x* sequence is constructed using the primitive polynomial $X^{25} + X^3 + 1$. The *y* sequence is constructed using the polynomial $X^{25} + X^3 + X^2 + X + 1$. The resulting sequences thus constitute the segments of a Gold sequences set. Sequence $c_{long,2,n}$ is a 16777232 chip shifted version of sequence $c_{long,1,n}$. Scrambling code generation is discussed in detail as follows.

Let $n_{23}\cdots n_0$ be the 24 bit binary representation of the scrambling sequence number n with n_0 denoting the least significant bit. The x sequence is denoted as x_n and depends on the scrambling sequence number n . Next, let $x_n(i), y(i)$ denote the i th symbol of the sequence x_n and y respectively. The m-sequences x_n and y are constructed as follows.

Set initial conditions as

$$\begin{aligned} &x_n(0) = n_0, x_n(1) = n_1, \cdots x_n(23) = n_{23}, x_n(24) = 1 \\ &y(0) = y(1) \cdots = y(23) = y(24) = 1 \end{aligned} \tag{4.12}$$

Recursively define subsequent symbols:

$$x_n(i + 25) = x_n(i + 3) + x_n(i) \text{ modulo } 2, i = 0, \ldots, 2^{25} - 27 \tag{4.13}$$

$$y(i + 25) = y(i + 3) + y(i + 2) + y(i + 1) + y(i) \text{ modulo } 2, i = 0, \ldots, 2^{25} - 27 \tag{4.14}$$

Define the binary Gold sequence z_n by:

$$z_n(i) = x_n(i) + y(i) \text{ modulo } 2, i = 0, \ldots, 2^{25} - 2 \tag{4.15}$$

Next, the real value Gold sequence Z_n can be defined as

$$Z_n(i) = \begin{cases} +1 & \text{if } z_n(i) = 0 \\ -1 & \text{if } z_n(i) = 1 \end{cases} \qquad \text{for } i = 0,1,\ldots 2^{25} - 2 \tag{4.16}$$

The real-value long scrambling sequences $c_{long,1,n}$ and $c_{long,2,n}$ are defined as follows.

$$\begin{aligned} &c_{long,1,n}(i) = Z_n(i), \qquad i = 0,1,\ldots 2^{25} - 2 \\ &c_{long,1,n}(i) = Z_n((i + 16777232) \text{ modulo } (2^{25} - 1)), \qquad i = 0,1,\ldots 2^{25} - 2 \end{aligned} \tag{4.17}$$

The complex value long scrambling sequence $C_{long,n}$, is defined as:

$$C_{long,n}(i) = c_{long,1,n}(i)(1 + j(-1)^i c_{long,2,n}(2\lfloor i/2 \rfloor)) \tag{4.18}$$

where $i = 0,1,\ldots 2^{25} - 2$ and $\lfloor \ \rfloor$ denotes rounding to the nearest lower integer.

RAKE Receiver and Maximum Ratio Combining (MRC) are used at the BS. The number of fingers is four. Assuming that the channels are perfectly estimated, both the phase distortion and the delay are known. The received signals are first realigned and phase compensated. Then, the signals are resampled, descrambled and despread before the MRC is used to generate the hard decisions. The Receiving process is illustrated below.

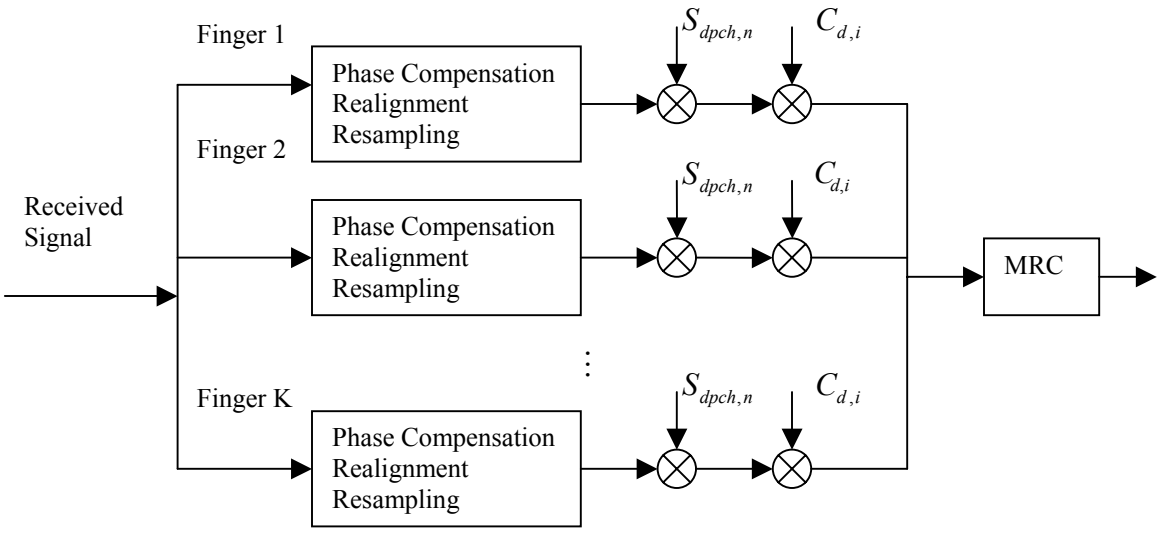

Fig 4.11 Receiver Structure

4.6 Smart Antenna Processing

Switched-beam and adaptive beamforming are used. The smart antenna processing are illustrated in Figure 4.9 below.

When signal $S_1, S_2, \ldots, S_N$ arrive, the antenna output $R_1, R_2, \ldots, R_N$ are generated according to the AoA θ. Switched beam beamformer multiplies the array output with the weight vectors, and chooses the weight vector which produces the maximum combining output to be the desired combining weight vector. Adaptive steering uses the array response as the desired weights. The array outputs are multiplied with the Hermitian of the combining weights in the combining process. The outputs of the combiner then go to the WCDMA receiver.

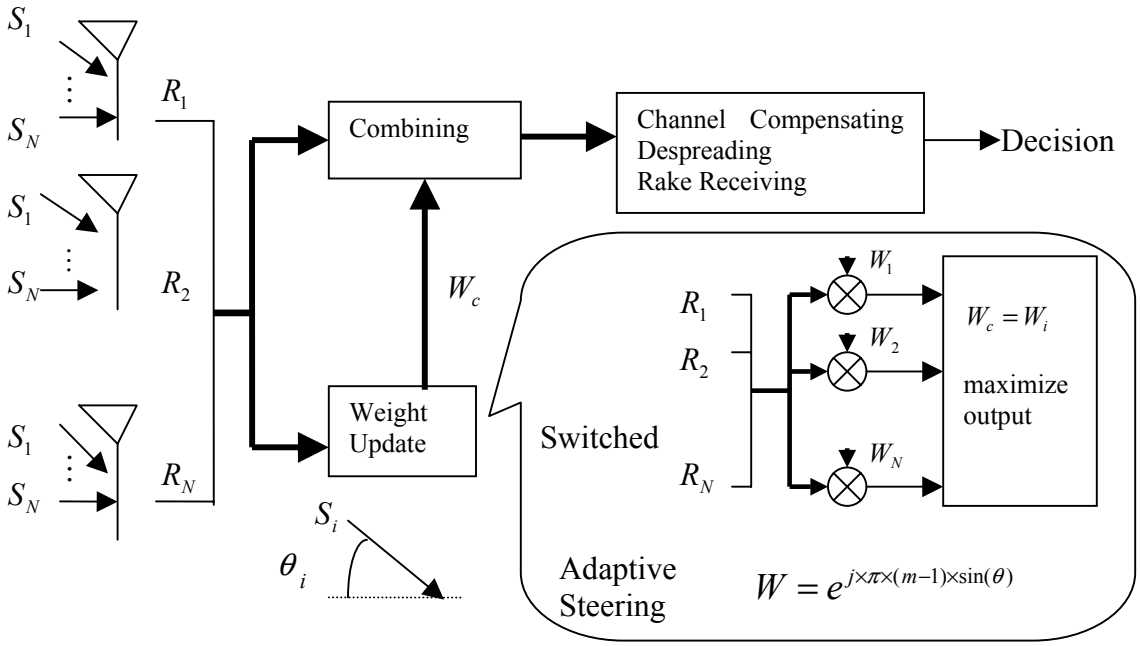

Fig 4.12 Smart Antenna Processing

4.7 Resource Management

We use power control based on constant power level in the simulator. The received power levels of every cell are the same. SINR are not balanced in this case since the interference varies in each cell. However, the interference level does not differ much since the mobiles tend to be uniformly distributed. The SINR balancing will improve the performance a little, but does not affect the simulation study much.

The TPC for power control has two bits instead of one in WCDMA proposal, but provide a more adaptive scheme to mitigate severe Doppler fade.

In order to simplify the simulation, power control commands are given by one BS in the active set identified as a controlling BS such that a single TPC command is received in each slot.

Pilot signals from different multipathe components are combined by MRC to generate a single estimation of the pilot strength. Angular diversity (through beam forming) is expected to smooth the fading effect and reduce power control errors. However, this expectation can not be met as shown in the simulation results in next chapter.

Handover is simulated based on IS-95 standard. Only the active set is simulated in order to cut down the complexity. An incoming call is added to active set if all the following condition satisfied.

. The pilot strength goes above T_ADD.
. The active set is not full.
. CAC gives permission.

Whenever the pilot strength drops below T_DROP, the BS is dropped from the active set without waiting for the timer to expire.

Call admission control and channel reservation are based on constant power level based PC scheme. Assuming that the received powers in every cell are the same, Equation (3.6), (3.7) become

$$R = \begin{cases} \min\{R(j) \mid j = k \text{ or } j \in \Omega(k)\}, & \text{if } R(j) > 0\}; \\ 0, & \text{otherwise} \end{cases} \tag{4.19}$$

where

$$R(j) = \begin{cases} \left| I_{TH} - I_k \right| , & \text{if } j = k; \\ \left| I_{TH} - I_k - L_m(h,k) \right|, & \text{if } j \in \Omega(k); \end{cases} \tag{4.20}$$

I_{TH} is the total interference and noise threshold, and I_k is the current interference in the k th cell.

Because of unbalanced SINR and constant signal power, HIM in section 3.4 is replaced by a handover interference threshold HI_{TH} . The total interference margin is renamed as total interference threshold TI_{TH} . The current interference margin CIM is replaced by the current interference CI . Therefore, The CAC and Channel Reservation can be illustrated as Figure 4.13 below.

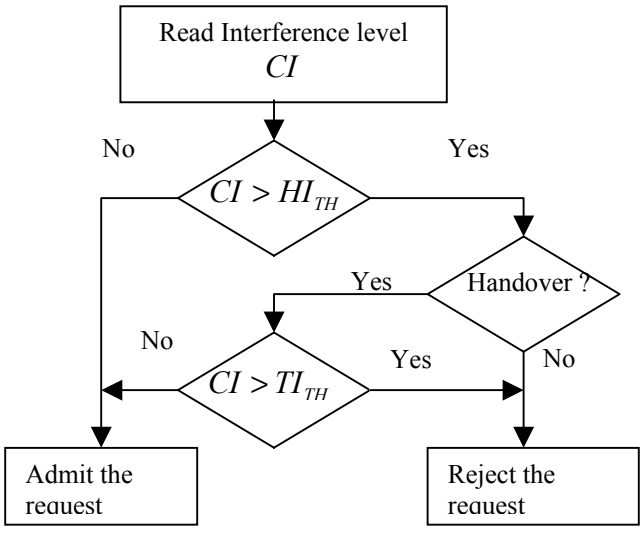

Fig 4.13 CAC and Channel Reservation Scheme

Chapter 5

Simulation Result and Discussions

This chapter discusses the simulation experiments and the results generated by the model described in Chapter four. The performances considered include bit error rate, power control rate, power control errors, handoff rate, call blocking rate and handoff failure rate, etc. Only the uplink scenario is considered in the following simulation experiments.

5.1 General Description of the Simulation Setup

Unless specified, simulation experiments follow the general setup described in this section. The Doppler frequency is 213 Hz. Power control rate is one command per slot (1500 Hz). The power control parameters are set as

pc_step	=	0.5dB	basic unit of increment or decrement
incre_step	=	3.2	multiplicity of increment (number of pc_step)
decre_step	=	3.2	multiplicity of decrement (number of pc_step)
sig_target	=	0dB	target signal power at the receiver
sig_th_low	=	-8dB	lower threshold for incre_step;
sig_th_high	=	8dB	higher threshed for decre_step;
pwr_ms_max	=	1.5 / t_drop	maximum MS power

The rule is that if the signal power is higher than sig_th_high, the transmitting power is decreased by pc_step multiplied by incre_step. Otherwise, if it is between sig_target and sig_th_high, the transmitting power is increased by pc_step. The same scheme applies when signal power is lower than sig_target. The scheme must use two bits in TPC instead of one, but is more capable of fighting fast fading. Furthermore, the transmitting power is adjusted such that the received signal power tends to reach the threshold in the opposite direction. Because signals in fading usually drops further continuously for several PC periods, adjusting the power a little bit more than just compensating the current fading will take into account the following fading during the PC delay.

A uniformly spaced linear array with 8 elements is used together with 120° sectoring in a cell. Sectoring gain is set as 6 dB. Sectoring is usually achieved through an antenna arrays. However, uniform attenuation of interference from other sections is assumed for simplicity. Spatial and temporal whiteness of the signals is assumed.

Only one DPCH is simulated with spreading gain set as 32. A 1D RAKE receiver with four fingers is used for MRC combining. Angular spread and diversity are not considered here.

5.2 Simulation Study in Single Cell Scenario

5.2.1 Single User BER Performance and Power Control

Figure 5.1 illustrates the amplitude of the signals at the receiver antenna input. Omni-directional antenna is used. Only fading effect applies without presence of noise, path lose and shadowing effect.

Figure 5.1 shows that because of the fading effect, signals are widely fluctuating. Fast power control mitigates the fading effect, but still can not catch up with the change of the channel when sharp and fast fading happens. Therefore, high pikes and deep abyss still exist along the curve with power control. The curve after power control is more likely to be smooth in slow fading circumstances.

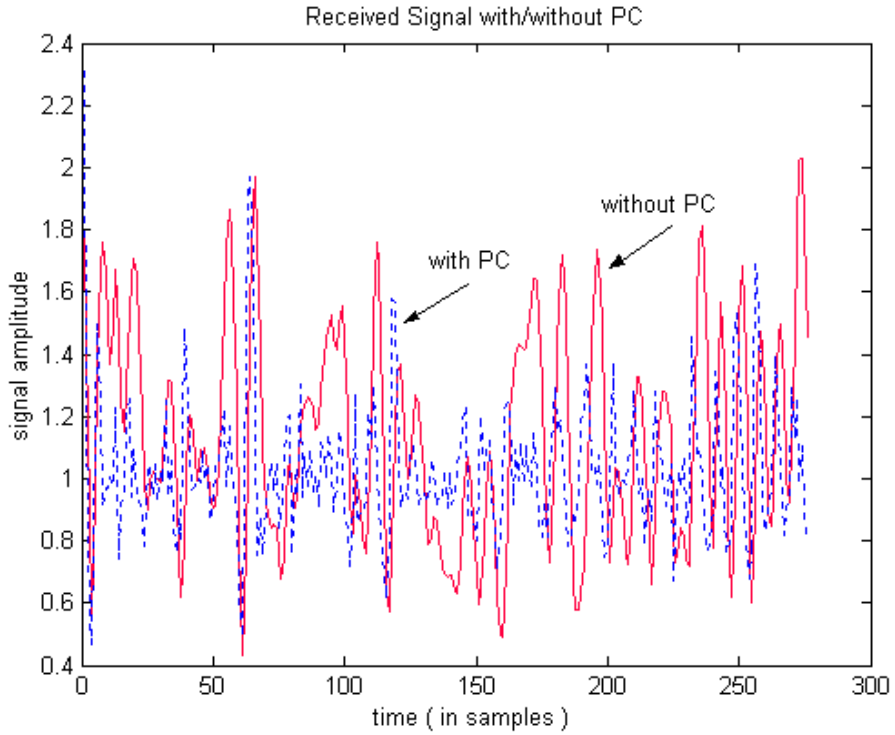

Fig 5.1 Received Signal at BS

Figure 5.2 illustrates the fading curves with different Doppler frequencies. As shown in the graph, fading channel with lower Doppler spreads changes more slowly and smoothly while that with higher Doppler spreads changes fast and sharply. It is easier to combat slow fading than fast fading by power control.

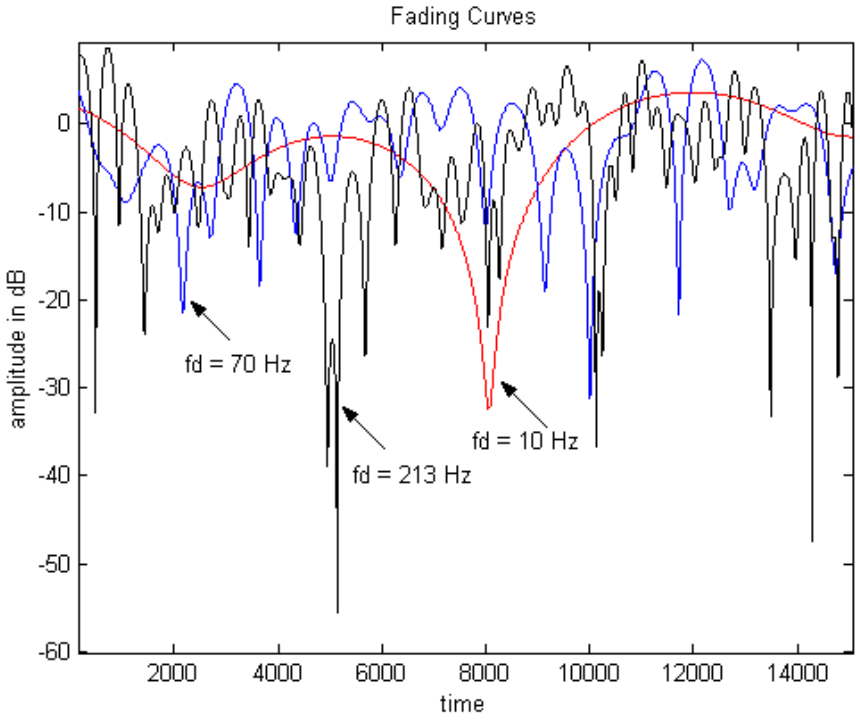

Fig 5.2 Fading Curves with Different Doppler Spreads

Figure 5.3 shows the link performance (BER) at the output of the receiver with fast power control applied to the system. The power control parameters are adjusted according to different fading situations. The parameters used for 213 Hz (Doppler spreads) are described before in Section 5.1. Parameters for 10 Hz and 100 Hz are as follows.

For 10 Hz, pc_step = 0.1dB; incre_step = 2; decre_step = 2; sig_target = 0dB; sig_th_low = -0.1dB; sig_th_high =0.1dB.

For 100 Hz, pc_step = 0.3dB; incre_step = 2; decre_step = 2; sig_target = 0dB; sig_th_low = -0.3dB; sig_th_high = 0.3 dB.

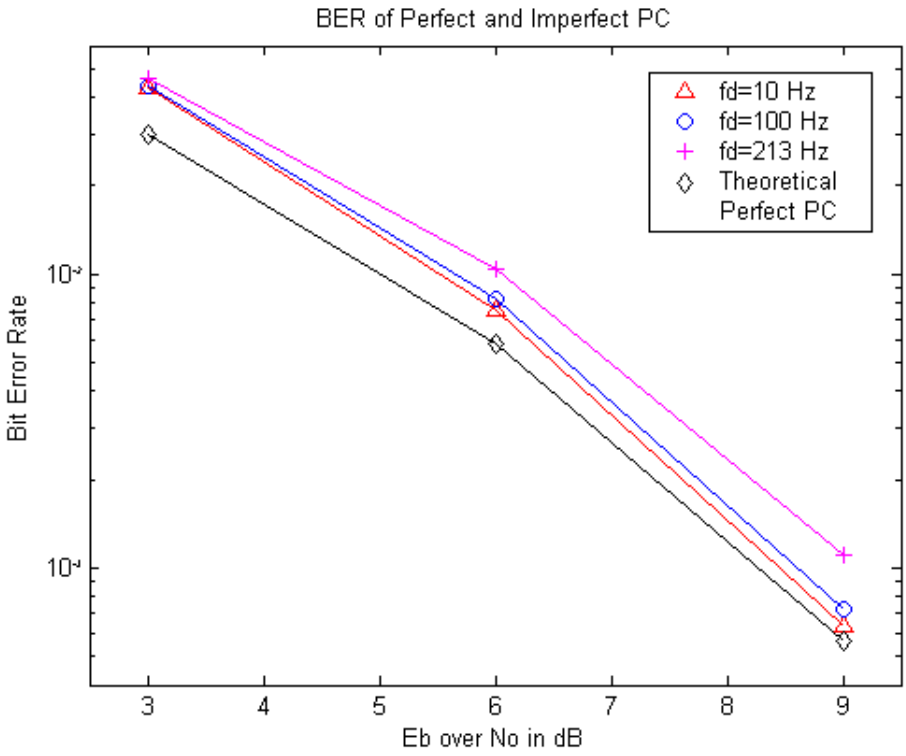

Fig 5.3 BER with PC under Different Doppler Spread

Result with theoretically perfect power control is derived using optimistic estimation of the BER in CDMA system considering the multipath effect.

$$P_e = Q\left(1\Big/\sqrt{\frac{N_0}{2E_b}\times\frac{K-1}{2N}}\right) \tag{5.1}$$

where K refers to the number of the multipath components, and N is the spreading gain. The powers of the multipath components are assumed to be equal after power control.

Figure 5.3 illustrates that bit error rate increases with higher Doppler spreads. Power control can mitigate the fading effect, especially in slow fading.

Figure 5.4 shows the power control error with respect to fading of different Doppler spreads and different diversity schemes. Consistent to figure 5.3, power control errors increase with the increase of the Doppler spreads.

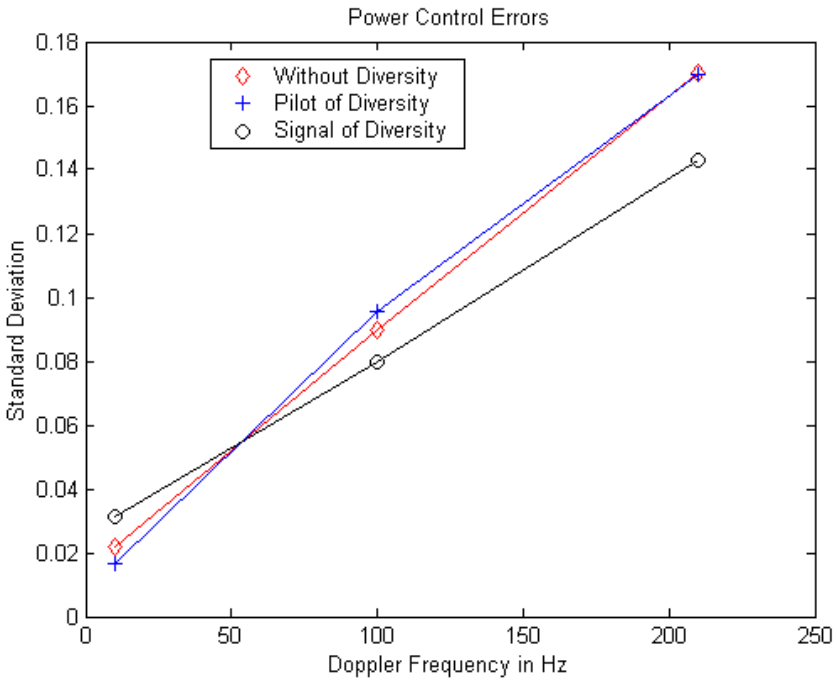

Fig 5.4 Power Control Error with Respect to Doppler Spreads and Diversity Schemes.

Power control schemes without exploring the diversity estimate the pilot strengths directly. Power control schemes exploring the diversity assume that multipath components are resolved perfectly by the smart antenna. The signal strengths of multipath components are combined according to the Maximum Ratio Combine (MRC) scheme into a single estimation of the signal power. Power control command is calculated based on this estimation.

It can be seen from Figure 5.4 that the PC errors (standard deviation) of the estimated pilot and the PC errors of the signal with diversity do not differ much from the PC errors of the signal without diversity.

Figure 5.5 further shows that the bit error rate does not improve by employing the diversity scheme in power control.

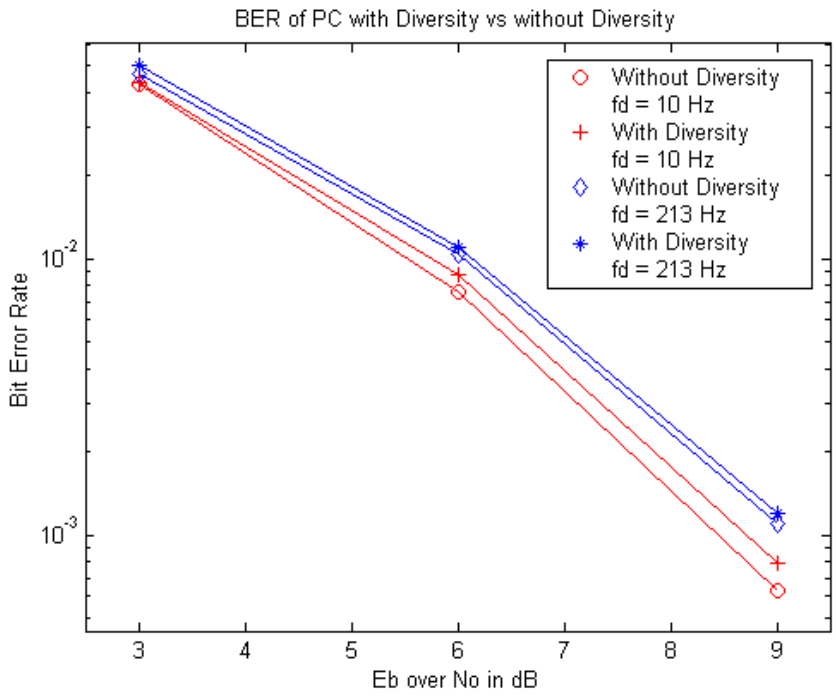

Fig 5.5 BER with Respect to Doppler Spreads and Diversity Schemes

Figure 5.6 illustrates how shadowing affects the performance. Slow power control compensates only the path loss and the shadowing effect. As shown in the figure, shadowing effect degrades the performance by a small amount when either fast PC or slow PC is applied.

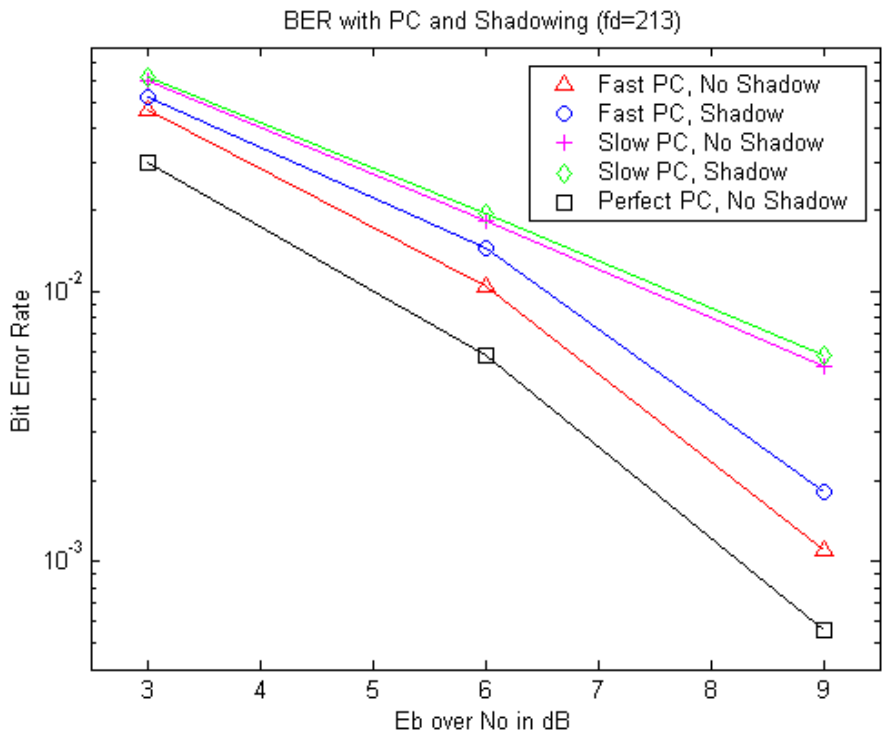

Fig 5.6 BER with Respect to Shadowing and Fast/Slow PC

5.2.2 Multi-user BER Performance and Smart Antenna

Figure 5.7 illustrates the BER performance with respect to fast and slow power control and cell sectoring when multiple (8) users are actively communicating to the BS in a cell. The AoA of the mobiles are uniformly between 0 and 2π.

It can be seen from Figure 5.7 that fast power control alone can significantly improve the performance. The BER curve with slow power control, no sectoring and no smart antenna levels off fast and remains at 0.02 with 12dB Eb/No. Sectoring can significantly reduce the BER. Fast power control can further reduce BER down below 0.001.

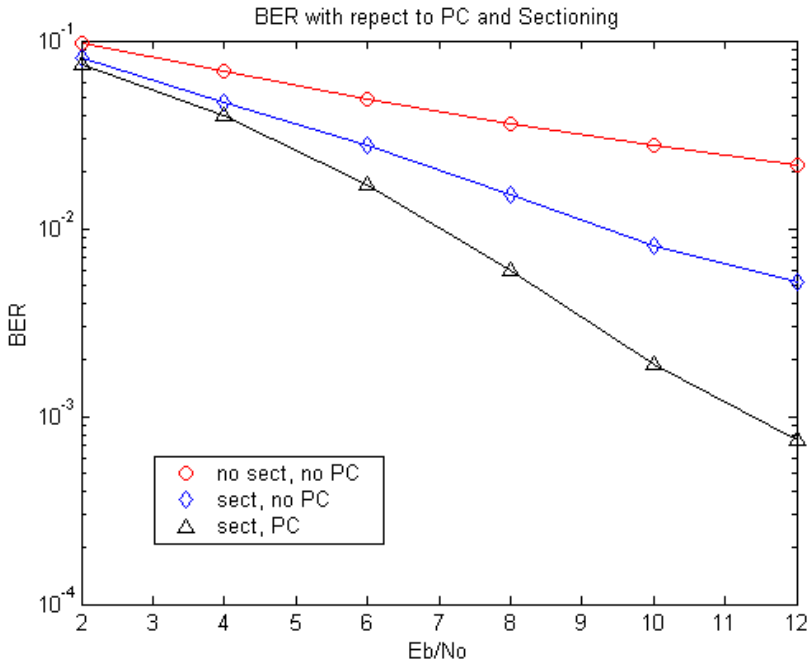

Fig 5.7 BER with respect to PC and Sectoring

Figure 5.8 illustrates the BER performance with different number of active mobiles in a cell and different types of antennas employed at the BS.

It is easy to see that with power control, but without a smart antenna, the BER curve levels off fast when system load increases. Either a switched beam or an adaptive array can generate much better performance than an omni-directional antenna. With a smart antenna, the BER degrades just a little when the number of users increases from 8 to 15. The BER degradation with an adaptive array is even smaller than that with a switched beam, and is trivial compared to that with no SA.

The BER with a smart antenna is much lower than that with just power control and no SA, which shows that the smart antenna can significantly increase the system capacity. The difference between the BER performance with an adaptive array and that

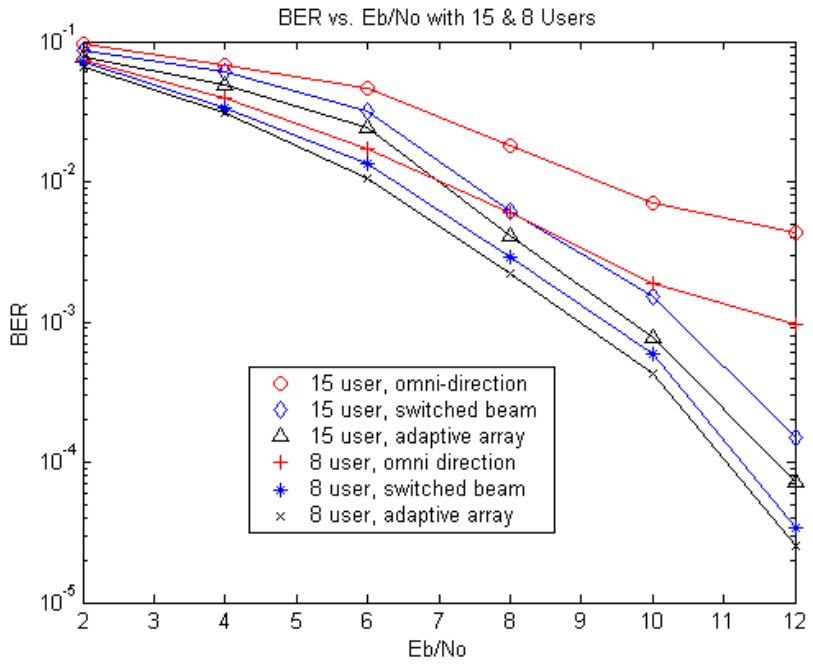

Fig 5.8 BER with respect to SA and Number of Users

with a switched beam increases when the system load goes up. However, it is still small compared to the overall performance.

Figure 5.9 shows the BER as a function of the number of users with Eb/No equal to 12dB. Similarly, the adaptive arrive and the switched beam generate comparable performances, but much better than that with omni-directional antennas. Figure 5.9 also shows that the BER levels off when system load approaches a high level. However, the BER with a smart antenna remains very low even with a large number of users. Thus, the system capacity is tremendously increased.

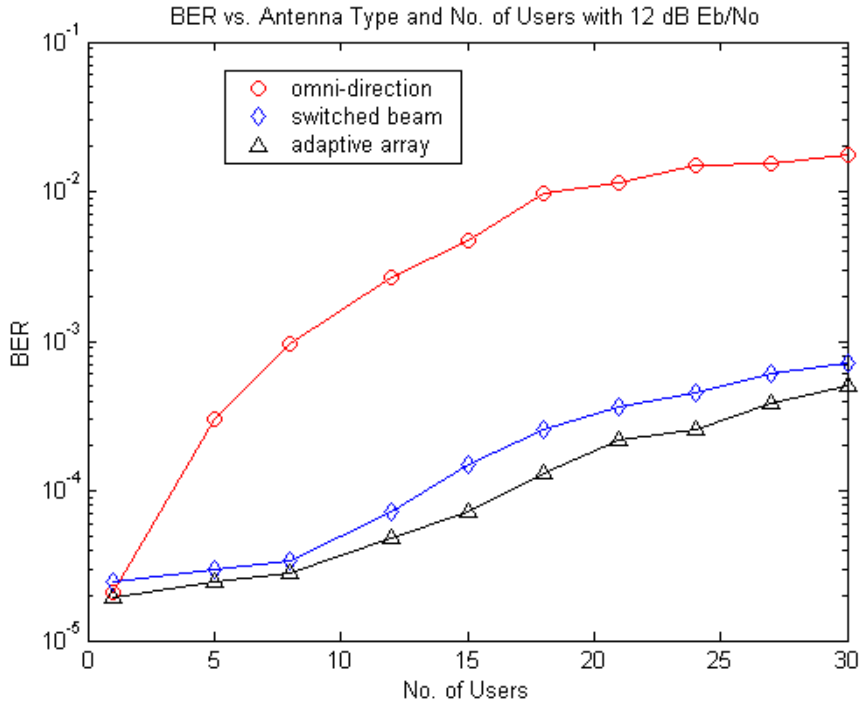

Fig 5.9 BER with respect to SA and No. of Users

Figure 5.10 illustrates the tradeoff of SA for lower PC rate. Eight users in a cell and the BS with an adaptive array are assumed in the experiment. The half rate PC (750 Hz) is similar to that in IS-95 (800 Hz).

We can see from Figure 5.10 that half rate PC without SA generates performance noticeably worse than that of slow PC with SA. This means that SA is better than fast PC in improving the performance. Also noticeable is that slow PC with SA and half rate PC with SA have similar performance compared to that of fast PC without SA. This shows that performance improvement by SA can be traded for the reduction of the PC rate. However, fast PC with SA gives much better performance than all other cases, showing the benefit of using SA in WCDMA systems.

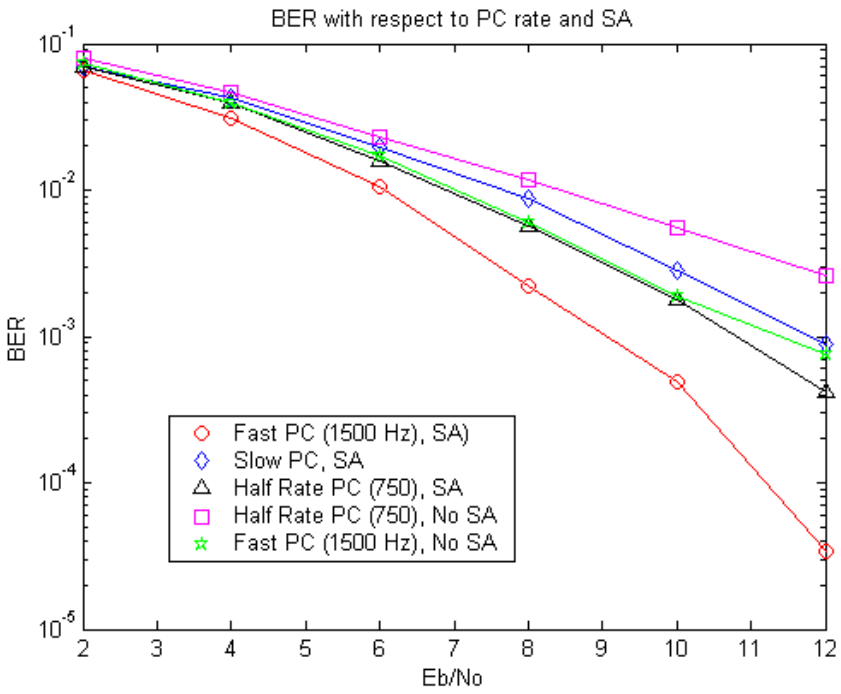

Fig 5.10 BER with respect to PC Rate and SA

5.2.3 Cell Capacity, Block/Drop Rate and Smart Antenna

Table 5.1 below shows the number of users with respect to the ratio of arrival and departure rate. The call admission and drop thresholds are set up as infinity. The measurements are the total interference and noise power level at the BS.

Arrival/Departure Ratio	2	6	10	14	18	22
Number of Users In the Cell	2.6	6.65	9.98	13.44	17.43	21.34

Table 5.1 Number of Users with respect to Arrival/Departure Ratio

It is clear from Table 5.1 that the number of users in the cell is equal to the ratio of the arrival rate and the departure rate, which is predicted by M/M/m/m queuing model when the number of servers (capacity) are infinite.

Figure 5.11 below shows the cell capacity with respect to the antenna types, call admission and call drop thresholds. The call holding time is set as infinity so that there are no call departures. 0.5 dB hysteresis means that the call drop threshold is set 0.5 dB above the call admission threshold. Otherwise, the call drop threshold is fixed at –13 dB.

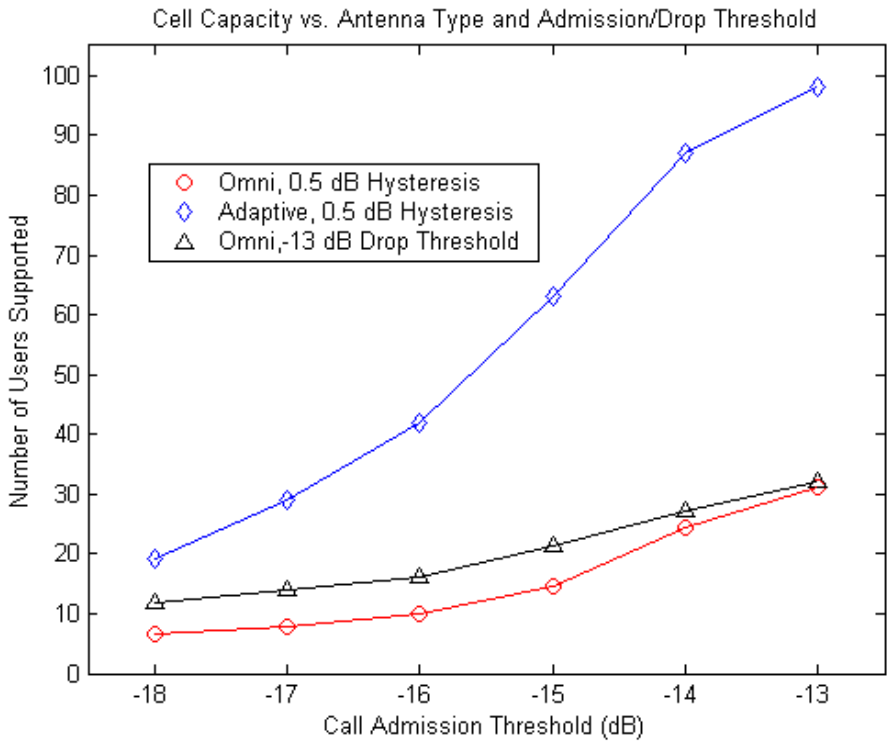

Fig 5.11 Cell Capacity with respect to Antenna,
Call Admission and Drop Threshold

Figure 5.11 shows that the cell capacity increases with the increase of the call admission threshold. Both the call admission and the call drop thresholds determine the

capacity of the cell. However, the major factor determining the capacity is the call admission threshold since it is below the call drop threshold. Larger hysteresis will increase the capacity, but just a little. On the other hand, smart antenna obviously increases the system capacity.

Figure 5.12 shows the number of users in a cell of finite capacity with call admission thresholds as –17 dB and call drop threshold as –16 dB. The estimated capacities are 10 users with an omni-directional antenna and 29 users with an adaptive array.

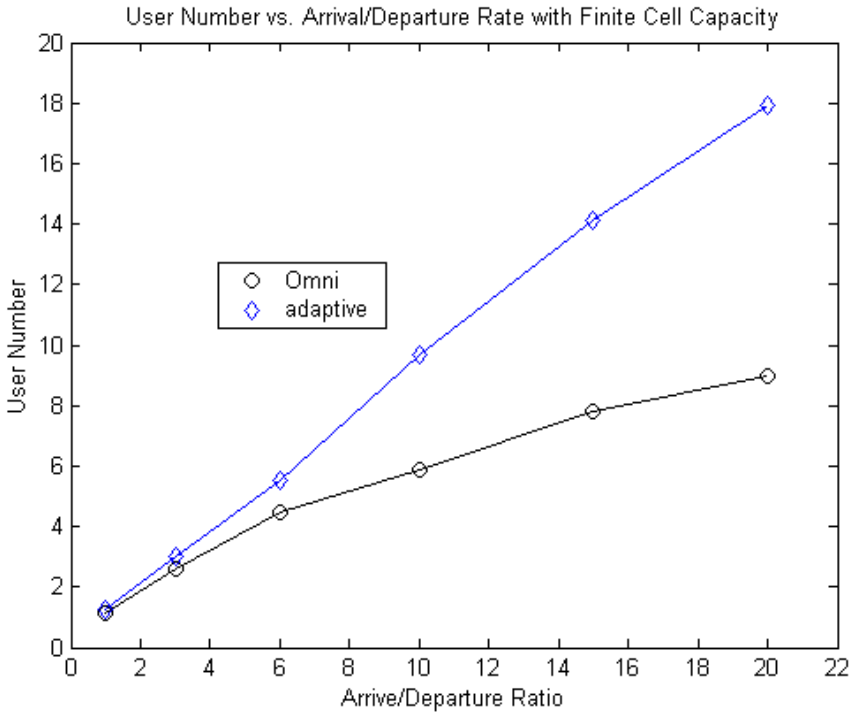

Fig 5.12 Number of Users with Finite Cell Capacity

It can be seen from the figure that with SA, there are many more users in the cell when the ratio of arrival rate over departure rate is large. For omni-directional antenna, there are just about 8 users remaining in the cell even if the ratio reaches 20, showing that the majority of the new call requests were rejected.

Figure 5.13 shows the call block and call drop rate with respect to the antenna types. The parameters are the same as above.

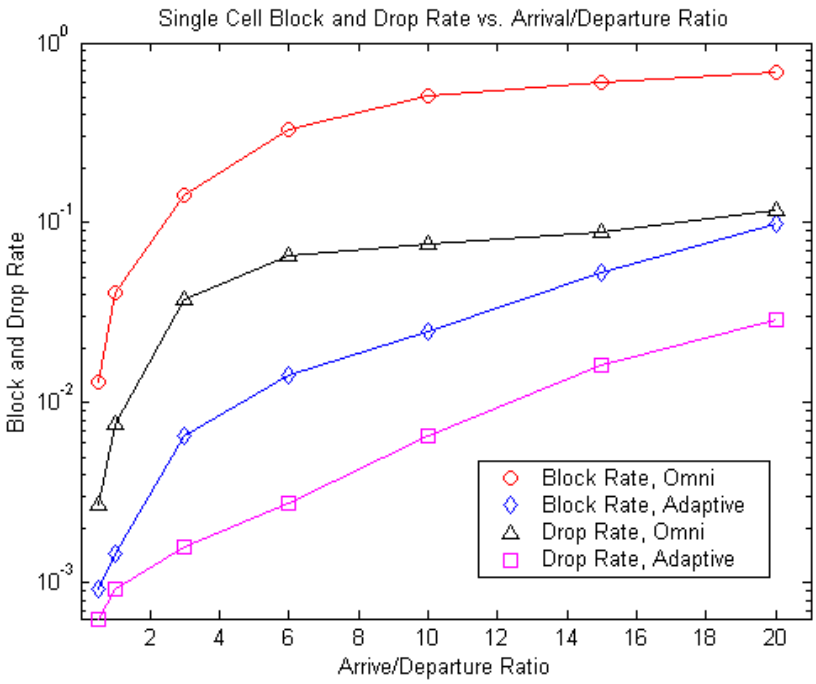

Fig 5.13 Block / Drop Rate and the Antenna

We can see from Figure 5.13 that the blocking rate with omni-directional antenna is very high. Smart antenna significantly reduces both the blocking probability and the dropping probability.

5.3 Simulation Study in Multi-cell Scenario

Simulation study in multi-cell (4 cells) scenario focuses on the role of smart antennas on soft handover and capacity reservation. We studied the handover failure rate and the handover rate with respect to soft handover region (SR), capacity reservation and smart antenna. Capacity is reserved for handover by setting a handover threshold higher than the call admission threshold, but lower than the call drop threshold.

Figure 5.14 shows the call drop rate with respect to antenna types and the capacity reservation. Parameters are as described in the next two paragraphs, and remain the same in the following experiments unless specified.

For omni-directional antennas, the small SR refers to adding the call to the candidate set if the mobile moves into 1/20 of the cell radius beyond the boarder, and dropping the call when it moves beyond 1/10 of the cell radius from the boarder. For large SR, the parameters are 1/8 when adding and 1/4 when dropping. For adaptive arrays, the small SR refers to 1/100 when adding and 1/200 when dropping, while large SR refers to 1/20 when adding and 1/10 when dropping.

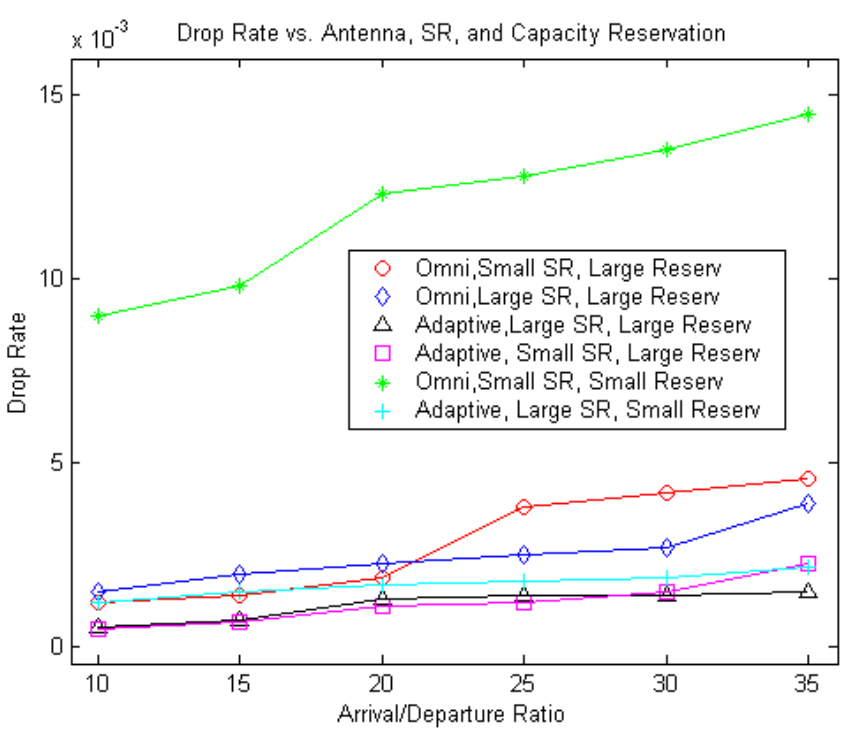

Fig 5.14 Call Drop Rate with respect to Antenna Types, SR, and Reservation

Large reservation refers to -19dB for denying admissions, -18 dB for blocking handovers and –16.5 dB for dropping ongoing calls. Small reservation refers to -18.2 dB

for denying admissions, -18 dB for blocking handovers and –16.5 dB for dropping ongoing calls.

From figure 5.14, we can see that the call drop rates do not differ much with respect to SR. The call drop rates go up considerably when the reservation is small. However, they can be driven back by smart antennas. The call drop rates with omni-directional antennas and large reservation are even higher than that with smart antennas, but small reservation. The call drop rates with smart antennas and large reservation are the lowest among all, but just a little bit lower than that with smart antenna and smaller reservation.

Figure 5.15 shows the handover rates with respect to antenna types and SR. The reservation is set as large, but is not relevant to the handover rate. From the figure, the handover rate is solely a function of SR.

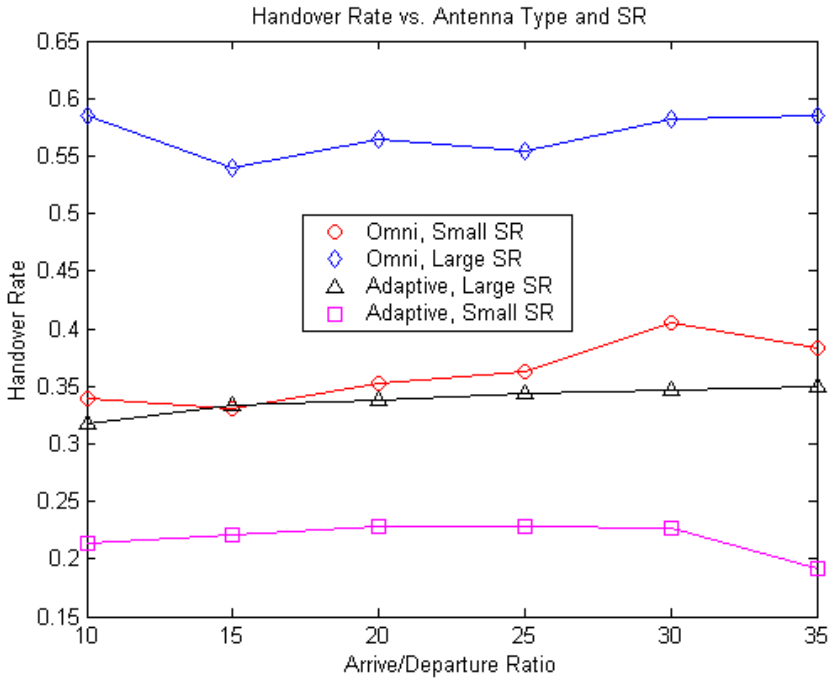

Fig 5.15 Handover Rate with respect to Antenna Type and SR

Figure 5.16 below shows the handover failure rates with respect to antenna types and SR. The reservation is set as large. It is easy to see that the reduction of handover failure rate by SR is very small. The reduction by smart antenna, on the other hand is significant. SR is mainly for seamlessly handover the call. Enlarging SR can reduce the handover failure rate a little bit just because a handover call can wait longer for the cell regaining its capacity before blocking the handover. The major factor affecting SR is the time period required to guarantee a seamless handover. Smart antennas have little to do in reducing the SR and corresponding soft handover rate.

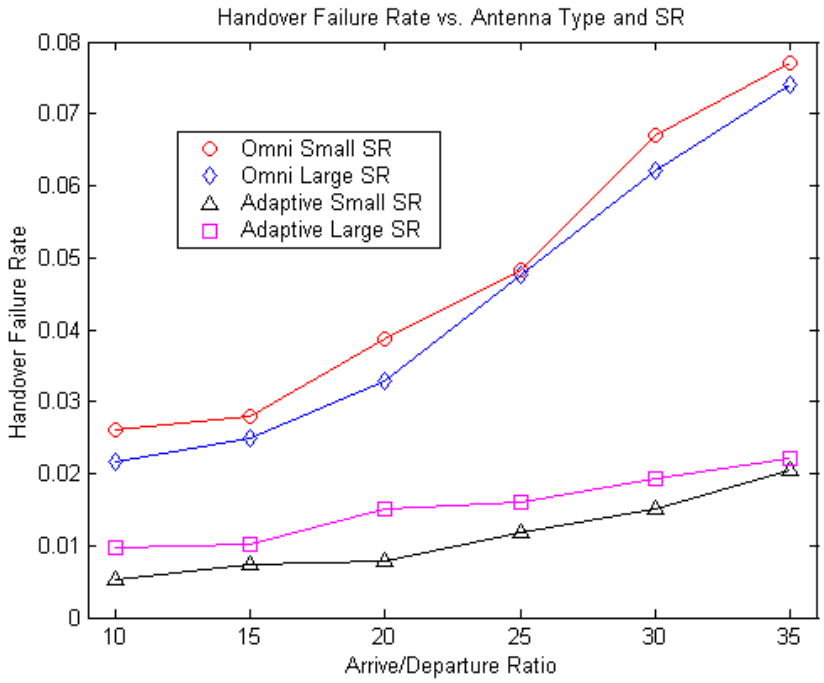

Fig 5.16 Handover Failure Rate with respect to Antenna and SR

Figure 5.17 shows the call block rates with respect to antenna types and SR. The reservation is set as large. Again, it is easy to see that SR has little influence on the call block rates whereas smart antennas reduce the call block rates significantly.

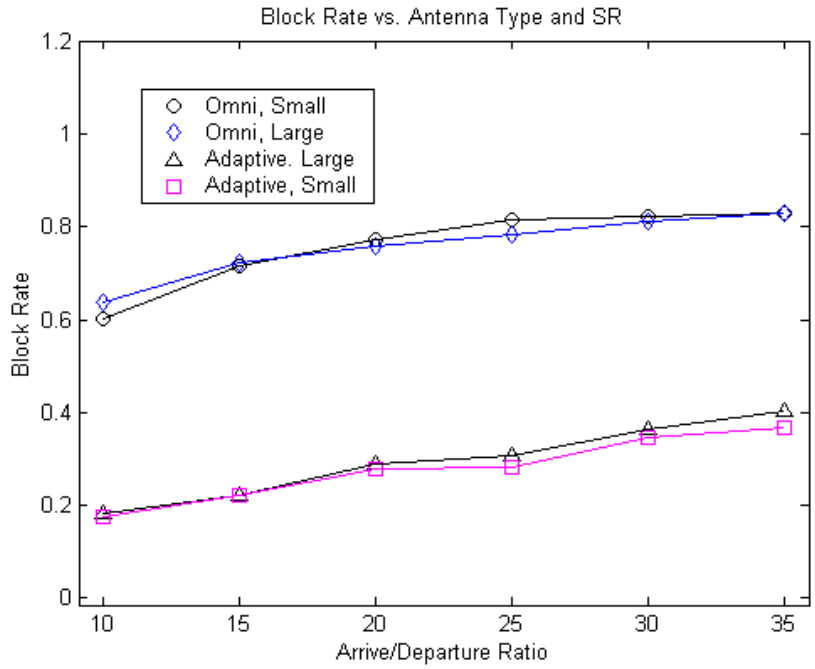

Fig 5.17 Call Blocking Rates with respect to Antenna Types and SR

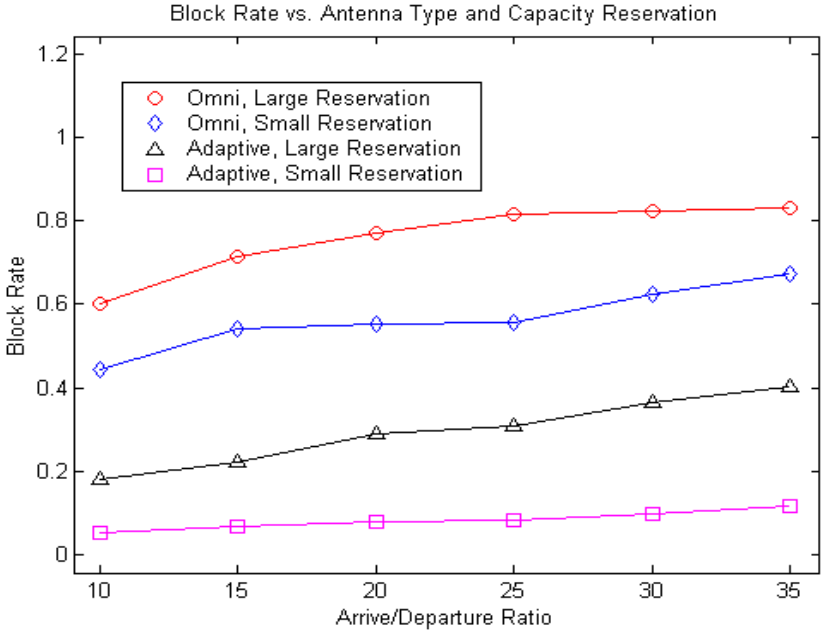

Fig 5.18 Call Blocking Rate with respect to Antenna and Reservation

Figure 5.18 shows the call blocking rates with respect to antenna types and reservation. Either reducing the capacity reservation or employing smart antennas reduces the call blocking probability considerably. Using smart antenna, among the two, is more effective in reducing the call blocking rates.

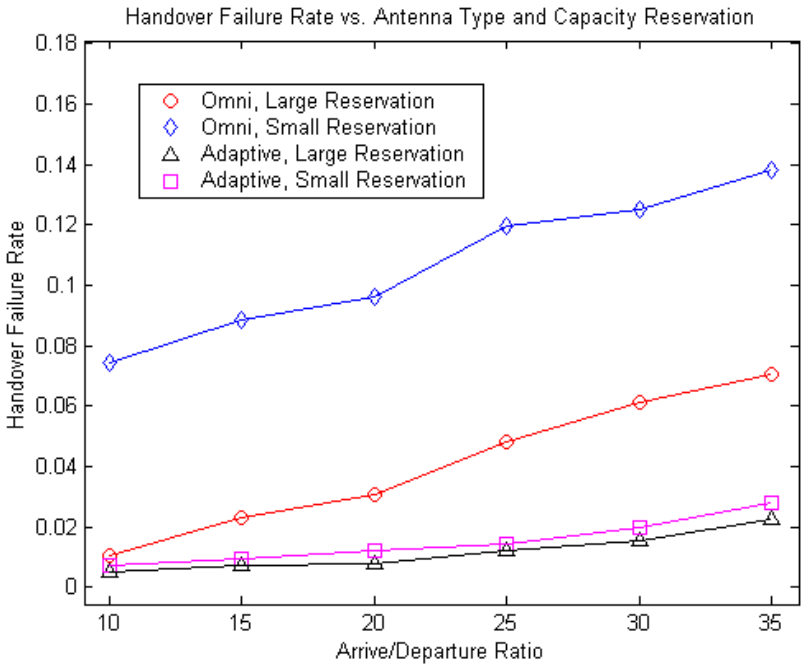

Fig 5.19 Handover Failure Rate with respect to Antenna and Reservation

Figure 5.19 shows the handover failure rates with respect to antenna types and reservation. It can be seen that contrary to the blocking rates in Figure 5.18, handover failure rates with small reservation is much higher than that with large reservation and omni-directional antenna. However, with smart antenna, the increase of the handover failure rates is very small when we change from large reservation to small reservation. Smart antenna can maintain the handover failure rates as if the reservation is not reduced. The reservation reduced can be used to accommodate more calls and the system capacity is increased, shown as the big reduction in the call block rates in Figure 5.18.

Chapter 6

Conclusion and Future Work

Although optional in 3G proposals, deploying smart antenna can significantly increase the capacity of the radio networks. In this thesis, we compare several aspects of different smart antenna algorithms including switched beam and adaptive arrays. A multi-cell simulation model is built which consists of six integrated components including a mobility and geographic model, an event simulator, a channel simulator, a WCDMA signal processor, a smart antenna processor and a resource management model. We also pursue simulation studies, investigating the benefit from smart antenna techniques to both the bit error rate (BER) performance improvement and the enhancement to the radio resource management schemes.

6.1 Conclusions

Adaptive arrays and switched beam antennas are two smart antenna (SA) approaches providing significant interference reductions in future cellular systems. Both algorithms have similar requirements on hardware. The computational complexity depends on individual algorithms. Algorithms such as CGA and MPL are designed to take advantage of the CDMA signal structures, and are more suitable than switched beam antennas when applied to CDMA systems with large number of users.

Both adaptive arrays and switched beam antennas generate comparable performances if the interference and noise signals are spatially and temporally white. Fully adaptive algorithms can produce much better performances than that of switched

beam if whiteness does not hold and the number of users is less than the number of array elements. However, they will fail when there are more users than array elements. Sub-optimal adaptive algorithms such as sub-optimal CGA and MPL are most likely the suitable algorithms for practical cellular systems due to their good performances, robustness, and low complexity.

Smart antenna techniques can significantly enhance the performances and capacity of the CDMA radio networks. With eight array elements, the capacity could be increased by a factor of 4. With moderate number of users, the BER will be improved by nearly 10^2 . Smart antennas also help to enhance the capability of radio resource management. The mobile transmitting power could be lower because of the interference reduction. Although the power control errors cannot be reduced by exploring the angular diversity provided by beamforming, the power control command rates can be reduced through the tradeoff with the interference reduction by smart antennas. On the second hand, smart antennas will significantly increase the system capacity and reduce the call blocking rates. Smart antennas also obviously reduce the handover failure rates. Therefore, the system capacity can be increased further by reducing the resources reserved for soft handover without increasing the handover failure rates. However, smart antenna does not play a big role in reducing soft handover rates. Handover rates can be reduced by decreasing SR, which generally does not obviously increase handover failure rates.

6.2 Future Works

Immediate follow up studies could be pursued in investigating smart antenna effect on performances and resource management in heterogeneous cell environments where a cell with an omni-directional antenna could suffer from his neighboring BS employing a smart antenna. The experiment can be done by setting the predefined parameter "bs_type" the proper value in the pre-processor. Another follow up is to study the issues with different traffic patterns, which may require a traffic pattern generator.

The simulator is open, and capable of integrating or replacing the original modules with new modules. New modules could include other smart antenna algorithms and resource management schemes, AoA spread models, 2-D rake receivers, sidelobe reduction algorithms, other propagation and channel modules. Some of the models have been introduced in Chapter two and three, such as SINR balanced power control algorithms, and statistics assisted handover, etc.

Another direction is to adopt the simulator as a platform in studying the network layer issues such as the end to end performance analysis and investigation in QoS, especially with multi-rate traffic (voice and data). Progress in this direction may require a multi-rate spreading/despreading schemes and channel coding. QoS schemes such as channel reservation and queuing could also be investigated. Queuing problems could be investigated by replacing call block clearing with specific queuing modules in the simulator.

Reference

[1] Harri Holma, Antti Toskala, *WCDMA for UMTS (Radio Access for Third Generation Mobile Communications)*, John Willy & Sons Ltd, West Sussex, England, 2001.

[2] Theodore S. Rappapport, *Wireless Communications (Principles and Practice)*, Prentice Hall PTR, New Jersey, 1996.

[3] Jerry D. Gibson, *The Mobile Communications Handbook*, CRC Press, 1996.

[4] M. Zeng, A. Annamalai, Vijay K. Bhargava, "Recent Advances in Cellular Wireless Communications," *IEEE Communication Magazine*, pp. 128-138, September, 1999.

[5] Francis Swarts, Pieter Van Rooyan, Ian Oppermann, Michiel P. Lotter, *CDMA Techniques for Third Generation Mobile Systems*, Kluwer Academic Publishers, Massachusetts, 1999.

[6] John Litva, Titus Kwok-Yeung Lo, *Digital Beamforming in Wireless Communications*, Artech House, Boston, 1996.

[7] Adrian O. Boukalov, Sven-Gustav Haggman, "System Aspect of Smart-Antenna Technology in Cellular Wireless Communications-An Overview," *IEEE Transactions on Microwave Theory and Techniques*, vol. 48, no. 6, pp. 919-929, June 2000.

[8] S. Anderson, U. Forssen, J. Karlsson, T. Witzschel, P. Fisher, and A.Krug, "Ericsson /Mannesmann GSM Field-trials with Adaptive Antennas," *Proc. IEEE 47th VTC*, pp. 1587–1591, 1997.

[9] S. Anderson, “Adaptive Antennas for GSM,” presented at the 5th Stanford Smart Antennas Mobile Wireless Communication Workshop, July 23–24, 1998.

[10] K. Molnar, “Space–time Processing in The Evolution of IS-136 System,” presented at the 5th Stanford Smart Antennas Mobile Wireless Communication Workshop, July 23–24, 1998.

[11] B. Hagerman, T. Osterman, K. J. Molnar, and G. E. Bottomly, “Field Test Performance Results for D-AMPS in PCS Bands with Array Processing,” *Proc. IEEE VTC’97*, Phoenix, AZ, pp. 1582–1586, 1997.

[12] J. H. Winters, “Forward Link Smart Antennas and Power Control for IS-136,” presented at the 5th Stanford Smart Antennas Mobile Wireless Communications Workshop, July 23–24, 1998.

[13] R. L. Cupo, G. Golden, C. Martin, and J. H. Winters, “A Four-element Adaptive Antenna Array for IS-136 PCS Base Stations,” in *Proc. IEEE VTC’97*, Phoenix, AZ, pp. 1577–1581, 1997.

[14] F. Adachi, “Application of Adaptive Antenna Arrays to W-CDMA Mobile Radio,” presented at the 5th Stanford Smart Antennas Mobile Wireless Communications Workshop, July 23–24, 1998.

[15] G. Tsulos, M. Beach, and J. McGeen, “Wireless Personal Communications for The 21st Century: European Technology Advances in Adaptive Antennas,” *IEEE Communication Magazine,* pp. 102–109, Sept. 1997.

[16] J. Monot, J. Thibault, P. Chevalier, F. Pippon, and S. Mayrague, “Smart Antenna Prototype for the SDMA Experimentation in UMTS and GSM/DCS1800 Network,” in *IEEE PIMCR’97*, Helsinki, Finland, pp. 33–337, 1997.

[17] J. Strandell, M. Wennstrom, A. Rydberg, T. Oberg, and O. Gladh, “Experimental Evaluation of An Adaptive Antenna for TDMA Mobile Telephony System,” in *Proc. PIMRC’97*, vol. 1, Helsinki, Finland, pp. 79–84, 1997.

[18] Paulo Cardieri, Theodore S. Rappaport*, Resource Allocation and Adaptive Antenna in Cellular Communications*, Ph.D. dissertation, Virginia Tech, Blacksburg, September 15, 2000.

[19] Jesse Buttler, Ralph Lowe, “Beam-Forming Matrix Simplifies Design of Electronically Scanned Antennas,” *Electronic Design*, pp. 170-175, April, 1961.

[20] R.C. Hansen, *Phased Array Antennas*, John Wiley & Sons Inc., New York, 1998.

[21] Seungwon Choi, Donghee Shim, Tapan K. Sarkar, “A Comparison of Tracking-Beam Arrays and Switching-Beam Arrays Operating in a CDMA Mobile Communication Channel,” *IEEE Antenna and Propagation Magazine*, vol. 41, no. 6, pp. 10-23, December, 1999.

[22] R. O. Schmidt, “Multiple Emitter Location and Signal Parameter Estimation," *IEEE Trans. Ant. and Prop.*, vol. AP-34, no. 3, pp. 276-280, 1986.

[23] R. Roy and T. Kailath, “ESPRIT Estimation of Signal Parameters via Rotational Invariance Techniques," *IEEE Trans. on Acoustics, Speech, and Signal Processing*, vol. 37, pp. 984-995, July 1986.

[24] D. Shim, S. Choi, "A New Blind Adaptive Algorithm Based on Lagrange's Formula for A Smart Antenna System in CDMA Mobile Communications," *IEEE Vehicular Technology Conference*, pp. 1160-1664, Ottawa, May 1998.

[25] Yash M. Vasavada, Thomas E. Biedka, Jeffrey H. Reed, "Code Gate Algorithms: A Blind Adaptive Antenna Array Beamforming Scheme for the Wideband CDMA Systems," The Thirty Fourth Asilomar Conference on Signals, Systems and Computers, vol. 2, pp. 1397 –1402, 2000.

[26] Donghee Shim, Seungwon Choi, "Should The Smart Antenna Be A Tracking Beam Array or Switching Beam Array," *IEEE 48th Vehicular Technology Conference*, vol. 1, pp. 494 –498, 1998.

[27] Seungwon Choi, Dongun Yun, "Design of an Adaptive Antenna Array for Tracking the Source of Maximum Power and Its Application to CDMA Mobile Communications," *IEEE Transactions on Antennas and Propagation*, vol. 45, no. 9, pp. 1393-1404, September 1997.

[28] Monica Dell'Anna, A. Hamid Aghvami, "Performance of Optimum and Sub-optimum Combining at The Antenna Array of A W-CDMA System," *IEEE Journal on Selected Areas in Communications*, vol. 17, no.12, pp. 2123-2137, December 1999.

[29] Joseph C. Liberti, "A Geographically Based Model for Line-Of-Sight Multipath Radio Channels," *IEEE 46th Vehicular Technology Conference*, vol. 2, pp. 844 –848, 1996.

[30] Joseph C. Liberti, Theodore S. Rappaport, "Analysis of CDMA Cellular Radio Systems Employing Adaptive Antennas in Multipath Environments," *IEEE 46th Vehicular Technology Conference*, vol. 2, pp. 1076-1080, 1996.

[31] ETSI TS 125 214, "Universal Mobile Telecommunications System (UMTS): Physical Layer Procedures (FDD)," 3GPP TS 25.214 version 4.0.0 Release 4, 2001.

[32] ETSI TR 25.922, "Universal Mobile Telecommunications System (UMTS): Radio Resource Management Strategies," 3GPP TR 25.922 version 4.0.0 Release 4, 2001.

[33] Tomohiro Dohi, Mamoru Sawahashi, Fumiyuki Adachi, "Performance of SIR Based Power Control in The Presence of None Uniformed Traffic Distribution", Fourth IEEE International Conference on Universal Personal Communications, pp. 334 –338, 1995.

[34] Zhao Liu, Magda El Zarki, "SIR-Based Call Admission Control for DS-CDMA Cellular Systems," *IEEE Journal on Selected Areas in Communications*, vol. 12, no. 4, pp. 638-644, May 1994.

[35] II Min Kim, Byung Cheol Shin, Dong-Jun Lee, "SIR-Based Call Admission Control Inter-cell Interference Prediction for DS-CDMA Systems," *IEEE Communication Letters*, vol.4 no.1, pp. 29-31, Jan. 2000.

[36] Sungmoon M. Shin, Cheol-Hye Cho, Dan Keun Sung, "Interference-Based Channel Assignment for DS-CDMA Cellular Systems," *IEEE Transactions on Vehicular Technology*, vol. 48, no. 1, pp. 233-239, Jan. 1999.

[37] Jin Weon Chang, Dan Keun Sung, "Adaptive Channel Reservation Scheme for Soft Handover in DS-CDMA Cellular Systems," *IEEE Transactions on Vehicular Technology*, vol. 50, no. 2, pp. 341-353, March 2001.

[38] Hyong-Goo Jeon, Seon-Ho Hwang, Soo-Kun Kwon, "A Channel Assignment Scheme for Reducing Call Blocking Rate in a DS-CDMA Cellular System," IEEE 6th

International Conference on Universal Personal Communications, vol. 2, pp.637-641, 1997.

[39] A. M. Law, W.D. Kelton, *Simulation Modeling and Analysis*, McGraw-Hill, New York, 1982.

[40] T. S. Rappaport, *Wireless Communications-Principle and Practice*, Prentice Hall, New Jersey, 1996.

[41] Alpha Concept Group, "Wideband Direct Sequence CDMA (WCDMA) Evaluation Document," Tdoc SMG 905/97, December 15-19, 1997.

[42] Duk Kyung Kim, Dan Keun Sung, "Characterization of Soft Handover in CDMA Systems," *IEEE Transactions on Vehicular Technology*, vol. 48, pp. 1195-1999, July 1999.

[43] ETSI TS 125 213, "Universal Mobile Telecommunications System UMTS): Spreading and Modulation," 3GPP TS 125.213 version 4.0.0 Release 4, March 2001.

[44] ETSI TS 125 401, "Universal Mobile Telecommunications System (UMTS): UTRAN Overall Description," 3GPP TS 25.401 version 4.0.0 Release 4, March 2001.

[45] Fakhrul Alam*, Simulation of Third Generation CDMA Systems* , M.S. thesis, Virginia Tech, Blacksburg, Deptember 15, 1999.

Abbreviations

AMPS	advanced mobile phone system
AoA	angle of arrival
AS	active set
BER	bit error rate
BS	base station
CAC	call admission control
CDMA	code division multiple access
CGA	code gate algorithm
CPICH	common pilot channel
DBF	digital beam forming
DCA	dynamic channel allocation
DDA	decision-direct Algorithms
DOA	direction of arrival
DPCCH	dedicated physical control channels
DPCH	dedicated physical channel
DPDCH	dedicated physical data channels
DSCMI	direct sample covariance matrix inversion
FCA	fixed channel allocation
FDD	frequency division duplex
FDMA	frequency division multiple access
FER	frame error rate
GSM	global system for mobile communications
IFFT	inverse fast Fourier transformation
LMS	least mean square

LOS	line of sight
MAHO	mobile assisted handover
MMSE	minimum mean square
MPL	maximum power lagrange
MS	mobile station
MSC	mobile switching center
MSIR	minimum signal to interference ratio
MV	minimum variance
OVSF	orthogonal variable spreading factor
PC	power control
PDF	probability distriburion funtion
PDF	power delay file
QoS	quality of service
RLS	recursive least square
RNC	radio network controller
RRM	radio resource management
SA	smart antenna
SF	spreading factor
SLR	sidelobe ratio
SR	soft handover region
TDD	time division duplex
TDMA	time division multiple access
UE	user equipment
UTRAN	universal terrestrial radio access networks
WCDMA	wideband code division multiple access

VITA

Yu Lei

Yu Lei was born in Chengdu, China on Oct. 29, 1969. He received his B.S. degree in Systems and Control from Chengdu University of Science and Technology. He started in the M.S. program of Virginia Tech at the fall of 1999., He joined MPRG in August 2000 and worked as a GRA with Dr. Annamalai in the area of smart antenna and radio resource management in CDMA systems.